

**EVALUACIÓN DEL MODELO CONSTITUTIVO PDMY02  
PARA CAPTURAR LA RESPUESTA DE SUELOS  
SOMETIDOS A CARGAS CÍCLICAS.**

**DIEGO MANZUR GUEVARA**

**Trabajo de grado para optar al título de Ingeniera Civil**

**DIRECTOR:**

**DAVID G. ZAPATA-MEDINA, Ph.D.**



**UNIVERSIDAD EIA  
INGENIERÍA CIVIL  
ENVIGADO  
2018**

**EVALUATION OF PDMY02 CONSTITUTIVE MODEL TO  
CAPTURE THE SOIL RESPONSE UNDER  
CYCLIC LOADINGS**

**BY**

**DIEGO MANZUR GUEVARA**

**COMMITTEE IN CHARGE**

**DAVID G. ZAPATA-MEDINA, Ph.D.**



**UNIVERSIDAD EIA  
CIVIL ENGINEERING  
ENVIGADO  
2018**

La información presentada en este documento es de exclusiva responsabilidad de los autores y no compromete a la EIA.

A una persona que me mostró desde su limitado conocimiento, lo bello de los números y la ciencia. Gracias Elkin.

La información presentada en este documento es de exclusiva responsabilidad de los autores y no compromete a la EIA.

## **AGRADECIMIENTOS**

A mi familia, mis padres, hermanas, tíos y primos, que sin ellos no estaría aquí escribiendo estas palabras. A mi director de trabajo de grado, quien me dio innumerables oportunidades para realizar investigación. A María del Pilar, a Rubén Darío, a Juan Fernando, a Jaqueline, a Javier, a Jorge, todos ellos profesores en todo el sentido de la palabra, quienes guiaron a un joven con todo virtudes y problemas, a empezar un nuevo camino. Amigos como Mateo y Héctor, los cuales son apoyo y motivación en este proyecto.

La información presentada en este documento es de exclusiva responsabilidad de los autores y no compromete a la EIA.

# TABLE OF CONTENTS

	Page.
1. INTRODUCTION .....	17
1.1 Problem statement .....	<b>¡Error! Marcador no definido.</b>
1.2 Justification.....	17
1.3 OBJECTIVES OF PROJECT .....	18
1.3.1 Main Objective.....	18
1.3.2 Specific Objectives .....	19
2. TECHNICAL BACKGROUND .....	20
2.1 Constitutive elasto-plastic models.....	20
2.2 Soil behavior under earthquake loading.....	22
2.3 Critical State Soil Mechanics .....	23
3. NUMERICAL MODELING OF MONOTONIC AND CYCLIC TRIAXIAL TESTS ON SANDS .....	35
3.1 PDMY 02 Constitutive Model .....	36
3.2 SSPbrickUP element .....	38
3.3 NUMERICAL MODEL.....	40
3.3.1 Mesh .....	40
3.3.2 Boundary conditions .....	40
3.3.3 Stages of loading.....	41
3.4 SOIL BEHAVIOR UNDER MONOTONIC LOADING.....	42
3.4.1 Sensibility analysis .....	48
3.5 SOIL BEHAVIOR UNDER cyclic LOADING .....	54

La información presentada en este documento es de exclusiva responsabilidad de los autores y no compromete a la EIA.

3.5.1	Individual calibration per individual test.....	55
3.5.2	Comparison between each set of parameters.....	67
3.6	Determination of sets per type of Dr .....	74
4.	PRELIMINARY NUMERICAL MODELING OF FREE FIELD CONDITIONS AT MANTA ECUADOR.....	82
4.1	SEISMICITY OF MANTA ECUADOR .....	82
4.1.1	Area of study .....	83
4.2	SUBSURFACE CONDITIONS.....	86
4.3	OPENSEES MODEL .....	88
4.3.1	VALIDATION AGAINST DEEPSOIL .....	91
5.	SUMMARY AND CONCLUSIONS.....	95
	REFERENCES .....	97
	APPENDIX A.....	100
	APPENDIX B.....	109

La información presentada en este documento es de exclusiva responsabilidad de los autores y no compromete a la EIA.

## LIST OF TABLES

Table 2.1 Applied stress paths and the stress points for cyclic loadings. (Matter & Jang, 2014) .....	24
Table 2.2 Recommended parameters per relative density for PDMY02 calibration (Khosravifar, 2013). .....	34
Table 3.1 CIU cyclic triaxial test results (Badanagki, 2016). .. <b>¡Error! Marcador no definido.</b>	
Table 3.2 Resume of stratigraphy and results of potential of liquefaction perforation P26-C7 Carrillo, J. (2018). Seismic analysis of Manta-Ecuador 2016 earthquake.....	42
Table 3.3 PDMY02 model parameters used for CID-TXC simulations (50kPa and 100kPa confining).....	44
Table 3.4 Parameters of PDMY02 model used to simulate the CIU-TXC test, and the variation respect the CID-TXC tests.....	47
Table 3.5 Resume of sets of parameters per test.....	67
Table 1.1 Resume of different set of parameters. ....	81
Table 4.1 DeepSoil model parameters.....	91

Page.

## LIST OF FIGURES

Figure 1.1 Volumetric and stress variations relationship.(Lu, 2006) <b>¡Error! Marcador no definido.</b>	21
Figure 2.1 Hyperbolic strain - stress relation.(Ti, 2014).....	21
Figure 2.2. Simulation results for a triaxial response for a linear and a nonlinear model.(Nieto Leal, Camacho-Tauta, & Ruiz Blanco, 2009) .....	21
Figure 2.3. Road displacement and embankment slope failure in Manta, Ecuador 2016..	22
Figure 2.4. Loss of bearing capacity in a silo foundation structure due liquefaction (1951). (McManus, 2016).....	22
Figure 2.5. Lateral spreadings of terrain and bridge foundations, Manta - Ecuador (2016) and Niigata (1964) respectively.....	23
Figure 2.6. Applied stress paths and the stress points for cyclic loadings (Matter & Jang, 2014) .....	24
Figure 2.7. Example of an engineering application of the triaxial test. (GDS, 2013) .....	25
Figure 2.8. OCR vs Undrained Strength Ratio and Shear Stress at failure from CK0U tests, (a) AGS Marine Sand Via SHANSEP and (b) James Bay Marine Sand via Recompression. (Ladd, 1995) .....	25
Figure 2.9. Granite rockfill (n=25.6%) (Vesic, 1969).....	26
Figure 2.10. CIU-TXC tests with different void ratio samples. ....	27
Figure 2.11. Relationship between void ratio and $\tan(\phi'_s)$ at different confining pressures in sands samples TXC tests. (Larsen & Ibsen, 2006) .....	28
Figure 2.12. Critical void ratio and critical state line in a TXC-CIU, TXC-CID and Simple CD test (Roscoe & Burland, 1970).....	28
Figure 2.13. Critical state definition (Roscoe & Burland, 1970). ....	29
Figure 2.14. Hysteretic curves from a cyclic triaxial test with a strain control.....	30
Figure 2.15. Variation in the $r_u$ value during cyclic loading process (Whittier 1989, Loma Prieta 1989, Imperial Valley 1979 y Loma Prieta 1989 earthquakes respectively) (Mercado Martínez Aparicio, 2016).....	31

La información presentada en este documento es de exclusiva responsabilidad de los autores y no compromete a la EIA.



Figure 2.16 Conic yield surfaces in a principal state of stress and deviatoric plane stress. (Elgamal et al., 2002).....	32
Figure 2.17 Lateral strains Vs Shear Stress and effective mean stress Vs Shear stress response of PDMY02 model. (Lu, 2006) .....	32
Figure 2.18 Back-bone stress-strain curve obtained from the yields surfaces. (Khosravifar, 2013) .....	33
Figure 3.1 Illustration of SSP brickUP element (in a column of soil and individual shape) (Fayun, Haibing, & Maosong, 2017).....	39
Figure 3.2 Diagram of constrains and fixies of model.....	41
Figure 3.3 CID-TXC test at different confining, conducted by University of Colorado at Boulder. ....	43
Figure 3.4 Deviatoric stress and excess pore water pressure (kPa) VS axial strain (%) comparison. ....	45
Figure 3.5 Confinement (kPa) VS Deviatoric stress (kPa) comparison.....	46
Figure 3.6 Shear strain (%) VS Shear modulus (MPa) comparison.....	46
Figure 3.7 Variation of confinement (kPa) VS deviatoric stress (kPa) with changes over c1 parameter. ....	48
Figure 3.8 Variation of axial strain (%) VS deviatoric stress (kPa) with changes over c1 parameter. ....	49
Figure 3.9 Variation of time (s) VS deviatoric stress (kPa) and confinement (kPa) VS deviatoric stress (kPa) with changes over c3 parameter. ....	50
Figure 3.10 Variation of axial strain (%) VS deviatoric stress (kPa) with changes over d1 parameter. ....	51
Figure 3.11 Variation of time (s) VS excess pore water pressure and confinement (kPa) VS deviatoric stress (kPa) with changes over d1 parameter. ....	52
Figure 3.12 Variation of time (s) VS deviatoric stress (kPa) and confinement (kPa) VS deviatoric stress (kPa) with changes over PT parameter. ....	53
Figure 3.13 Deviatoric stress (kPa) VS Axial strain (%) and confinement (kPa) respectively Test #1. ....	55

La información presentada en este documento es de exclusiva responsabilidad de los autores y no compromete a la EIA.

Figure 3.14 $r_u$ VS Time (s), Axial Strain (%) VS $u$ (kPa) and Time (s) VS Deviatoric stress (kPa) respectively Test #1. ....	56
Figure 3.15 Deviatoric stress (kPa) VS Axial strain (%) and confinement (kPa) respectively Test #2. ....	57
Figure 3.16 $r_u$ VS Time (s), Axial Strain (%) VS $u$ (kPa) and Time (s) VS Deviatoric stress (kPa) respectively Test #2. ....	58
Figure 3.17 Deviatoric stress (kPa) VS Axial strain (%) and confinement (kPa) respectively Test #3. ....	59
Figure 3.18 $r_u$ VS Time (s), Axial Strain (%) VS $u$ (kPa) and Time (s) VS Deviatoric stress (kPa) respectively Test #3. ....	60
Figure 3.19 Confinement (kPa) VS Deviatoric Stress (kPa) and $r_u$ VS Time (s) respectively Test #4. ....	61
Figure 3.20 Time (s) VS Deviatoric stress (kPa) and Axial strain (%) VS Deviatoric stress (kPa) respectively Test #4. ....	62
Figure 3.21 Deviatoric stress (kPa) VS Axial strain (%) and confinement (kPa) respectively Test #5. ....	63
Figure 3.22 $r_u$ VS Time (s), Axial Strain (%) VS $u$ (kPa) and Time (s) VS Deviatoric stress (kPa) respectively Test #5. ....	64
Figure 3.23 Deviatoric stress (kPa) VS Axial strain (%) and confinement (kPa) respectively Test #6. ....	65
Figure 3.24 $r_u$ VS Time (s), Axial Strain (%) VS $u$ (kPa) and Time (s) VS Deviatoric stress (kPa) respectively Test #6. ....	66
Figure 3.25 Comparison between all sets of parameters to reproduce test #1 conditions.	68
Figure 3.26 Comparison between all sets of parameters to reproduce test #2 conditions.	69
Figure 3.27 Comparison between all sets of parameters to reproduce test #3 conditions.	70
Figure 3.28 Comparison between all sets of parameters to reproduce test #4 conditions.	71
Figure 3.29 Comparison between all sets of parameters to reproduce test #5 conditions.	72
Figure 3.30 Comparison between all sets of parameters to reproduce test #6 conditions.	73
Figure 3.31 Simulation results of average set modeling test #1 conditions.....	75

La información presentada en este documento es de exclusiva responsabilidad de los autores y no compromete a la EIA.

Figure 3.32 Simulation results of average set modeling test #2 conditions.....	76
Figure 1.1 Simulation results of average set modeling test #4 conditions. ....	78
Figure 1.2 Simulation results of average set modeling test #5 conditions. ....	79
Figure 1.3 Simulation results of average set modeling test #6 conditions. ....	80
Figure 4.1 Tectonic condition of study region (Gutscher, Malavieille, Lallemand, & Collot, 1999). ....	82
Figure 4.2 Local tectonic conditions (GEOESTUDIOS S.A, 2016). ....	83
Figure 4.3 Barrio Tarqui location, Manta Ecuador. ....	83
Figure 4.4 Damages over the infrastructure of Tarqui suburb (GEOESTUDIOS S.A, 2016). ....	84
Figure 4.5 Distribution of stratigraphic profiles in Tarqui, Manta (GEOESTUDIOS S.A, 2016). ....	84
Figure 4.6 Altimetry data (GEOESTUDIOS S.A, 2016). ....	85
Figure 4.7 Profile D (GEOESTUDIOS S.A, 2016). ....	86
Figure 4.8 Accelerograms at different locations (GEOESTUDIOS S.A, 2016).....	86
Figure 4.9 Comparison between field obtained and convolution obtained (15m depth) accelerogram (GEOESTUDIOS S.A, 2016). ....	87
Figure 4.10 Response spectrum at surface at ARS1 zone.....	87
Figure 4.11 Fourier spectrum.....	87
Figure 4.12 Shear beam test mesh.....	89
Figure 4.13 Vertical Displacement (km 0+750) .....	90
Figure 4.14 Maximum ru value achieved in different depths. ....	90
Figure 4.15 Excess of pore water pressure ratio in time.....	91
Figure 4.16 Degradation of stiffness due shear strain at different depths (GEOESTUDIOS S.A, 2016).....	92
Figure 4.17 Damping due shear strain at different depths (GEOESTUDIOS S.A, 2016). .	92

La información presentada en este documento es de exclusiva responsabilidad de los autores y no compromete a la EIA.

Figure 4.18 Response spectrum comparison..... 93  
Figure 4.19 Shear strain comparison. .... 93

Page.

## LIST OF APPENDIXES

APPENDIX A Opensees code for an isotopically consolidated undrained triaxial test (CIU TXC test).....	100
APPENDIX B MATLAB code for plotting graphics and illustrations.....	109
	Page.

## **GLOSARY**

CID: Consolidated Isotropic Drained conditions.

CIU: Consolidated Isotropic Undrained conditions.

PDMY02: Pressure Depend Multi Yield constitutive model.

PBD: Performance Based Design

TXC: Triaxial Compression Test

TXE: Triaxial Extension Test

## RESUMEN

La simulación numérica alrededor de proyectos geotécnicos se está convirtiendo gradualmente en una herramienta principal para diseñar estructuras con una filosofía de diseño basada en desempeño que permite no solo determinar la estabilidad de las construcciones, sino también una respuesta contra diferentes condiciones de carga, como sísmica, eólica o marítima. que son capaces de crear condiciones únicas que fuerzan al elemento de las estructuras a funcionar de formas diferentes a las que fueron diseñadas. Con esto en mente, un grupo de ecuaciones matemáticas deben ser capaces de reproducir la respuesta mecánica en diferentes condiciones de carga y capturar los cambios internos en el suelo y su comportamiento. Es por esto que se selecciona un modelo constitutivo basado en múltiples superficies de fluencia para tratar de capturar la respuesta mecánica de una arena que proviene de Manta, Ecuador, en condiciones monótonas y cíclicas y comparar los resultados numéricos con datos de pruebas de laboratorio. El modelo constitutivo propuesto para este estudio es el modelo Pressure Depend Multi Yield 02 (PDMY02) desarrollado por el profesor Ahmed Elgamal en UCSD, el que considera múltiples superficies de fluencia para obtener una respuesta mecánica diferente en diferentes condiciones de esfuerzo-deformación (p. Ej. Dilatación o comportamiento contractivo del suelo).

Tomando en consideración la formulación matemática del modelo PDMY02, la capacidad de reproducir diferentes esfuerzos hizo que este modelo sea capaz de determinar el inicio de la licuefacción y predecir los asentamientos inducidos debido a eventos sísmicos, producto del exceso de disipación de la presión del agua intersticial. El caso de estudio presentado en esta investigación, el suburbio de Tarqui, ubicado en la ciudad de Manta, el 16 de abril de 2016 se vio afectado por un terremoto de magnitud 7.8 en la escala de Richter, y sobre este lugar, se desarrolló un proceso de licuación, donde daños en edificios estructurales como carretera o puentes fueron producidos.

Este trabajo presenta los resultados de una optimización manual de los parámetros del modelo constitutivo PDMY02 para tres pruebas de TXC monotónicas y para seis pruebas de TXC cíclicas, una simulación numérica preliminar de la respuesta de campo libre basada en la calibración triaxial cíclica.

En general, el modelo presenta una respuesta precisa en la fase de contracción, con una sobre predicción de la respuesta a extensión, y es capaz de predecir en un análisis inicial, el inicio de la licuefacción y el comportamiento posterior a dicho fenómeno.

La información presentada en este documento es de exclusiva responsabilidad de los autores y no compromete a la EIA.

## ABSTRACT

Numerical simulation around geotechnical projects is gradually becoming a main tool to design structures with a performance-based design philosophy that allows not only to determine the stability of constructions, but also a response against a different load conditions, like seismic, wind or marine loads, that are able to create unique conditions that force the elements of the structures to work in different ways to those that were designed. With that in mind, a group of mathematical equations must be capable to reproduce the mechanical response at different loading conditions and capture the internal changes in soil materials and its behavior. That is why a constitutive model based on multiple yield surface concept is selected to try to capture the mechanical response of a sand that comes from Manta, Ecuador, under monotonic and cyclic conditions and compare the numerical results with a laboratory test data. The constitutive model proposed for this study is Pressure Depend Multi Yield 02 model (PDMY02) developed by professor Ahmed Elgamal in UCSD, it takes into account multiple yield surfaces to get a different mechanical response at different stress-strains conditions (e.g. dilatancy or contractive soil behaviors).

Taking into consideration the mathematical formulation of PDMY02 model, the capacity to reproduce different stress made this model capable of determining the onset of liquefaction and predict the induced settlements due to seismic events caused by excess pore water pressure dissipation. The case of study presented in this research, Tarqui suburb, which is located in Manta city, in April 16<sup>th</sup> of 2016 was affected by a 7.8 Richter scale magnitude earthquake, and over this location, a liquefaction process was developed, where damages on structural buildings as road or ports were produced.

This work presents the results of a manual optimization of PDMY02 constitutive model parameters for three monotonic TXC tests and for six cyclic TXC tests, a preliminary numerical simulation of free field response based on cyclic triaxial calibration.

In general, the model presents an accurate response in the contraction phase, with an overprediction of extension response, and a capability to predict in an initial analysis, the onset of liquefaction and post liquefaction behavior.



# 1. INTRODUCTION

## 1.1 AREA OF WORK

Significant advances in the last 40 years have led us to performance-based earthquake engineering. It basically attempts to predict and quantify the behavior of structures under seismic loadings (Kramer, Arduino, & Shin, 2008). Commercial suites such as Plaxis and Flac are examples of state-of-the-practice tools to model freefield and soil-structure interaction conditions for a wide range of geo-structures. The performance-based design philosophy has been refined in recent years as technological developments have made it possible to incorporate numerical tools to improve the capabilities of predicting soil stress distributions, deformation or strain fields, and forces in structural elements., such as excavation props, foundations, dams and tunnels (Kramer et al., 2008). However, all numerical tool employed for dynamic analyses require a proper definition of the seismic input motion, a suitable constitutive soil model, and an adequate soil characterization. This research focuses on evaluating an advance constitutive soil model that can represent adequately cyclic soil behavior and its intrinsic stiffness degradation, hysteretic damping, accumulated deformations, pore pressure built-up, and volumetric changes.

The liquefaction phenomena and its numerical modeling are of interest in this work. This soil instability is attributed to the loss of interstitial frictional forces due to continuous change of pore pressures leading to an associated loss of shear strength and stiffness. (Petalas & Galavi, 2013) This phenomenon produces an increase of deformations, that result in a decrease of bearing capacity of soil, which induces large settlements in nearby infrastructure (Stark, Olson, Kramer, & Youd, 1989). Traditionally, the potential of liquefaction is evaluated based on the cyclic resistance of the soil with respect to the shear strength, which define a safety factor against liquefaction. Field correlations and laboratory testing are the standard practice to define the cyclic resistance of a soil deposit. However, little to none information regarding induced ground movements is obtained. Given the complexity of the phenomenon (Lopez-caballero & Modaressi, 2008), it is necessary to use an advanced constitutive soil model that can capture not only the onset of liquefaction due to pore water pressure build-up, but also the volumetric change due to re-sedimentation or consolidation after the earthquake (Galavi, Petalas, & Brinkgreve, 2013). Several constitutive soil models have been proposed to capture post liquefaction behavior. Among those are UBC3D (Petalas & Galavi, 2013), PM4SAND (Boulanger & Ziotopoulou, 2015), and PDMY02 (Elgamal, Yang, & Parra, 2002). UBC3D has been proved to work well to define the onset of liquefaction (Mercado Martínez Aparicio, 2016). However, it fails to adequately simulate the volumetric change due to reconsolidation after liquefaction (Mercado Martínez Aparicio, 2016). PM4Sand which is implemented in FLAC has all the potential to capture this phenomenon. However, it requires the input of 23 parameters and their determination is difficult. In this thesis, the PDMY02 soil model is evaluated for this purpose. Initially, a boundary value problem of a triaxial test is created in the FEM software OPENSEES to calibrate the soil

La información presentada en este documento es de exclusiva responsabilidad de los autores y no compromete a la EIA.

parameter against monotonic and cyclic triaxial testing. Then, a free field model in OPENSEES is created to simulate a deposit subjected to a seismic event and validated with other numerical tools such as DEEPSOIL.

## **1.2 JUSTIFICATION**

The basic ingredients for liquefaction are loose deposit of clean sand, saturated conditions and rapid loading such as those generated by earthquakes and detonations. The entire Pacific coast as well as the lower and upper parts of the Atlantic coast of Colombia meet the necessary conditions to be potential places for the occurrence of this phenomenon. (Colombian regulation of earthquake resistant construction, 2010) (García Núñez, 2007). Then, a methodology where a mechanical view of the soil from the elasto-plastic point of view prevails, can predict the behavior of these structures under short cyclic dynamic loads, thus achieving a high level of service in the long term and that its operation is not affected suddenly, causing a high risk for different localities surrounding such infrastructures, as considerable monetary losses, while generating the possibility of analyzing this type of phenomena from an affordable point of view to both technical, logistical and economic level (Seed, 1987), because despite the high level of training required for the management of these IT solutions, due to the shortage of equipment for dynamic triaxial testing not only in the region but also in the country, they put this type of alternatives as a valuable resource for the dynamic analysis of foundation is (Stark et al., 1989).

Now, being able to determine how the behavior of a structure (using elasto-plastic models) before its construction (Kramer, 2008) under sporadic cyclic loads (mainly seismic forces) will be able to identify possible critical points of failure, which are required design and / or build following standards of both material quality and construction processes, thus allowing them to be infrastructures with a high level of security, ensuring not only their uninterrupted operation due to catastrophic events, but a guarantee for the areas surrounding the structure that their safety and integrity will not be at risk.

## **1.3 OBJECTIVES OF PROJECT**

### **1.3.1 Main Objective**

Evaluate the capacity of PDMY02 constitutive model to capture the soil response under cyclic loading triaxial conditions, through the verification of residual values between the experimental and simulation results, three monotonic triaxial tests and 6 cyclic triaxial tests.

La información presentada en este documento es de exclusiva responsabilidad de los autores y no compromete a la EIA.

### 1.3.2 Specific Objectives

- To obtain the back-bone characteristic curves that indicates the soil behavior under a loading condition, through a data recompilation of granular and “cohesive” soil tests, that includes index properties, oedometer test, static and cyclic triaxial tests with interne deformation measures to determinate the mechanical response of soil.
- To model in the finite element software OpenSees contour problems that represent the oedometric and triaxial conditions using the PDMY02 constitutive model to obtain the back-bone characteristic curves.
- To compare the numeric response with the triaxial test observe response.
- To analyze the numeric data, taking into consideration the parametric function of model, to determinate the coherency of data, giving recommendations to implement PDMY02 constitutive model in geotechnical engineering applications.

## 2. TECHNICAL BACKGROUND

### 2.1 CONSTITUTIVE ELASTO-PLASTIC MODELS

Taking in consideration the behavior of the soil, it is not just controlled by elastics dynamics, others methodologies tries to explain the relationship between strain and stress conditions, working together along the deformation process in the medium of analysis (Kamalzare, Dove, Flint, Green, & Rodriguez-marek, 2016). For example, Hardening Soil constitutive model, use the incremental elasticity model from Duncan-Chang (Seed, 1987), which one is based in a elastoplastic lineal ratio, who takes as reference the preconsolidation load to adjust the behavior of soil (Stark & Vettel, 1991). The next equation show is represented in the next illustration.

$$\frac{1}{2 * E_{50}} * \frac{q}{1 - \frac{q}{q_a}} = \varepsilon * a$$

(Stark & Vettel, 1991)

Where:

- $E_{50}$  is the Young's modulus at 50% of ultimate stress.
- $\varepsilon$  is the strain of soil.
- $a$  is a parameter that change in function of soil behavior, as the Young's modulus and the ultimate stress.
- $q$  is the deviatoric stress.
- $q_a$  is the ultimate stress that can be applied to soil.

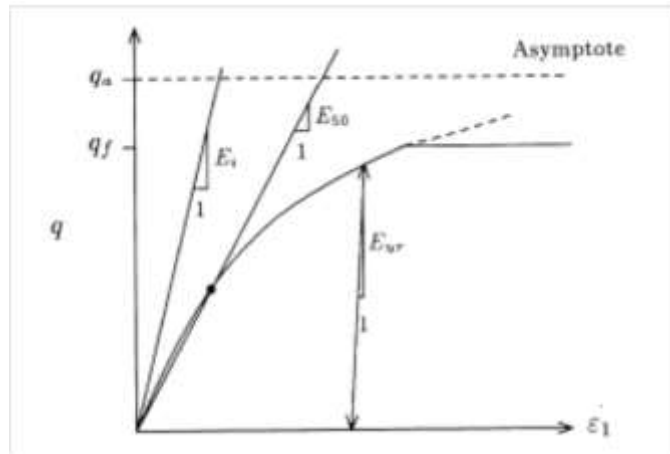


Figure 2.1 Hyperbolic strain - stress relation.(Ti, 2014)

In the next illustration, is represented two constitutive models, a linear and nonlinear model (Mohr-Coulomb and Hardening Soil models) for a triaxial test representation.

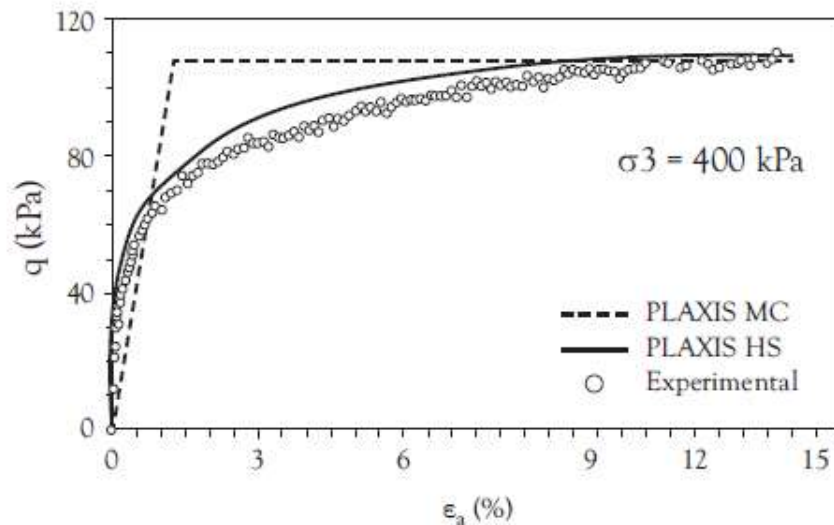


Figure 2.2. Simulation results for a triaxial response for a linear and a nonlinear model.(Nieto Leal, Camacho-Tauta, & Ruiz Blanco, 2009)

La información presentada en este documento es de exclusiva responsabilidad de los autores y no compromete a la EIA.

## 2.2 SOIL BEHAVIOR UNDER EARTHQUAKE LOADING

The phenomenological process of liquefaction occurs principally in a poorly graded sand, saturated, which ones at a cyclic load process, the grains lose contact between each other's (the interstitial frictional forces disappears because a continuous change of pore pressure, the amount of water is not capable to dissipate, which lead to an associated los of shear strength and stiffness. This phenomenon produces an a increase of deformations, that result in a decrease of bearing capacity of soil, which induces a high settlements in all kind of infrastructures around (Stark et al., 1989). This behavior is only capable to reproduce taken into consideration the elasto-plastic response of soils. At next will appeared different images that show post liquefaction process.



**Figure 2.3. Road displacement and embankment slope failure in Manta, Ecuador 2016.**

(Grunauer, 2017)



**Figure 2.4. Loss of bearing capacity in a silo foundation structure due liquefaction (1951). (McManus, 2016)**

La información presentada en este documento es de exclusiva responsabilidad de los autores y no compromete a la EIA.



**Figure 2.5. Lateral spreadings of terrain and bridge foundations, Manta - Ecuador (2016) and Niigata (1964) respectively.**

Other type of destructive effect induced by liquefaction process is the lateral spreading of foundations, mechanism that could unconfined the piles or induce a lateral movement of shallow foundations, which causes different stresses conditions around the structure, creating a instability producing tilting or even collapse.

### **2.3 CRITICAL STATE SOIL MECHANICS**

Monotonic triaxial test.

Because the initial condition stress is produce by its own weight and loading charges (foundations for example), the monotonic loading process and its results for an initial study of mechanical behavior of soils is crucial to determinate not just the resistance values, also the stiffness response. That is because the stress path induced to a soil sample will allow know under sort type of stress condition, the parameter that reproduce in a better way, the stress-strain relation. Because of different ways to charge a sample of soil, under a triaxial chamber, the loading process could be applied under these four conditions:

**Table 2.1 Applied stress paths and the stress points for cyclic loadings. (Matter & Jang, 2014)**

Test	Description
RTXE	Reduced triaxial extension test, decreasing axial stress with constant radial stress
TXC	Triaxial compression test, increasing axial stress with constant radial stress
RTXC	Reduced triaxial compression test, decreasing radial stress with constant axial stress
TXE	Triaxial extension test, increasing radial stress with constant axial stress

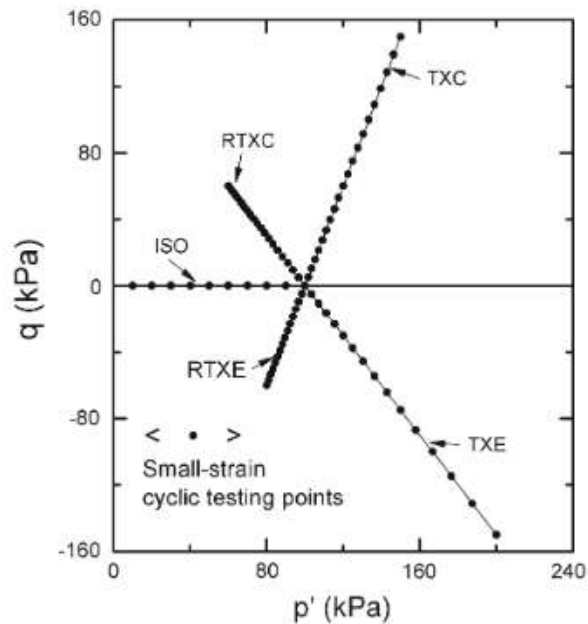


**Figure 2.6. Applied stress paths and the stress points for cyclic loadings (Matter & Jang, 2014)**

These four conditions of stress path try to reproduce the stress pattern that is applied in a point of soil medium, which depends majorly of relative position to geometry and structures respectively. Taking that into analysis consideration, for example in a slope where the failure zone follows a circular-parabolic trajectory, the better way to characterize a stratum soil by anisotropy non induced (Carrillo & Casagrande, 1944) mechanic response is recreate a different loading process, where to determinate the behavior that governate the crown of slope, the TXC test reproduce in a major aprox. way the stress in situ condition, or at the



base of a slope, a TXE test could induce the most possible strains around the sample. This is represented in the next figure.

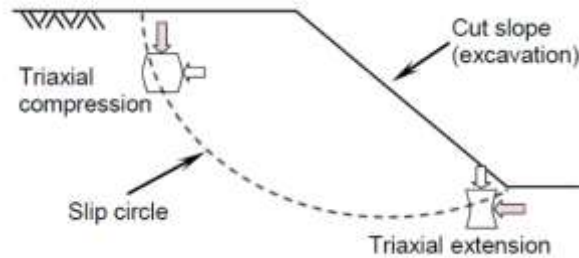


**Figure 2.7. Example of an engineering application of the triaxial test.** (GDS, 2013)

Now, due to the inherent anisotropy condition of soils, the way that a sample response to a determinate stress path is by definition different (Carrillo & Casagrande, 1944), where for example to granular soils, the grain size distribution, the grain shape, the mineral grains and the density, affects the strength at shear failure, and this is show in the next figure, where for the same sand sample, with a reconstituted process getting the same void ratio, describe a different mechanical response, because a different stress path.

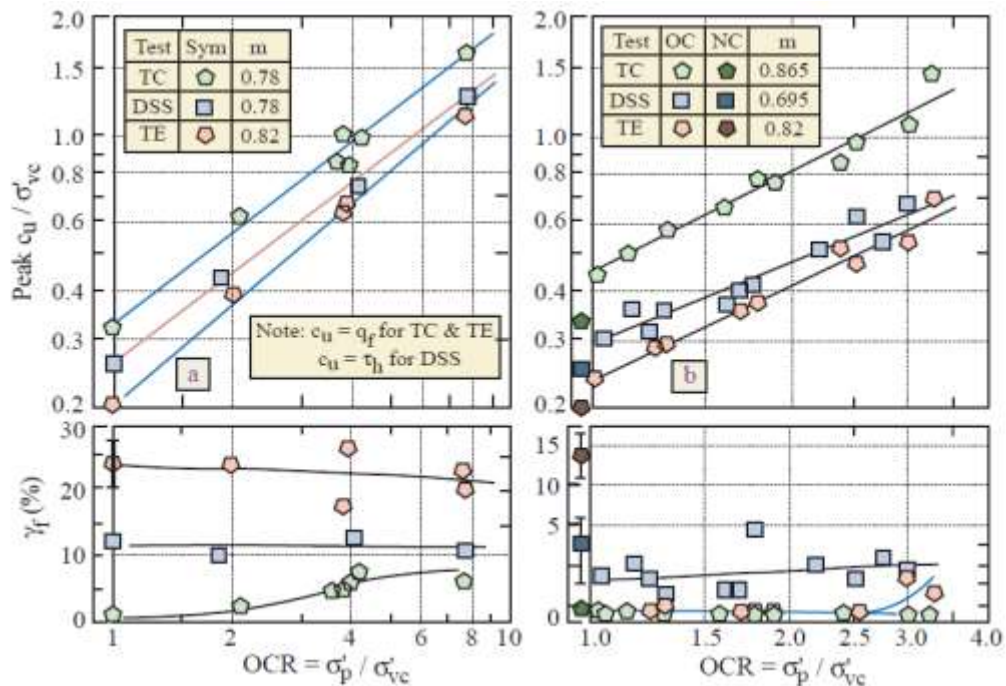


**Figure 2.8. OCR vs Undrained Strength Ratio and Shear Stress at failure from CK0U tests, (a) AGS Marine Sand Via SHANSEP and (b) James Bay Marine Sand via Recompression.** (Ladd, 1995)

La información presentada en este documento es de exclusiva responsabilidad de los autores y no compromete a la EIA.

The previously natural conditions could be synthesized in these 4 factors which ones defines the shear strength:

- Mineral friction.
- Particle Rearrangement
- Dilatancy
- Particle breakage

Due a series of testing (CIU-TXC) on dense sands at very high consolidation stress, with a increment around the confinement pressure, the behavior of soil, not just the mechanical response (increasing confinement will increase stress failure), the volumetric process will be different (increasing confinement pressure the dilatancy tendency will be canceled, with a contraction process that domain the volumetric changes). That is show in the next figure.

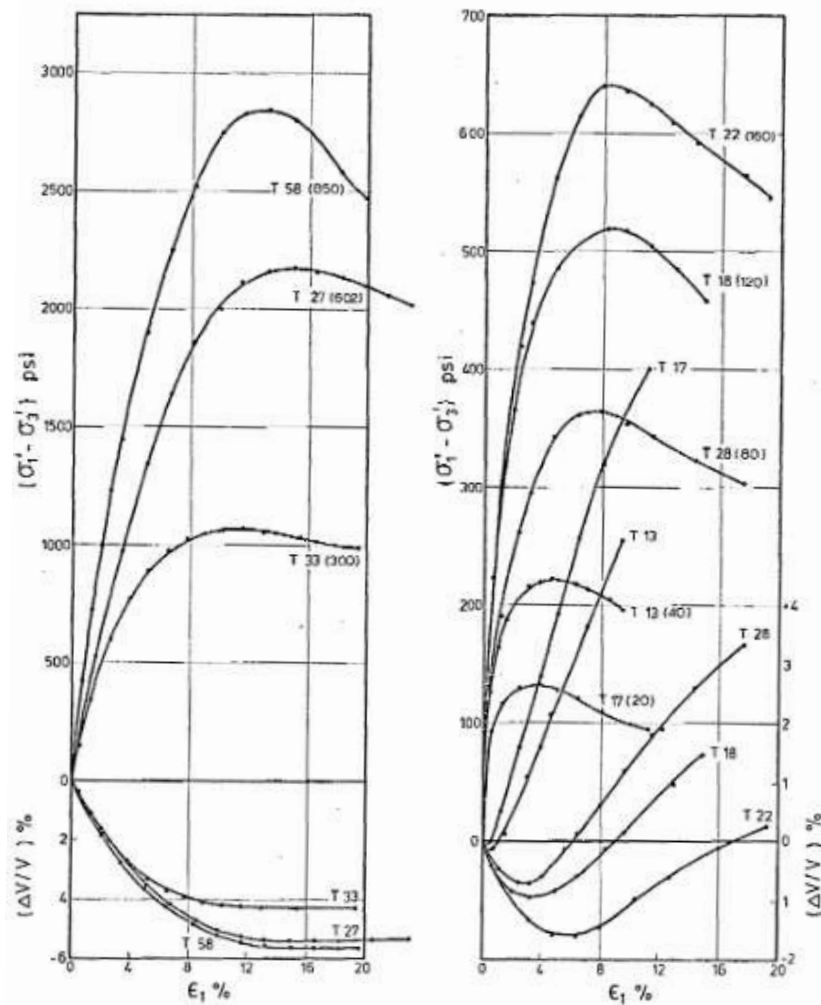


**Figure 2.9. Granite rockfill (n=25.6%) (Vesic, 1969)**

La información presentada en este documento es de exclusiva responsabilidad de los autores y no compromete a la EIA.

Additionally, the relation between the void ratio (particle rearrangement factor) and the mechanical and volumetric response is directly and inversely proportional, where the shear strength will increase with a dense sand sample, and the volumetric decrease with a loose one, and for a future analysis, for a loose sample of sand, the gain of excess pore pressure will be developed, against samples with higher void ratio. This could be see in the next figure.

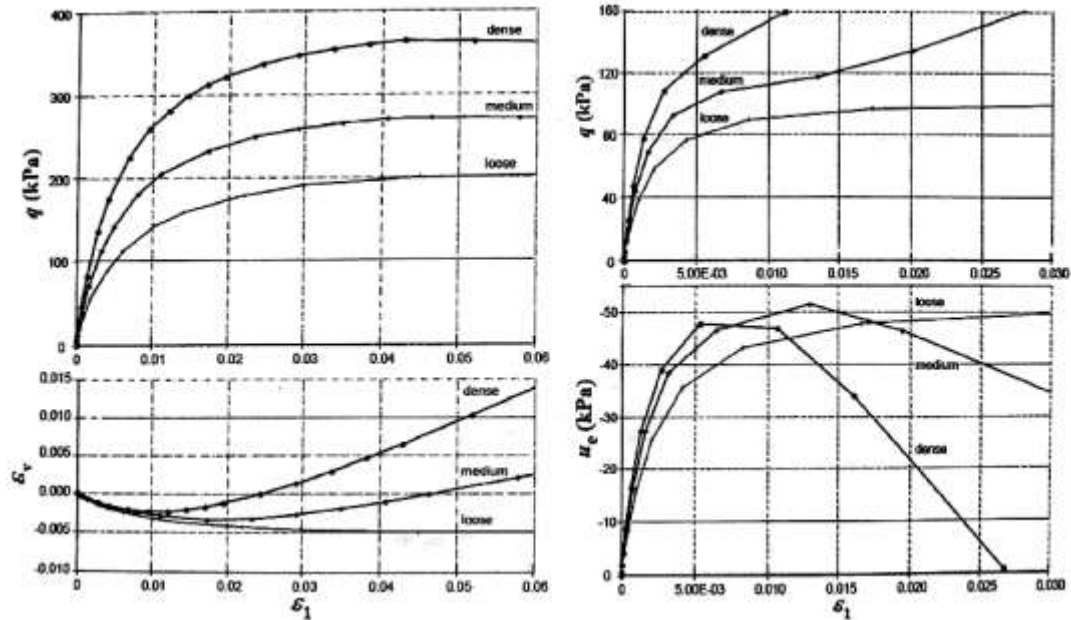


**Figure 2.10. CIU-TXC tests with different void ratio samples.**

On the other hand, the confinement will change the resistance value, principally because at high stress conditions, the mineral friction, particle rearrangement and dilatancy process will not be developed, against the pure resistance of grains at shear stress, majorly produce particle breakage, when there is not another possible way of failure, which is lower than the other resistance process (Figure 2.11. Relationship between void ratio and  $\tan(\varphi'_s)$  at different confining pressures in sands samples TXC tests. **(Larsen & Ibsen, 2006)**).

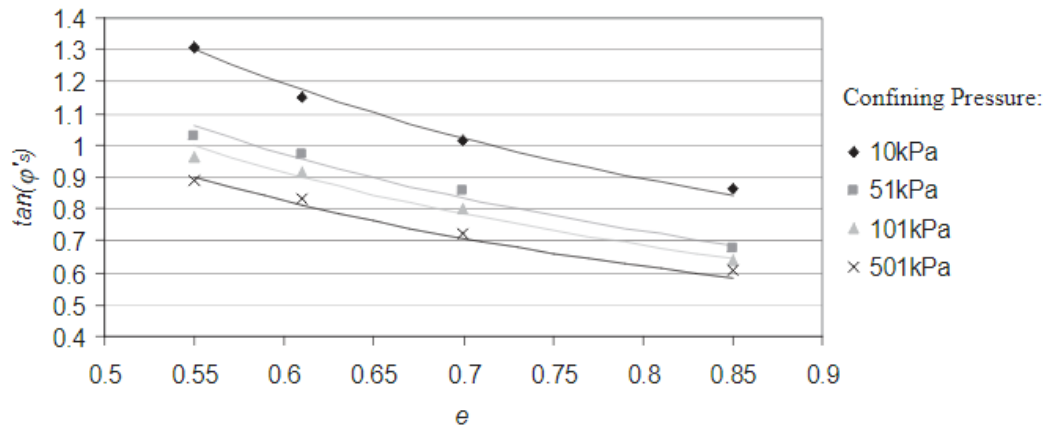


**Figure 2.11. Relationship between void ratio and  $Tan(\varphi'_s)$  at different confining pressures in sands samples TXC tests. (Larsen & Ibsen, 2006)**

In the volumetric section, the definition of critical void ratio is basic, due it is the pore condition to which a sample tend at failure regardless the density, and at this point, the definition of “loose” or “dense” depends only of void ratio, not of density of soil.

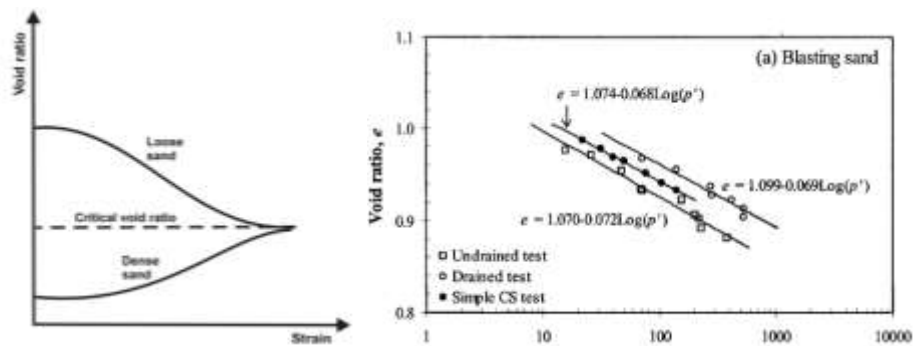


**Figure 2.12. Critical void ratio and critical state line in a TXC-CIU, TXC-CID and Simple CD test (Roscoe & Burland, 1970).**

At the end of this section, the definition of critical state failure statement, will considered not just a constant deviatoric stress and volumetric strain as shows in the Figure 2.13. Critical state definition (**Roscoe & Burland, 1970**), also as the achievement of a critical void ratio, because it will be independent mechanical and volumetric state of stress loading.

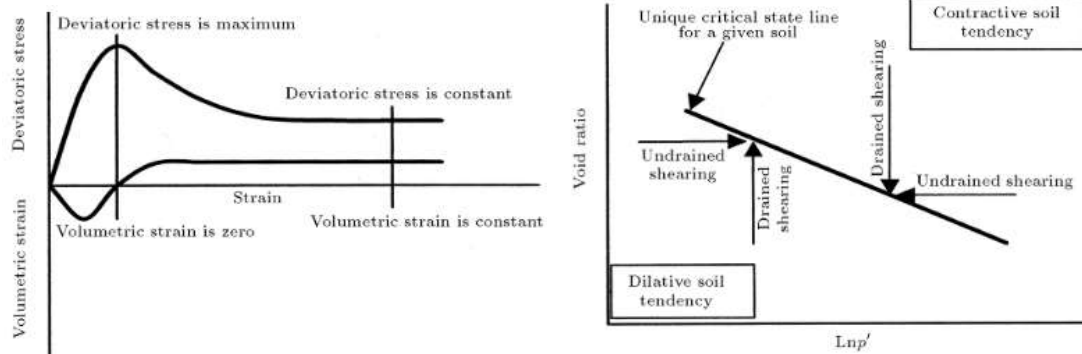


**Figure 2.13. Critical state definition (Roscoe & Burland, 1970).**

### Cyclic triaxial test.

An approximation to explain the behavior of soil through elasto-plastic constitutive model, requires a sore type of calibration, not just for the static loading process, but the cyclic and hysteretic loading process that allows to know the response at different strain – stress level, and it becomes a higher relevance when the phenomena to study is detonated by a cyclic loading conditions as liquefaction is.

A way to compare to type of data results, in this case experimental and simulation results and to obtain an objective conclusion is using a residual value, to quantify the capability of the numerical simulation in capturing the dynamic response of the constitutive model used. A positive residual indicates that numerical prediction underestimated experimental observations (Karimi, Z. and dashti, 2015). Residual value is defined as:

$$\text{Residual } X = \log \left( \frac{X_{\text{experimental}}}{X_{\text{numerical result}}} \right)$$

Now, to obtain experimental results, a cyclic triaxial must check these conditions:

- Sample preparation

The soil sample must satisfy a height and a diameter length (around 30cm and 15 cm respectively), this to secure that tilting and buckling will not occur (the failure of the sample must be a shear failure) for the sake of the determination of shear strength parameters. Additionally, the sample must be or saturated or not saturated, and consolidated or not consolidated (isotropic or  $K_0$  consolidated) before the failure process begins (Campos Sigüenza, 1992).

La información presentada en este documento es de exclusiva responsabilidad de los autores y no compromete a la EIA.

- Loading and unloading cycles execution.

The different load periods as the magnitude of this ones must be considerate in function of the purpose of the test, as accelerogram scale in function of the spectral response of the structures around the soil to study. This values will determinate the shape of the hysterical curves (Campos Sigüenza, 1992).

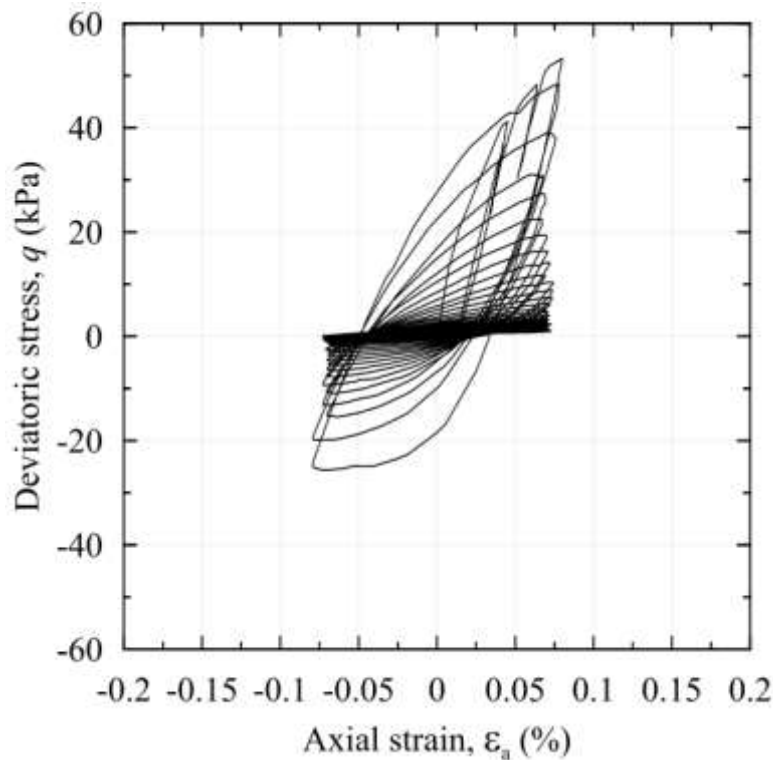


**Figure 2.14. Hysteretic curves from a cyclic triaxial test with a strain control.**

Potential of liquefaction in a soil due stress conditions.

Usually the potential of liquefaction is express in function of excess pore pressure ratio, where the initial vertical effective stress is comparted with the same value at different time in the loading process, when must the time this process is generated by earthquakes. When this parameter achieves values around 0.6 or 0.7, the loss of bearing capacity product of a decreasing of shear strength (loss of contact and normal forces between the grains) will create a deformation produce by it is own weight or loads that coming from structures foundations (Wu, Kammerer, Riemer, Seed, & Pestana, 2004). At next the  $r_u$  formulation is show.

La información presentada en este documento es de exclusiva responsabilidad de los autores y no compromete a la EIA.

$$r_u = 1 - \left( \frac{\sigma'_v}{\sigma'_{v0}} \right)$$

Where

$\sigma'_v$  is the variable in time vertical effective stress.

$\sigma'_{v0}$  is the initial vertical effective stress.

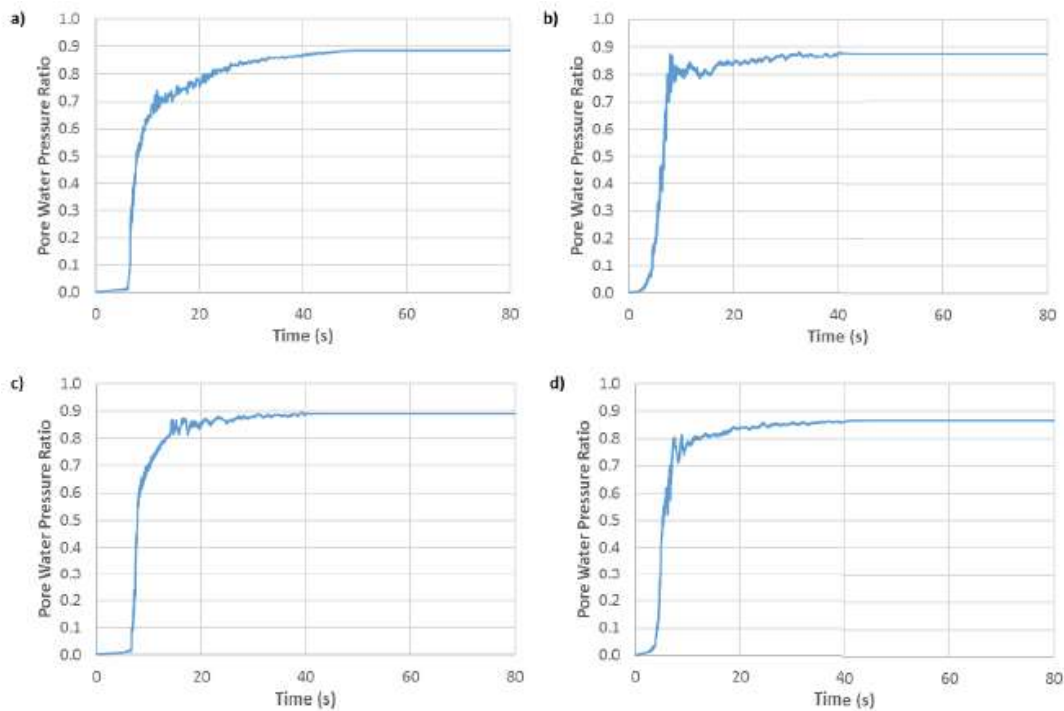


**Figure 2.15. Variation in the  $r_u$  value during cyclic loading process (Whittier 1989, Loma Prieta 1989, Imperial Valley 1979 y Loma Prieta 1989 earthquakes respectively) (Mercado Martínez Aparicio, 2016)**

#### Pseudo-elastic constitutive models for liquefaction

To select a constitutive model, it must be based in the capability to reproduce not just the nonlinear mechanic behavior of soils, so the loss of shear strength due increase of pore pressure, in a critical state and with a direct relationship with confinement, which allow capture excess pore pressure under monotonic or cyclic process loading.

La información presentada en este documento es de exclusiva responsabilidad de los autores y no compromete a la EIA.

One of these models that satisfies these conditions is the PDMY02, developed by professor Ahmed Elgamal (Elgamal et al., 2002), based in multy yield plastic failure surfaces, where the failure criteria is defined by these conic surfaces, where the dilatancy and contraction behaviors is associated directly with the shear strain (Karimi & Dashti, 2016).

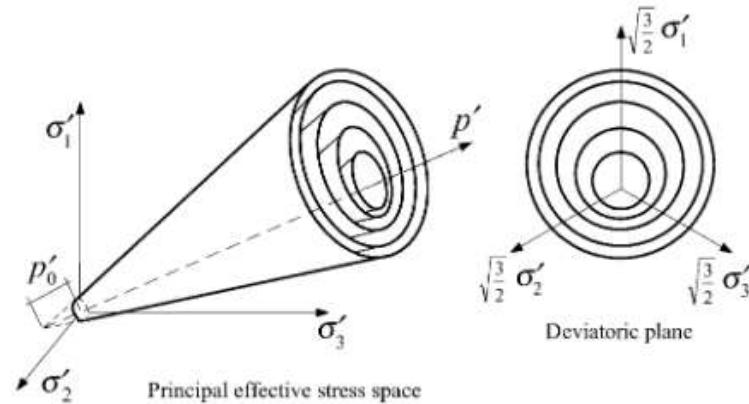


**Figure 2.16 Conic yield surfaces in a principal state of stress and deviatoric plane stress.** (Elgamal et al., 2002)

The flow rule that govern the model is a non-associative rule, where the parametrization is described for two phases:

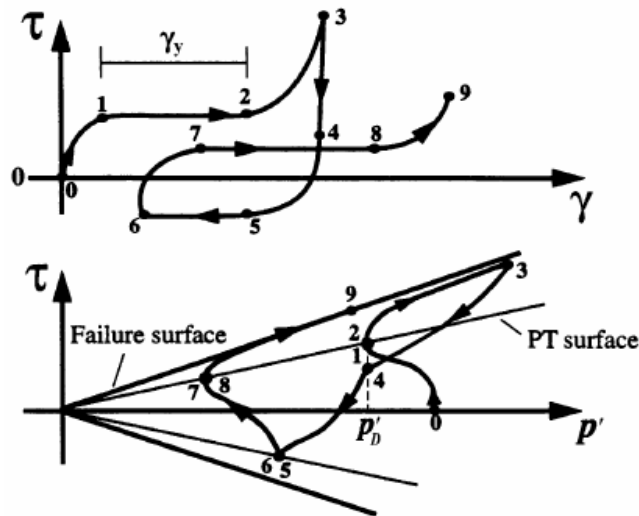


**Figure 2.17 Lateral strains Vs Shear Stress and effective mean stress Vs Shear stress response of PDMY02 model.** (Lu, 2006)

Where the contraction process is developed with this formulation:

La información presentada en este documento es de exclusiva responsabilidad de los autores y no compromete a la EIA.



Contraction [ $(\tau < \tau_{PT})$  or  $(\tau > \tau_{PT} \text{ y } \dot{\epsilon} < 0)$ ]

$$P'' = -\left(1 - \frac{\tau}{\tau_{PT}}\right)^2 * (c_1 + \epsilon_c * c_2) * \left(\frac{p' + p'_0}{p_{atm}}\right)^{c_3}$$

Where  $c_1$ ,  $c_2$  and  $c_3$  are model parameters and  $\epsilon_c$  represents the accumulative volumetric strain (positive for dilatancy and negative for contraction). The term  $\epsilon_c * c_2$  indicates the fabric damage where a high dilatancy generates a high rate of contraction in the next cycle of loading. (Khosravifar, 2013)

Dilatancy [ $(\tau > \tau_{PT} \text{ y } \dot{\epsilon} > 0)$ ]

$$P'' = \left(\frac{\tau}{\tau_{PT}} - 1\right)^2 * (d_1 + \gamma_d^{d_2}) * \left(\frac{p' + p'_0}{p_{atm}}\right)^{-d_3}$$

Where  $d_1$ ,  $d_2$  and  $d_3$  are model parameters and  $\gamma_d$  is the accumulated octahedral lateral strain from the beginning of dilatancy cycle, where the dilatancy rate increased by the increase of lateral strain produce this time by a shear stress by cycle (Khosravifar, 2013).

This is directly related with the nonlinear response of the model, that describe a back-bone stress-strain.

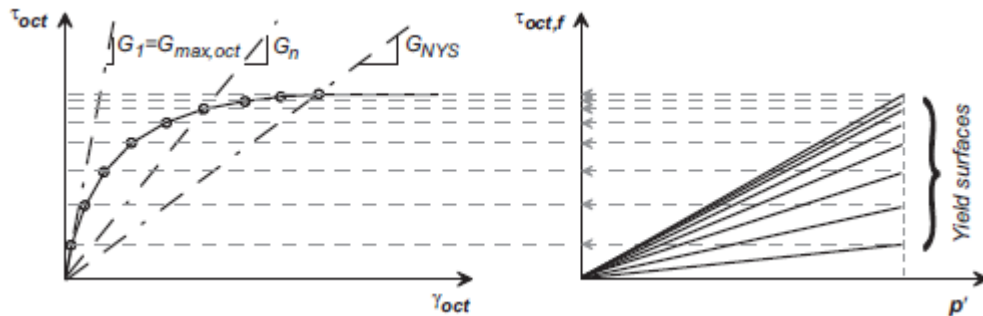


**Figure 2.18 Back-bone stress-strain curve obtained from the yields surfaces.**  
(Khosravifar, 2013)

At next is presented a table which contents a recommended value of all different parameters from the model.

La información presentada en este documento es de exclusiva responsabilidad de los autores y no compromete a la EIA.

**Table 2.2 Recommended parameters per relative density for PDMY02 calibration (Khosravifar, 2013).**

	<b>Dr=30%</b>	<b>Dr=40%</b>	<b>Dr=50%</b>	<b>Dr=60%</b>	<b>Dr=75%</b>
<b>rho (ton/m3)</b>	1.7	1.8	1.9	2	2.1
<b>refShearModul (kPa, at p'r=80 kPa)</b>	6x104	9x104	10x104	11x104	13x104
<b>refBulkModu (kPa, at p'r=80 kPa)</b>	16x104	22x104	23.3x104	24x104	26x104
	(K0=0.5)	(K0=0.47)	(K0=0.45)	(K0=0.43)	(K0=0.4)
<b>frictionAng (°)</b>	31	32	33.5	35	36.5
<b>PTAng (°)</b>	31	26	25.5	26	26
<b>peakShearStra (at p'r=101 kPa)</b>	0.1				
<b>refPress (p'r, kPa)</b>	101				
<b>pressDependCoe</b>	0.5				
<b>C1,C2</b>	0.087	0.067	0.045	0.028	0.013
<b>C3</b>	0.18	0.23	0.15	0.05	0
<b>d1,d2</b>	0	0.06	0.06	0.1	0.3
<b>d3</b>	0	0.27	0.15	0.05	0
<b>e</b>	0.85	0.77	0.7	0.65	0.55

La información presentada en este documento es de exclusiva responsabilidad de los autores y no compromete a la EIA.

### 3. NUMERICAL MODELING OF MONOTONIC AND CYCLIC TRIAXIAL TESTS ON SANDS

The main objective of this investigation is determine if this constitutive model (PDMY02) reproduces the mechanical and volumetric response of a liquefaction process on sands soils. In this work, the PMDY02 model and its controlling parameter are calibrated to capture the response of monotonic and cyclic triaxial tests completed as part of the seismic study and testing program conducted in Manta, Ecuador after the earthquake of April 16<sup>th</sup>, 2016. It was a 7.8Mw seismic event that induced liquefaction in both free field and foundation soil supporting 1 and 2 story-floor buildings. For this work, 4 monotonic and 6 cyclic triaxial tests were available. Table 3.3 list the cyclic tests and the employed testing parameters. All the tests were completed with reconstituted samples to target in-situ void ratio and were isotropically reconsolidated..

**Table 3.1 CIU cyclic triaxial test results (Badanagki, 2016).**

Test #	B-value (%)	$p'$ (kPa)	$D_r$ (%)	$\Delta$ (mm)	$\varepsilon$ (%)	$\gamma$ (%)	No. of cycles to reach $r_v=0.99$	$q_{max}$ (kPa)	CSR	$f$ (Hz)
1	97.5	100	31	0.10	0.070	0.105	20	53.27	0.346	1
2	99.5	100	33	0.40	0.286	0.429	3	59.76	0.388	1
3	98.0	100	34	0.25	0.179	0.2685	7	56.80	0.369	1
4	99.6	100	87	0.10	0.070	0.105	236	72.00	0.468	1
5	99.1	100	84	0.35	0.250	0.375	26	109.32	0.711	1
6	97.0	100	86	0.68	0.486	0.729	5	152.00	0.988	1

Initially, the constitutive model is calibrated against monotonic triaxial tests under drained and undrained conditions. As described previously, the parameter to determine the result approximation is residual values, the same process is used for cyclic results. The principal parameters that control the stress-strain response during monotonic loading are the ones related to the stiffness. They are chosen based on the relative density of the samples. Once the model is calibrated against the monotonic test results and correctly describe the backbone stress-strain curve, a sensibility analysis is made to try to understand the individual response of each parameter of PDMY02 constitutive model, where the objective is to know the effect of parameters principally on the degradation of stiffness, the accumulation of pore water pressure and loss of bearing capacity.

After this process, a manual optimization is propose to get a set of parameters that allow capture the mechanical response of each cyclic test in an individual way, secondly is checked if each set of parameters is capable to capture the response of other ones cyclic

test, but with a poor response to get at the same time a good approximation with a single set of parameters for all six tests, an average set over each parameter is adjusted to reproduce the cyclic triaxial responses for samples with similar relative densities. In this calibration stage the contraction and dilatancy parameters ( $c_1, c_2, c_3$  and  $d, d_2, d_3$ ) are adjusted to better reproduced the mechanical and volumetric responses.

### 3.1 PDMY 02 CONSTITUTIVE MODEL

#### Formulation

The PDMY 02 model is plasticity model formulation based on multi-yield surface methodology, which ones have conical shape (into a 3D stress space). The last surface defines the failure criteria and internal surfaces (n number of surface) define the hardening space, as show in the Figure 2.18 Back-bone stress-strain curve obtained from the yields surfaces. **(Khosravifar, 2013)**.

#### Yield function

Based into the classical plasticity convention, where elasticity is due a linear and an isotropic response, and the plasticity comes from the nonlinearity an inherent and induced anisotropy (Hill, 1950). The yield surfaces, taken into consideration the previous idea, are defined in J2 yield surface formulation (second invariant). The formulation is at next:

$$\tilde{\sigma}' = \begin{bmatrix} \sigma'_{11} & \sigma_{12} & \sigma_{13} \\ \sigma_{21} & \sigma'_{22} & \sigma_{23} \\ \sigma_{31} & \sigma_{32} & \sigma'_{33} \end{bmatrix} = \begin{bmatrix} \sigma'_1 & 0 & 0 \\ 0 & \sigma'_2 & 0 \\ 0 & 0 & \sigma'_3 \end{bmatrix}$$

$$I_1 = tr(\tilde{\sigma}'), \quad I_2 = \frac{1}{2}(\tilde{\sigma}' : \tilde{\sigma}' - tr(\tilde{\sigma}')^2), \quad I_3 = det(\tilde{\sigma}')$$

Volumetric (mean effective stress) and deviatoric stress are defined as:

$$p' = \frac{\sigma'_1 + \sigma'_2 + \sigma'_3}{3}, \quad \tilde{s} = \tilde{\sigma}' - p'\tilde{I} = \begin{bmatrix} \sigma'_{11} - p' & \sigma_{12} & \sigma_{13} \\ \sigma_{21} & \sigma'_{22} - p' & \sigma_{23} \\ \sigma_{31} & \sigma_{32} & \sigma'_{33} - p' \end{bmatrix}$$

Deviatoric stress invariant are defined as:

$$J_1 = tr(\tilde{s}) = 0$$

$$J_2 = \frac{1}{2}(\tilde{s} : \tilde{s} - tr(\tilde{s})^2) = \frac{1}{2}(\tilde{s} : \tilde{s})$$

La información presentada en este documento es de exclusiva responsabilidad de los autores y no compromete a la EIA.

$$J_3 = \det(\tilde{s})$$

Now, the yield surface is defined by equaling the second invariant to a constant:

$$J_2 = \frac{M^2 p'^2}{3}$$

Where  $M$  is the slope of  $p'$ - $q$  stress space failure line, then we get:

$$\frac{3}{2}(\tilde{s} : \tilde{s}) - M^2 p'^2 = 0$$

With an  $\alpha$  that is a second order deviatoric tensor, which one defines the center of the yield surface in a deviatoric stress subspace, we get:

$$f = \frac{3}{2}(\tilde{s} - p' \tilde{\alpha}) : (\tilde{s} - p' \tilde{\alpha}) - M^2 p'^2 = 0$$

On the other hand, assuming a small cohesion at zero confining pressure, the apex of conical shape moves towards negative confining pressure ( $p'_{ref}$ ). If no cohesion is used, to not get numerical problems and ambiguity in defining the normal vector to yield surface, the value will be a small constant (0.01kPa) (Khosravifar, 2013).

$$f = \frac{3}{2}(\tilde{s} - (p' + p'_{ref}) \tilde{\alpha}) : (\tilde{s} - (p' + p'_{ref}) \tilde{\alpha}) - M^2 (p' + p'_{ref})^2 = 0$$

Hardening rule

The model considerate a deviatoric kinematic hardening rule, that allows to generate hysteretic response (stiffness degradation and irrecoverable deformations) due cyclic shear loadings (Elgamal et al., 2002), which implies the yielding surfaces will move in stress space within the failure surface.

Flow rule

Due a necessity to control the volumetric strains, the use of a non-associative flow rule becomes crucial to reduce the overpredicted response on those strains. It is divided into a deviatoric and volumetric components:

$$\tilde{Q} = \tilde{Q}' + Q'' \tilde{I}$$

And

$$\tilde{P} = \tilde{P}' + P'' \tilde{I}$$

La información presentada en este documento es de exclusiva responsabilidad de los autores y no compromete a la EIA.

Where  $\tilde{Q}$  and  $\tilde{P}$  are the deviatoric components of the normal vector to yield surface and plastic potential surface respectively.  $Q'' \tilde{I}$  and  $P'' \tilde{I}$  are volumetric components respectively. Product of non – associative proposal,  $Q'' \neq P''$  (Khosravifar, 2013).

Now, to define the volumetric component of plastic potential surface, we invoke the previous equations showed in Pseudo-elastic constitutive models for liquefaction topic, where in function of a new variable (Phase Transformation angle PT) and the actual stress state of soil, the definition of change around volumetric parameters will be due contraction or dilation phenomena.

### **3.2 SSPBRICKUP ELEMENT**

Because of necessity not just to obtain the total stresses and strains, but to get the effective response of soil (effective stresses, pore water pressure and excess pore water pressure) to characterize the liquefaction phenomena (and post liquefaction soil behavior too), in the FEM numerical simulations, the element will need to provide this information, and it need to be fully coupled element, to considerate not just the effects over the soil, but the water if it exists in the analysis. That is the main reason to use the SSPbrickUP element, for use in dynamic 3D of fluid-soil interaction analysis (“SSPbrickUP Element,” 2017), where a mixed displacement-pressure formulation is used (Zienkiewicz & Shiomi, 1984).

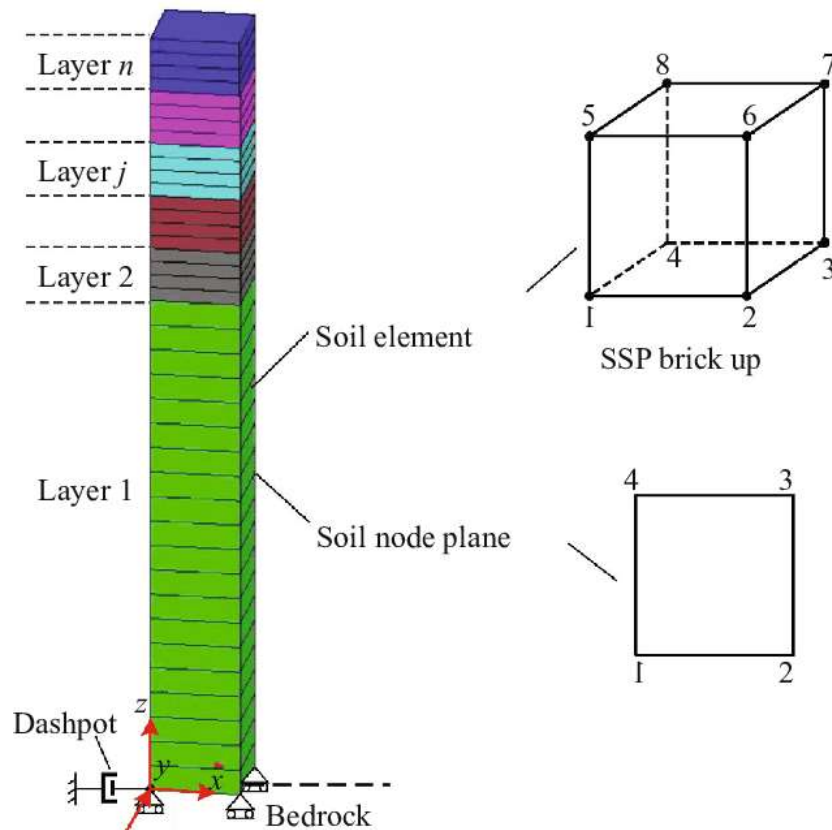


**Figure 3.1 Illustration of SSP brickUP element (in a column of soil and individual shape) (Fayun, Haibing, & Maosong, 2017).**

An equal order interpolation for displacement and pressure calculation, thus the element does not pass the inf-sup condition, because of that is not fully acceptable in the limit of use (incompressible-impermeable limit) (“SSPbrickUP Element,” 2017). To stabilize the equal order interpolation, an  $\alpha$  parameter is needed, that follows the next formulation:

$$\alpha = \frac{h^2}{(4 * (Ks + \frac{4}{3}Gs))}$$

Where  $h$  is the height of the element, and  $Ks$  y  $Gs$  are the bulk and shear modulus for the solid phase (“SSPbrickUP Element,” 2017).

Besides this parameter, exists another recommendation of use (“SSPbrickUP Element,” 2017).

1. This element will only work in dynamic analysis,
2. For saturated soils, the mass density should be the saturated mass density.

La información presentada en este documento es de exclusiva responsabilidad de los autores y no compromete a la EIA.

3. Fixing the pore pressure degree of freedom (dof 4) will allow create water pressure (effective stress condition).

### **3.3 NUMERICAL MODEL**

#### **3.3.1 Mesh**

The definition of mesh used to characterize the monotonic and cyclic response is based principally on numerical facility, due to the fact OpenSees requires not just a high computational effort, but the condition of instability properly from elements objects, and because the definition of every single parameter of numerical solution (e.g. integrator method, constrains definitions, type of non-linear equations system solver) increases times and computational cost of modeling. Is because of that a single element is used to captures stress-strain response for every single situation of analysis and considering the reflection of waves as a limitation of this model, as is see it in **Appendix A**, the use of Rayleigh damping is not higher than 2%. The use of a 3D element based on 8 nodes, requires the definition of same quantify, and because of this type of tests (triaxial tests) the layer of soil is not too big (around 0.30m), the own weight of soil will not create significative gravitational stresses, stage that is not evaluated on this project. With that in mind, and because of reduction possible solving problems, the size of element is defined as one meter in all three directions.

#### **3.3.2 Boundary conditions**

About the boundaries and constrain conditions, just a single element (1 of total 8) is fixed against the 3 degrees of freedom (3 displacements DoF's and a pore water pressure DoFs in case of effective conditions). The node fixed is by definition node #1 located in the origin of coordinate system (0,0,0) and the others 3 are just restrained against vertical displacement.

On the other hand, all 4 nodes (the upper nodes) are constrained against vertical displacements, when all of them are subjected to same magnitude and direction of displacement. A diagram of mesh and fixed definition is presented at next.



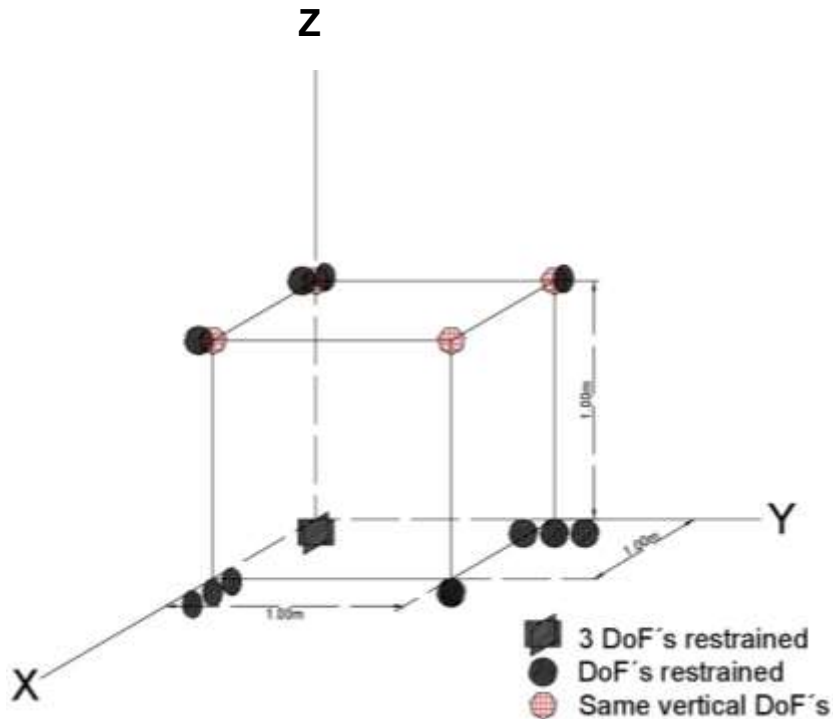


Figure 3.2 Diagram of constraints and fixies of model.

### 3.3.3 Stages of loading

Due to the isotropic consolidation test condition, an initial phase of loading is needed to secure the correct initial stress state at failure stage. With that in mind, a first initial isotropic consolidation is defined, creating a stage of loading applied directly over nodes (for the 3 lower nodes the load is defined in X and Y axis, and in all upper ones the loading is defined in all directions) with the consideration of create a contraction of element (i.e. in case of node 1,0,0 the loadings are defined in a contrary direction of X axis and a positive direction of Y axis). The magnitude of this loads is product of confinement reached in the lab test multiplied by  $0.25\text{m}^2$  (i.e. if  $p' = 100\text{kPa}$  then the load apply over the node in one direction is 25 kN).

After this initial stage of consolidation, the failure stage for both types of monotonic load comes from a linear strain control process, where the limit of this process of loading is defined by last value of strain-strain reported in laboratory test (30% of axial strain in both monotonic drained and undrained cases). And for cyclic test, all of them were loaded by a sinusoidal load, where the amplitude is defined by maximum axial strain of each test (view **Table 3.1**) starting with a compression stage and with displacement rest over the displacement achieve with consolidation phase.

### 3.4 SOIL BEHAVIOR UNDER MONOTONIC LOADING

For the sake of starting a calibration process, a selection of drained and undrained tests that allow compare the response in terms of capability of capture not just the resistance or stiffness degradation under a monotonic loading, but at the same time the volumetric changes are need it, besides the capability of capture the accumulation of pore water pressure under a single monotonic loading respectively. Now, a group of TXC tests is provided to realize the analysis previously describe, which one comes from the location of Manta, a city of Ecuador that April 16<sup>th</sup> of 2016, was an earthquake who produce a several damages not just the urbane infrastructure, but the port of Manta where in many cases, a liquefaction phenomenon occurred (Nikolaou, Vera-Grunauer, & Gilsanz, 2016).

The soil material corresponds to a stratum of sand (0.00m to 20.00m), classified as a SM (SUCS), provide from *calicata* C7, that ordinary methodologies (factor of safety ratio between CRR and CSR) at this point indicates a potential liquefaction behavior as is show in the next table.

**Table 3.2 Resume of stratigraphy and results of potential of liquefaction perforation P26-C7 Carrillo, J. (2018). Seismic analysis of Manta-Ecuador 2016 earthquake.**

Input Data								Liquefaction Susceptibility
Strat a	Depth (m)	N <sub>SPT</sub>	Clasificati on(USCS)	Fines Conte nt (%)	%W	L.L. (%)	I.P. (%)	FS <sub>11q</sub>
1	0.30							-
2	0.75	19	SM	18	15			-
3	1.20	15	SP-SM	7	6			-
4	1.65	16	SP-SM	7	6			-
5	2.10	10	SP-SM	7	6			0.47
6	2.55	21	SP	5	16			0.82
7	3.00	23	SP	5	16			0.86
8	3.45	12	SP	5	16			0.39
9	3.90	16	SM	22	24			0.59
10	4.35	14	SM	22	24			0.48
11	4.80	11	SM	22	24			0.38
12	5.25	9	SM	20	27			0.32
13	5.85	10	SM	14	22			0.30
14	6.30	48	SM	22	25			>2.00
15	9.00	100	SM	19	25			>2.00
16	12.00	100	SM	19	22			>2.00
17	14.50	100	SP-SM	8	25			>2.00
18	17.00	100	SP-SM	8	27			>2.00
19	19.55	100	SM	15	28			>2.00
20	20.00	56	SM	15	30			>2.00

Because of that condition, a series of triaxial test had be done (2 CID-TXC, 1 CID-TXC and 6 Cyclic TXC) to try to characterize the mechanic response of the potential liquefiable layer.

La información presentada en este documento es de exclusiva responsabilidad de los autores y no compromete a la EIA.

At next, is presented the results of 2 CID-TXC tests, and their corresponding simulations results, where is see that mechanical response, stiffness, volumetric change and resistance can be reached at different level of confinement. The model PDMY02 is capable to reproduce an initial contraction process, follow it by a dilation process. On the other hand, there is a loss of resistance at high values of strain (over 15% of axial strain), that cannot be reproduce.

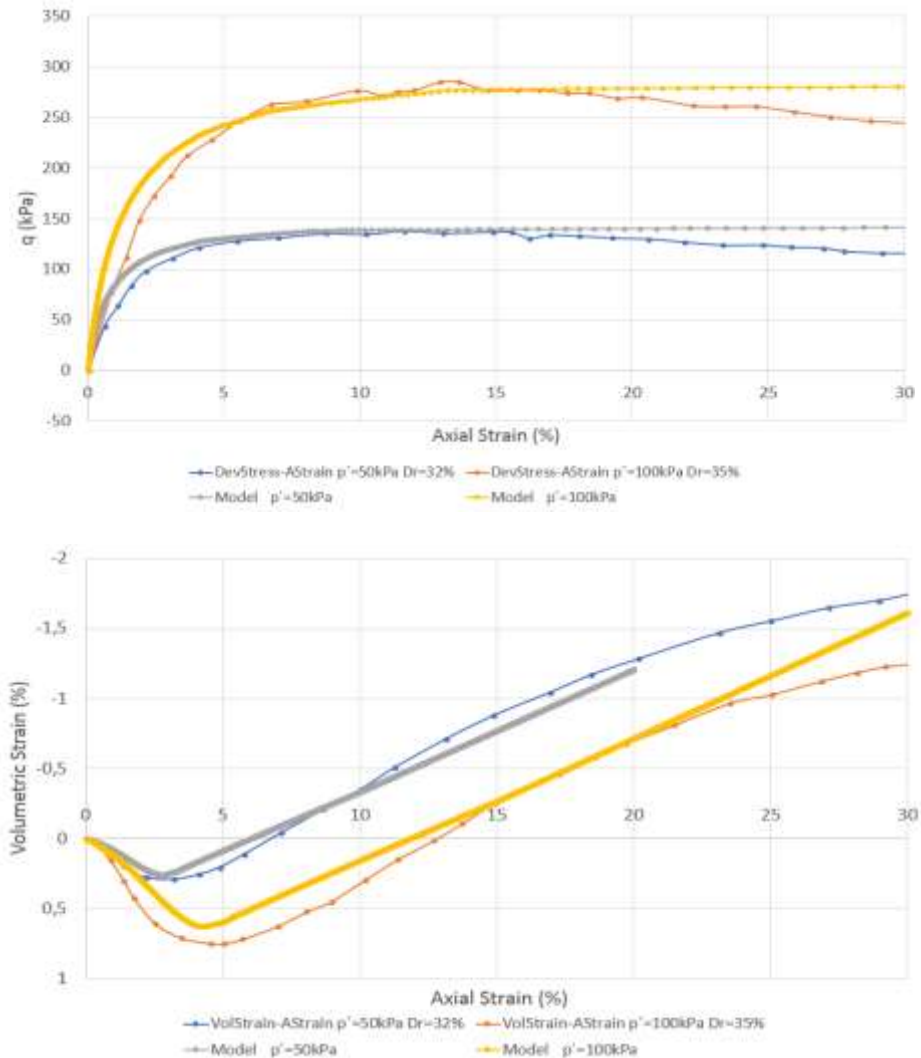


**Figure 3.3 CID-TXC test at different confining, conducted by University of Colorado at Boulder.**

**Table 3.3** shows the soil parameters used for these simulations, that where obtained shear wave velocity for a mean value of 150 m/s.

La información presentada en este documento es de exclusiva responsabilidad de los autores y no compromete a la EIA.

**Table 3.3 PDMY02 model parameters used for CID-TXC simulations (50kPa and 100kPa confining).**

Parameter	Dr=32% to 35% CID Tests
set massDen	1.9
set refG (Mpa)	60000
set refB (Mpa)	180000
set frinctionAng (°)	34.5
set peakShearStrain (%)	0.15
set refPress (kPa)	101
set pressDependCoe (-)	0.5
set phaseTransAng (°)	30
set contractionParam1 (-)	0.06
set contractionParam2 (-)	4
set contractionParam3 (-)	0.21
set dilationParam1 (-)	0.1
set dilationParam2 (-)	3
set dilationParam3 (-)	0.2
set liqParam1 (-)	1
set liqParam2 (-)	0
set noYieldSurf (-)	30
set void (-)	0.74
set cs1 (-)	0.9
set cs2 (-)	0.02
set cs3 (-)	0
set pa (kPa)	101
set c (-)	0.1

Once the drained tests simulations results were obtained, a second process of calibration was done, to reproduce the undrained behavior of the same layer of sand. At first step, the same values of drained simulations were used to try get the experimental, but due the undrained condition, the volumetric and shear modulus had to be increased to get the appropriated response. The results are show at next figures.

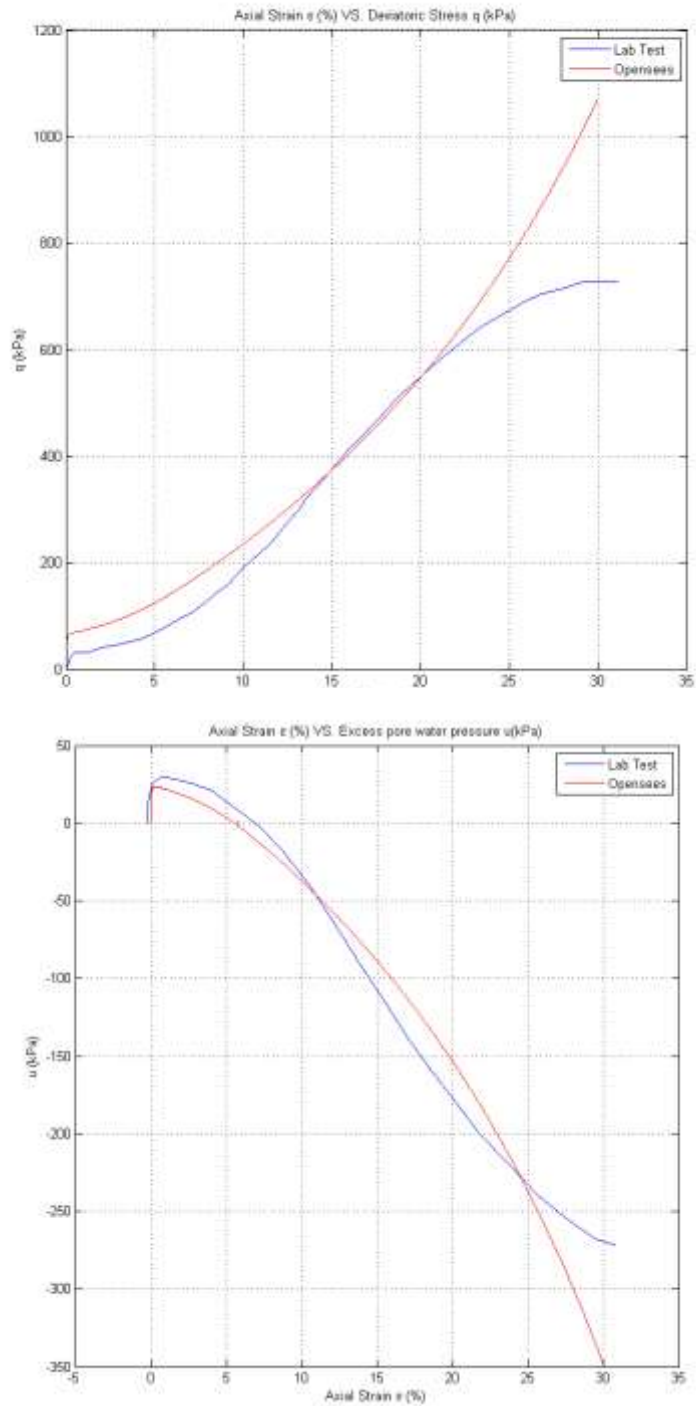


**Figure 3.4 Deviatoric stress and excess pore water pressure (kPa) VS axial strain (%) comparison.**

La información presentada en este documento es de exclusiva responsabilidad de los autores y no compromete a la EIA.

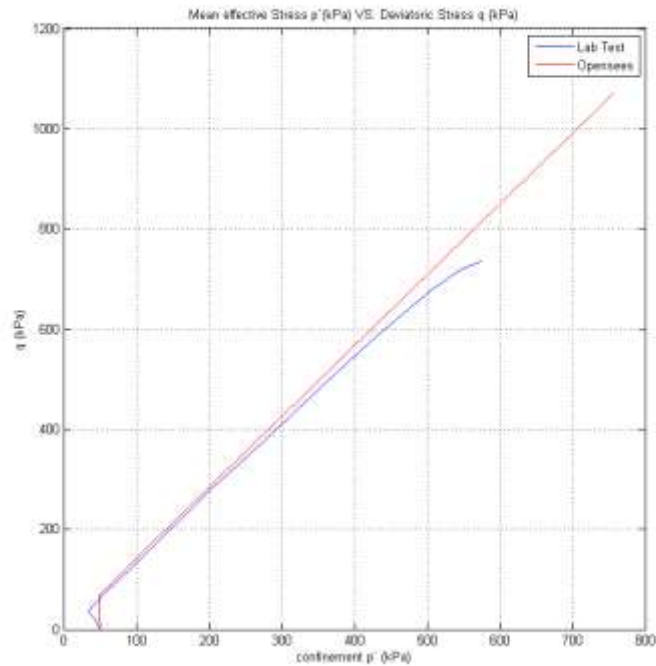


**Figure 3.5 Confinement (kPa) VS Deviatoric stress (kPa) comparison.**

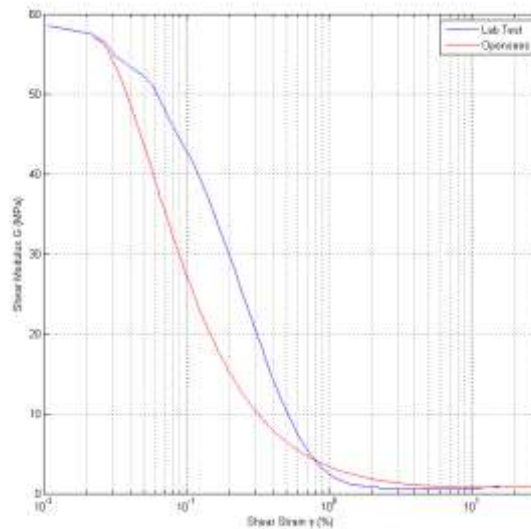


**Figure 3.6 Shear strain (%) VS Shear modulus (MPa) comparison.**

As see it in the **Figure 3.4** and **Figure 3.5**, the tendency is correct for both cases, but a higher value of deviatoric stress indicates the model over predict the bearing capacity of soil, despite the fact exist a higher loss of stiffness at strains levels around 0.01% to 1%, that concludes an underpredict response at lower (0.01% to 1%) deformations and overpredict

La información presentada en este documento es de exclusiva responsabilidad de los autores y no compromete a la EIA.

response at higher deformations (up to 1%). At next is presented the parameters used to simulate the CIU-TXC test, and the variation of parameters respect the CID-TXC tests.

**Table 3.4 Parameters of PDMY02 model used to simulate the CIU-TXC test, and the variation respect the CID-TXC tests.**

Parameter	Dr=32% to 35% CID Tests	Dr=32% to 35% CIU Tests	Variation CID-CIU Parameters
set massDen	1.9	1.9	0%
set refG (Mpa)	60000	200000	233%
set refB (Mpa)	180000	303000	68%
set frinctionAng (°)	34.5	34.9	1%
set peakShearStrain (%)	0.15	0.15	0%
set refPress (kPa)	101	101	0%
set pressDependCoe (-)	0.5	0.5	0%
set phaseTransAng (°)	30.	31.8	6%
set contractionParam1 (-)	0.06	0.045	-25%
set contractionParam2 (-)	4	5	25%
set contractionParam3 (-)	0.21	0.15	-29%
set dilationParam1 (-)	0.1	0.1	0%
set dilationParam2 (-)	3	3	0%
set dilationParam3 (-)	0.2	0.15	-25%
set liqParam1 (-)	1	1	0%
set liqParam2 (-)	0	0	0%
set noYieldSurf (-)	30	30	0%
set void (-)	0.74	0.7	-5%
set cs1 (-)	0.9	0.9	0%
set cs2 (-)	0.02	0.02	0%
set cs3 (-)	0	0.7	0%
set pa (kPa)	101	101	0%
set c (-)	0.1	0.1	0%

As is see it in **Table 3.4**, the main variation is around the elastic parameters, phase transformation angle and over c1, c2 and c3 parameters, which indicates the high sensibility those parameters over the mechanic response of simulations, thing that is going to be analyze later.

La información presentada en este documento es de exclusiva responsabilidad de los autores y no compromete a la EIA.

### 3.4.1 Sensibility analysis

Known the high variability over all the parameters, because of the effect of them on the predict mechanical response, a sensibility analysis over the parameters that in all the calibrations processes and because the mathematical formulation of plastic potential rule, present evidence of the relevance in the configuration of response in deviatoric as volumetric changes. Because of this, 4 parameters had been selected to be characterize individual over an initial set (set of parameters of test #2).

- Contraction parameter #1

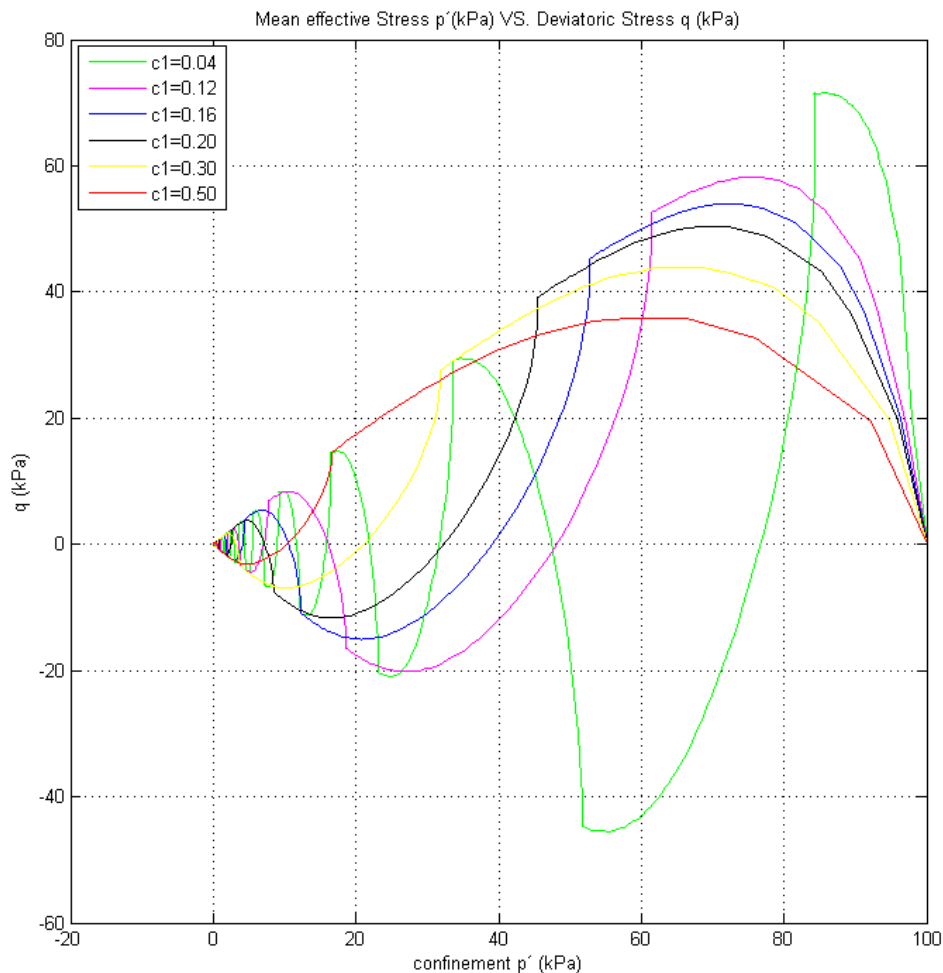


**Figure 3.7 Variation of confinement (kPa) VS deviatoric stress (kPa) with changes over  $c1$  parameter.**



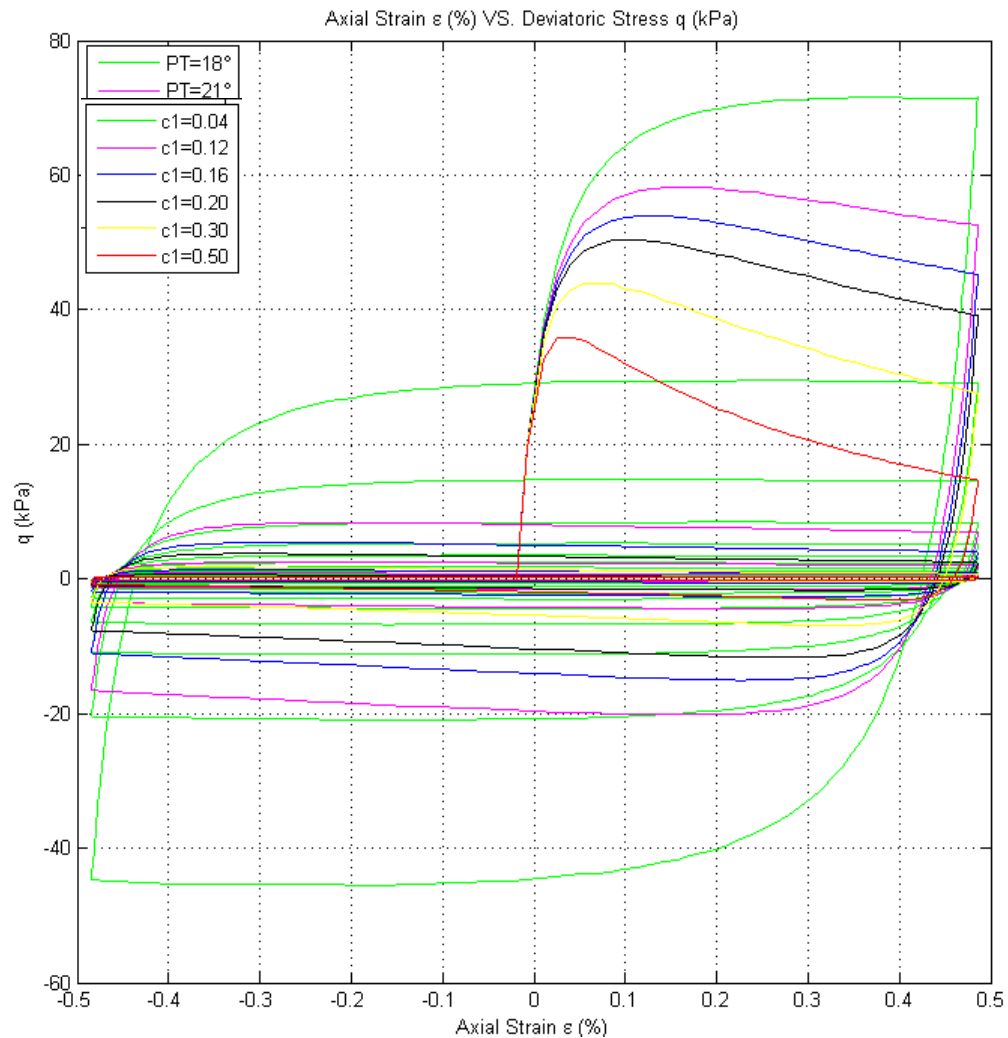


**Figure 3.8 Variation of axial strain (%) VS deviatoric stress (kPa) with changes over c1 parameter.**

As is see it, in the **Figure 3.7** and **Figure 3.8**, when the parameter  $c_1$  increases, the value of deviatoric stress reduces, which indicates a loss of bearing capability and consequently a higher increase in the volumetric strains, as expected because the formulation of plastic potential rule.

- Contraction parameter #3

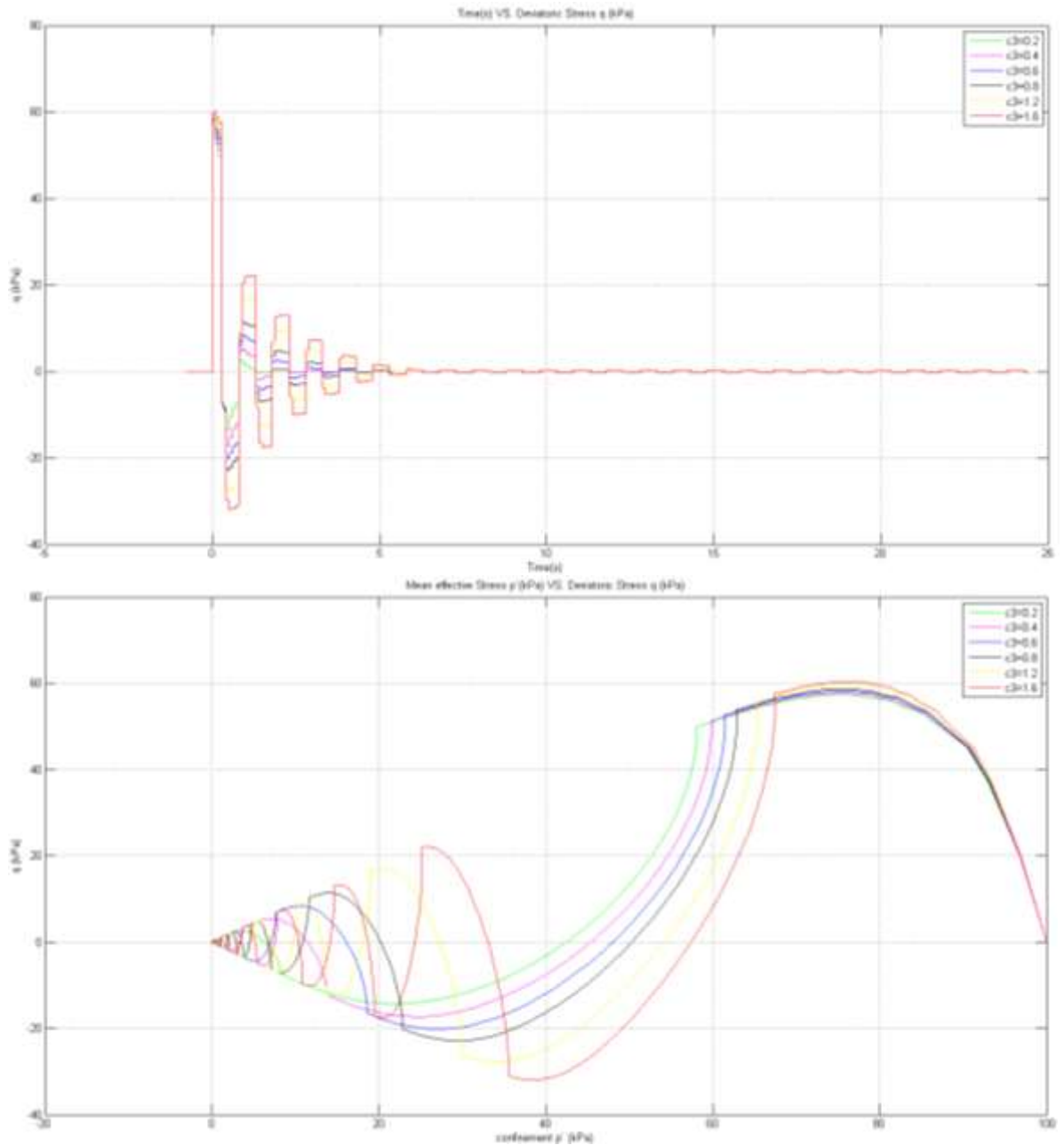


**Figure 3.9 Variation of time (s) VS deviatoric stress (kPa) and confinement (kPa) VS deviatoric stress (kPa) with changes over  $c_3$  parameter.**

La información presentada en este documento es de exclusiva responsabilidad de los autores y no compromete a la EIA.

Taking into consideration the plastic potential function:

$$\tilde{P} = \tilde{P}' + P'' \tilde{I}$$

And the volumetric component:

$$P'' = -\left(1 - \frac{\tau}{\tau_{PT}}\right)^2 * (c_1 + \varepsilon_c * c_2) * \left(\frac{p' + p'_0}{p_{atm}}\right)^{c_3}$$

With low values of  $c_3$  makes the volumetric component minor ( $P''$ ), something that just let the deviatoric component of strain ( $\tilde{P}'$ ), that every time step becomes higher creating a bigger contractive phenomenon, with a direct relation of loss of bearing capacity (a higher potential of liquefaction).

- Dilation parameter #1

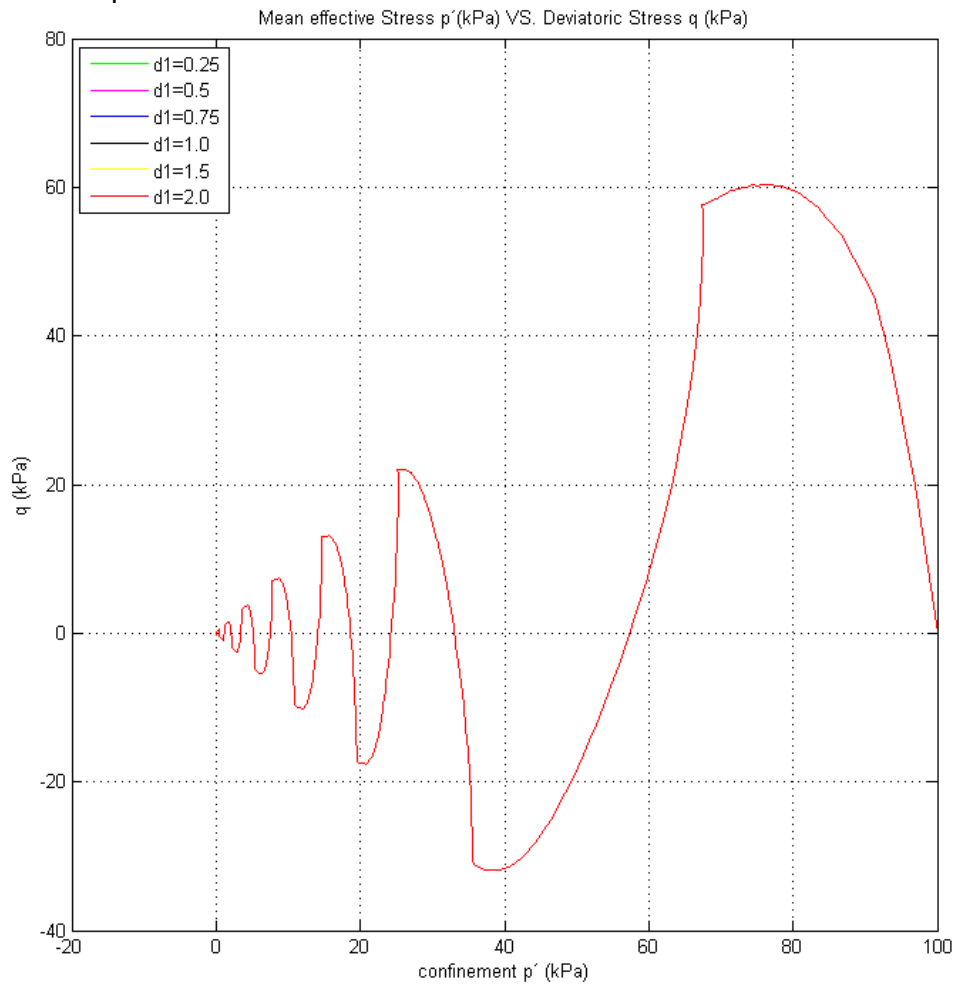


**Figure 3.10 Variation of axial strain (%) VS deviatoric stress (kPa) with changes over d1 parameter.**

La información presentada en este documento es de exclusiva responsabilidad de los autores y no compromete a la EIA.

With the **Figure 3.10**, is identified the fact that dilation parameters do not interfere with the mechanical prediction of model where the response of soil is purely contractive (Phase Transformation Angle > Friction Angle).

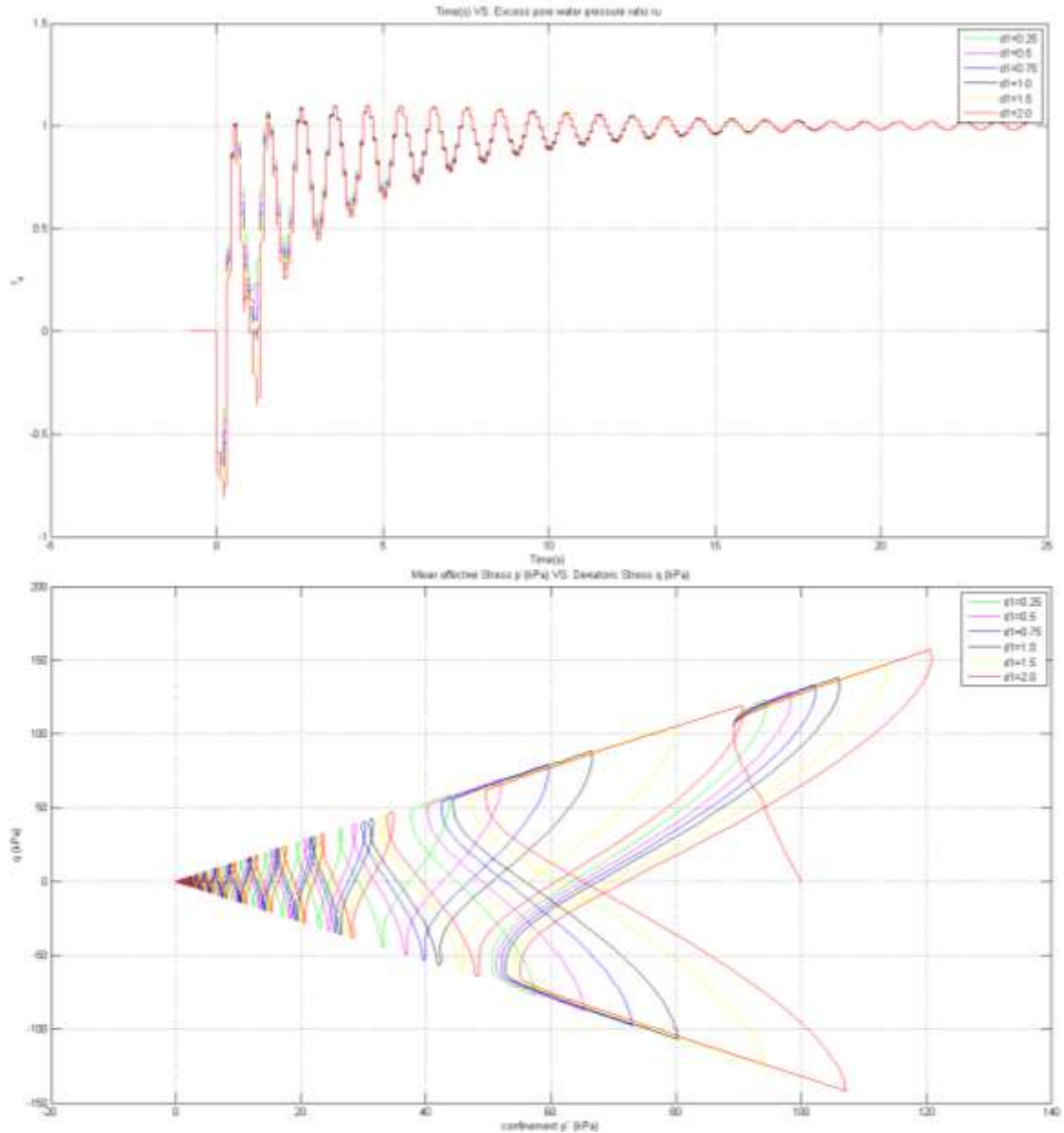


**Figure 3.11 Variation of time (s) VS excess pore water pressure and confinement (kPa) VS deviatoric stress (kPa) with changes over d1 parameter.**

Taking into consideration the plastic potential function:

La información presentada en este documento es de exclusiva responsabilidad de los autores y no compromete a la EIA.

$$\tilde{p} = \tilde{p}' + P'' \tilde{I}$$

And the volumetric term in the dilatancy phase:

$$P'' = \left(\frac{\tau}{\tau_{PT}} - 1\right)^2 * (d_1 + \gamma_d^{d_2}) * \left(\frac{p' + p'_0}{p_{atm}}\right)^{-d_3}$$

A higher value of parameter  $d_1$ , is a direct positive effect over the volumetric changes ( $P''$ ), that will create not just some bigger loops, but allow the possibility of dissipating the excess pore water pressure as see in the **Figure 3.11**.

- Phase transformation angle with constant friction angle ( $23^\circ$ ).

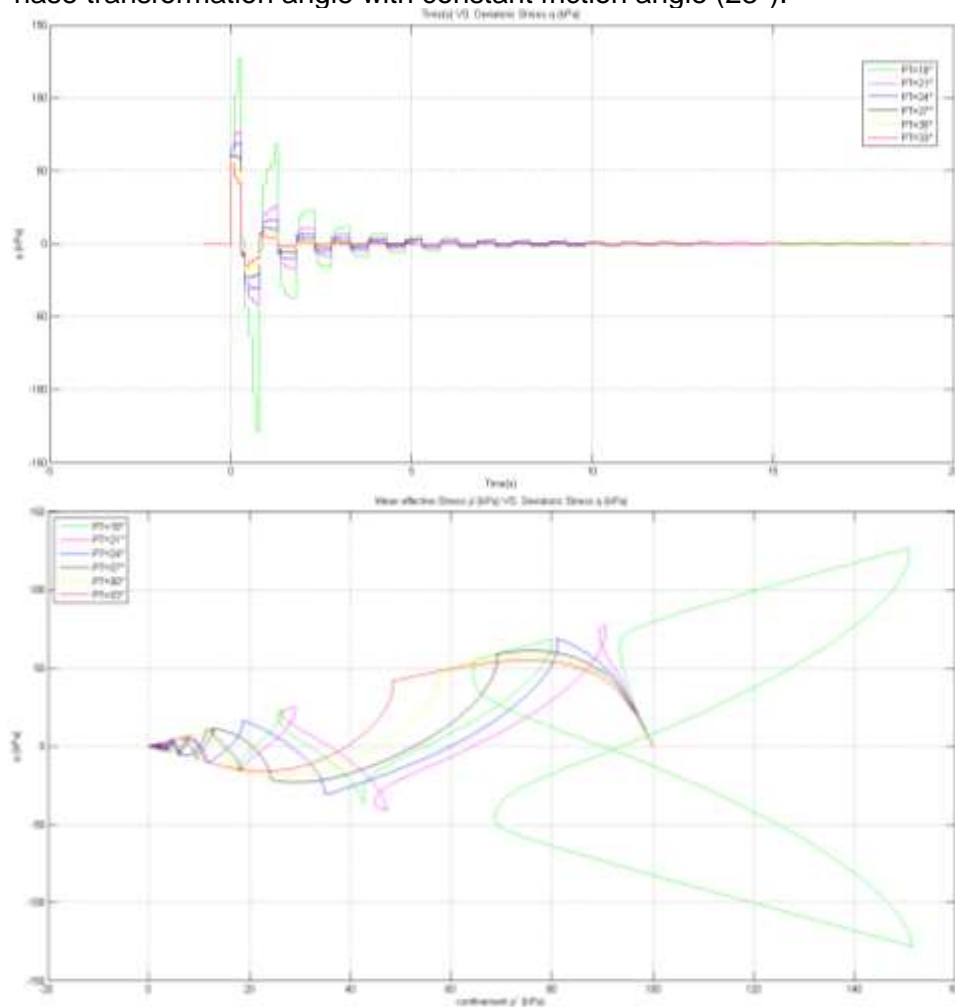


**Figure 3.12** Variation of time (s) VS deviatoric stress (kPa) and confinement (kPa) VS deviatoric stress (kPa) with changes over PT parameter.

La información presentada en este documento es de exclusiva responsabilidad de los autores y no compromete a la EIA.

Around the PT angle exists two responses depending of relation between this parameter and friction angle.

- PT < FA

On these cases, green and magenta lines in the

**Figure 3.12**, invoking the volumetric term of the potential plastic rule:

$$P'' = \left(\frac{\tau}{\tau_{PT}} - 1\right)^2 * (d_1 + \gamma_d^{d_2}) * \left(\frac{p' + p'_0}{p_{atm}}\right)^{-d_3}$$

If a lower PT value is input, then first term  $\left(\frac{\tau}{\tau_{PT}} - 1\right)^2$  will be higher, developing a major positive value of volumetric term, generating a dilatancy phenomenon and higher values of bearing capacity (higher deviatoric stresses).

- PT > FA

On these cases, the other ones in the

**Figure 3.12**, invoking the volumetric term of the potential plastic rule:

$$P'' = -\left(1 - \frac{\tau}{\tau_{PT}}\right)^2 * (c_1 + \varepsilon_c * c_2) * \left(\frac{p' + p'_0}{p_{atm}}\right)^{c_3}$$

If a higher PT value is input, the first term  $\left(1 - \frac{\tau}{\tau_{PT}}\right)^2$  will tend to maximum value of 1 and the volumetric term will be more negative, indicating a contraction phenomenon, an increase of excess of pore water pressure and a loss of bearing capacity (due a loss of deviatoric stress) and a potential liquefaction process will be developed.

### 3.5 SOIL BEHAVIOR UNDER CYCLIC LOADING

After two calibration process and taking into consideration the importance of the cyclic response to predict not just the liquefaction but the post-liquefaction behavior of soil (elements for a performance-based design/analysis), over six cyclic TXC test that had be done over the same sand, for 2 types of relative density and for different levels of control strain, a third calibration process is done, firstly individually and secondly taking a set of parameters for low and high densities.

La información presentada en este documento es de exclusiva responsabilidad de los autores y no compromete a la EIA.

The resume of laboratory work is presented in the **Table 3.1 CIU cyclic triaxial test results (Badanagki, 2016)**.

### 3.5.1 Individual calibration per individual test

The first step is to calibrate every single test in an individual process, taking the CID-TXC test parameters as a start point. At next is presented the results per test.

- **CIU-Cyclic TXC Test #1 strain control ( $\epsilon=0.070\%$ ,  $D_r=31\%$   $p' = 100\text{kPa}$ ).**

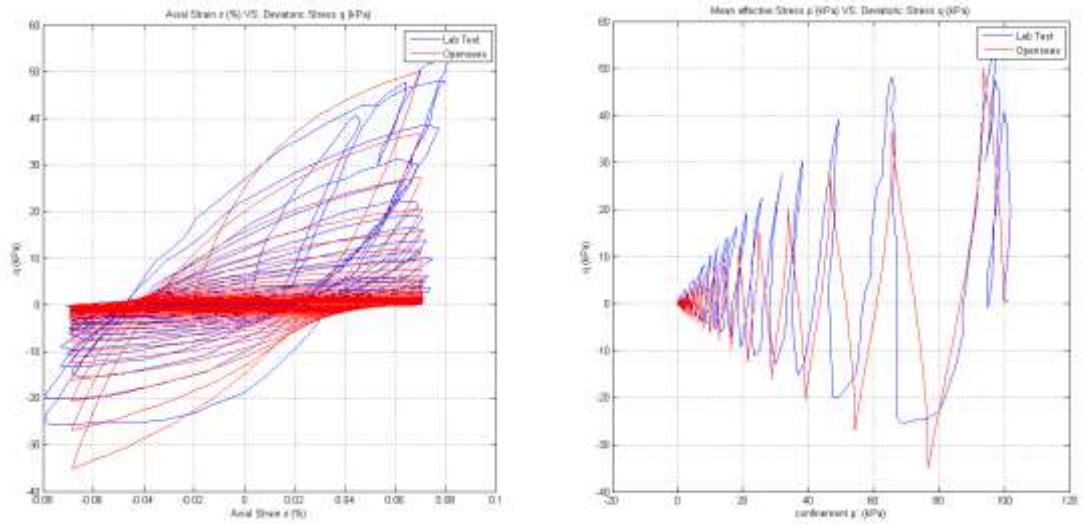


**Figure 3.13 Deviatoric stress (kPa) VS Axial strain (%) and confinement (kPa) respectively Test #1.**

La información presentada en este documento es de exclusiva responsabilidad de los autores y no compromete a la EIA.

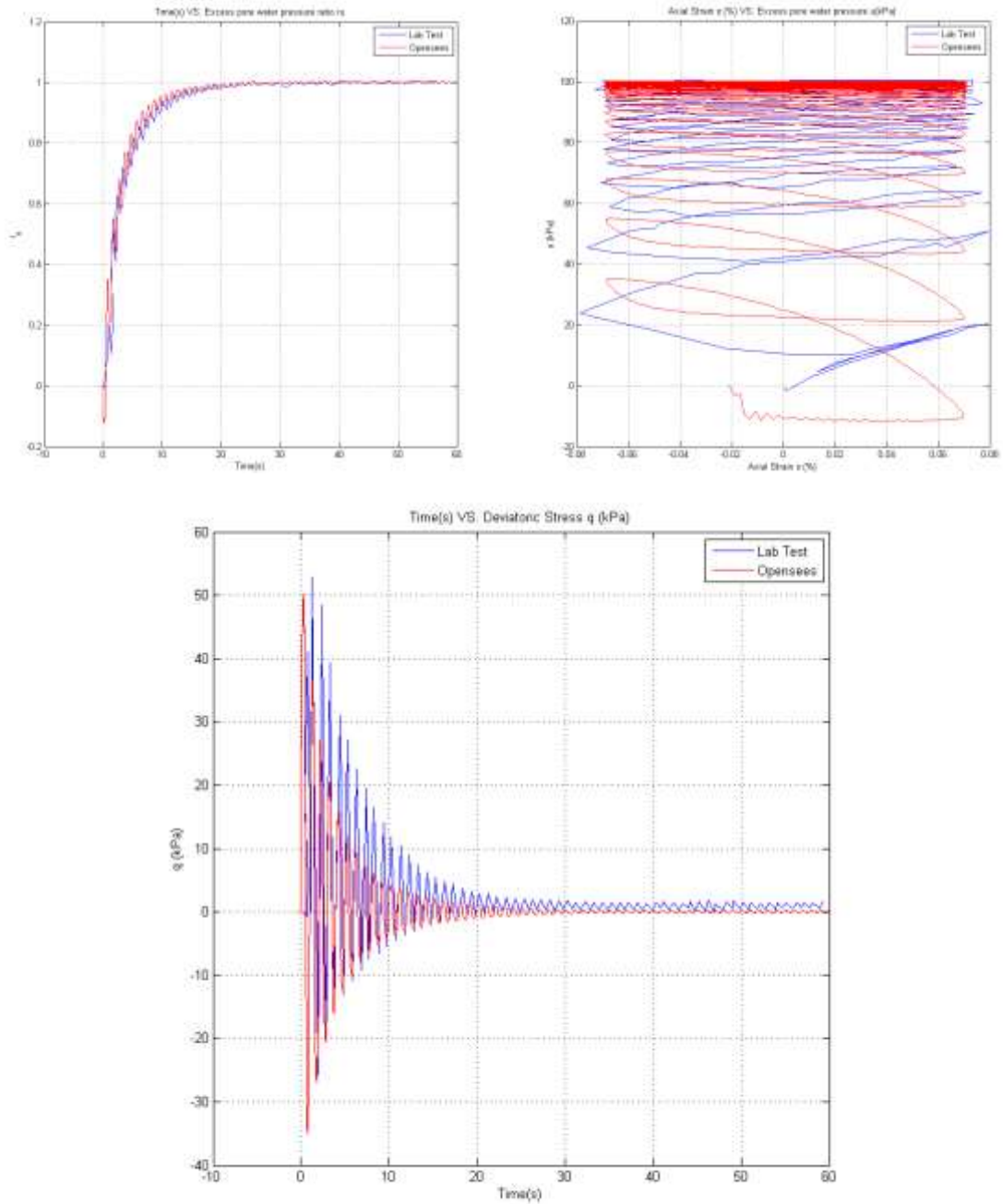


**Figure 3.14  $u$  VS Time (s), Axial Strain (%) VS  $u$  (kPa) and Time (s) VS Deviatoric stress (kPa) respectively Test #1.**

La información presentada en este documento es de exclusiva responsabilidad de los autores y no compromete a la EIA.



As is see it in the **Figure 3.13**, exist a good match for extension loading process, but in the compression part of cycle, and underpredict of deviatoric stress occurs despite the first peak of compression is achieved, and **Figure 3.14** is clearer to see it. At level of pore water accumulation, the model produces an accurate response.

- **CIU-Cyclic TXC Test #2 strain control ( $\epsilon=0.286\%$ ,  $Dr=33\%$   $p' = 100\text{kPa}$ ).**

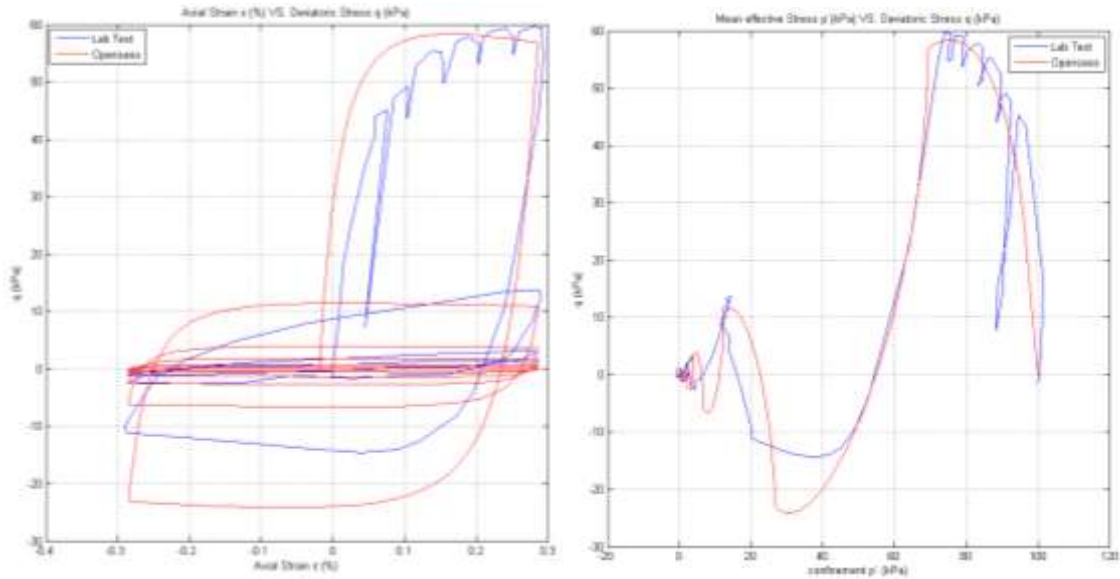


**Figure 3.15 Deviatoric stress (kPa) VS Axial strain (%) and confinement (kPa) respectively Test #2.**

As is show it in the **Figure 3.15**, the overprediction of deviatoric stress occurs in the extension part of cycle. In the **Figure 3.16** is show the accurate match in the generation excess of pore water pressure.

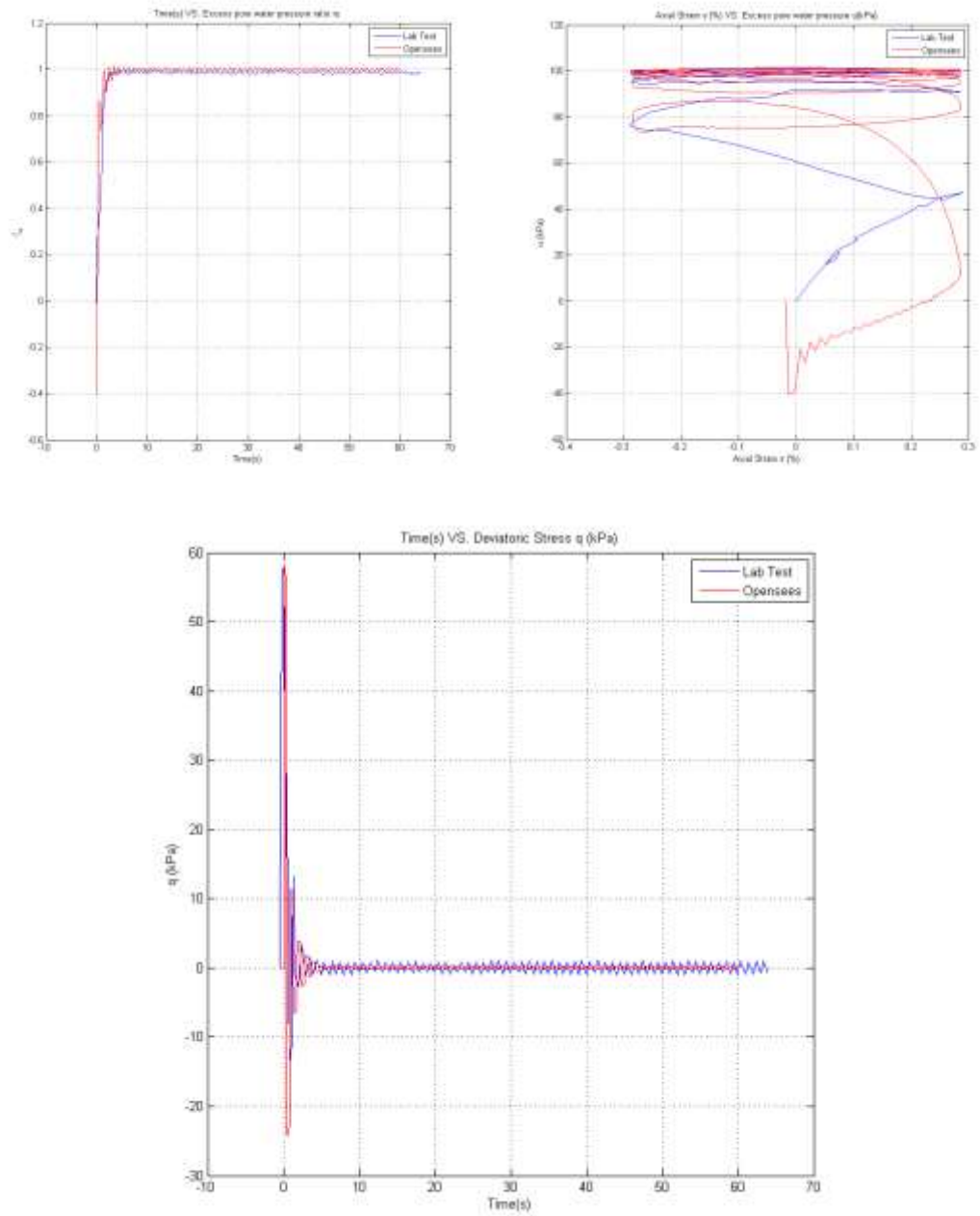


**Figure 3.16  $u$  VS Time (s), Axial Strain (%) VS  $u$  (kPa) and Time (s) VS Deviatoric stress (kPa) respectively Test #2.**

La información presentada en este documento es de exclusiva responsabilidad de los autores y no compromete a la EIA.

- CIU-Cyclic TXC Test #3 strain control ( $\epsilon=0.179\%$ ,  $D_r=34\%$   $p' = 100\text{kPa}$ ).

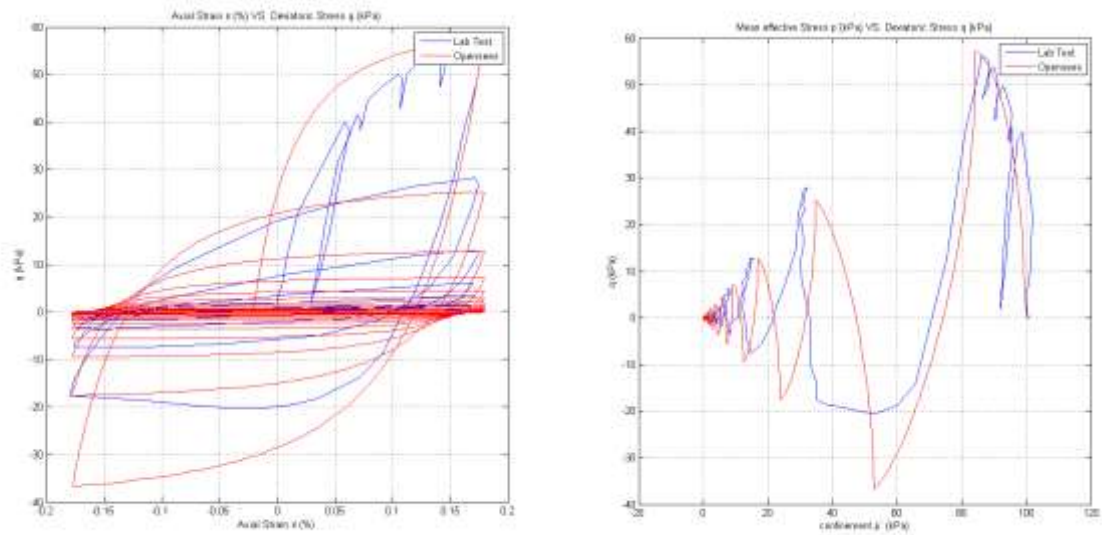


**Figure 3.17 Deviatoric stress (kPa) VS Axial strain (%) and confinement (kPa) respectively Test #3.**

As is show it in the **Figure 3.17**, the overprediction of deviatoric stress occurs in the extension part of cycle, the same pattern that test #2, besides the loss of deviatoric stress is not occurs with the same path in the extension process, something that in the compression part, the match of peaks is more accurate. In the **Figure 3.18** is show the accurate match in the generation excess of pore water pressure.

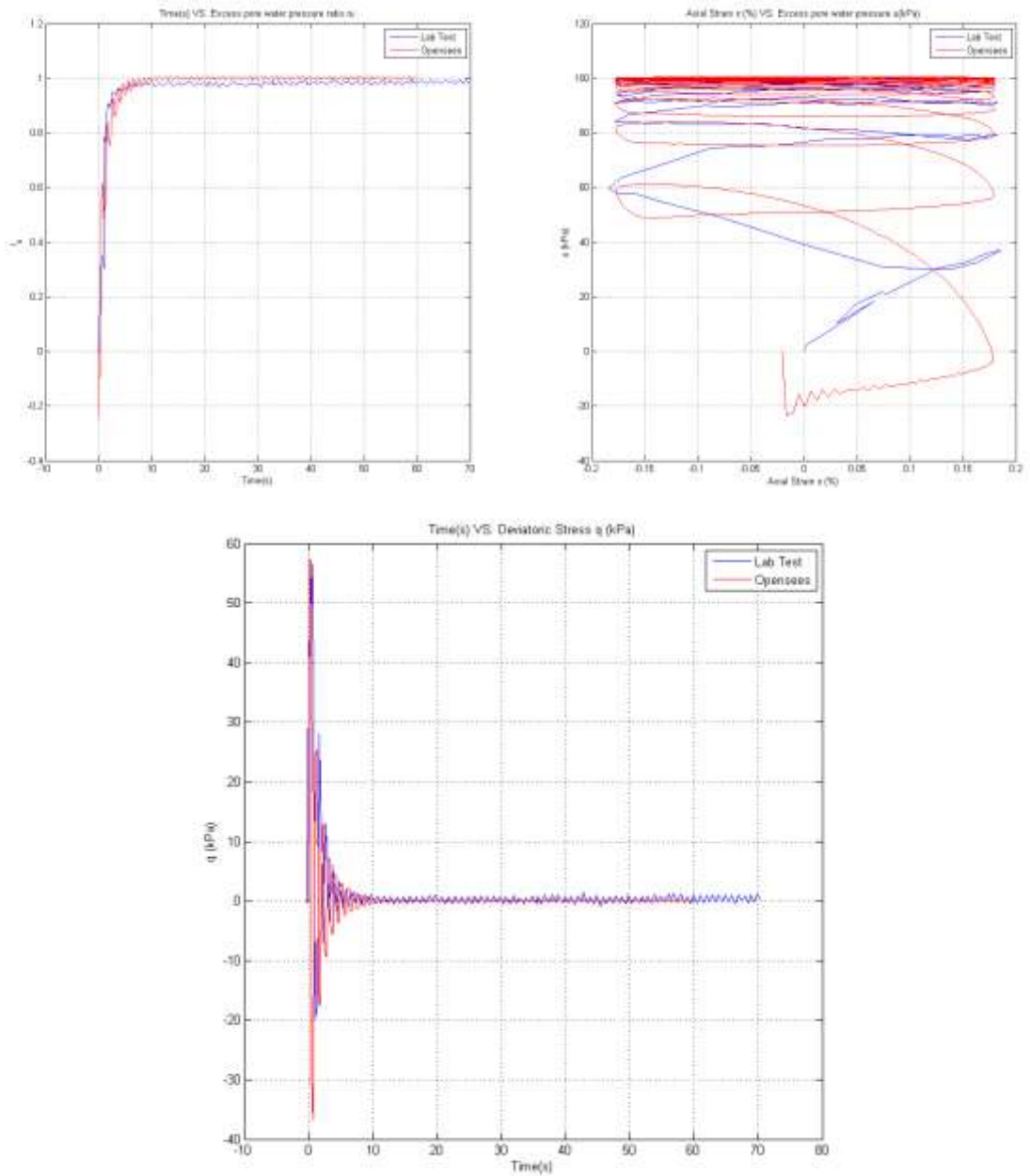


**Figure 3.18  $u$  VS Time (s), Axial Strain (%) VS  $u$  (kPa) and Time (s) VS Deviatoric stress (kPa) respectively Test #3.**

La información presentada en este documento es de exclusiva responsabilidad de los autores y no compromete a la EIA.

- CIU-Cyclic TXC Test #4 strain control ( $\epsilon=0.070\%$ ,  $Dr=87\%$   $p' = 100\text{kPa}$ ).

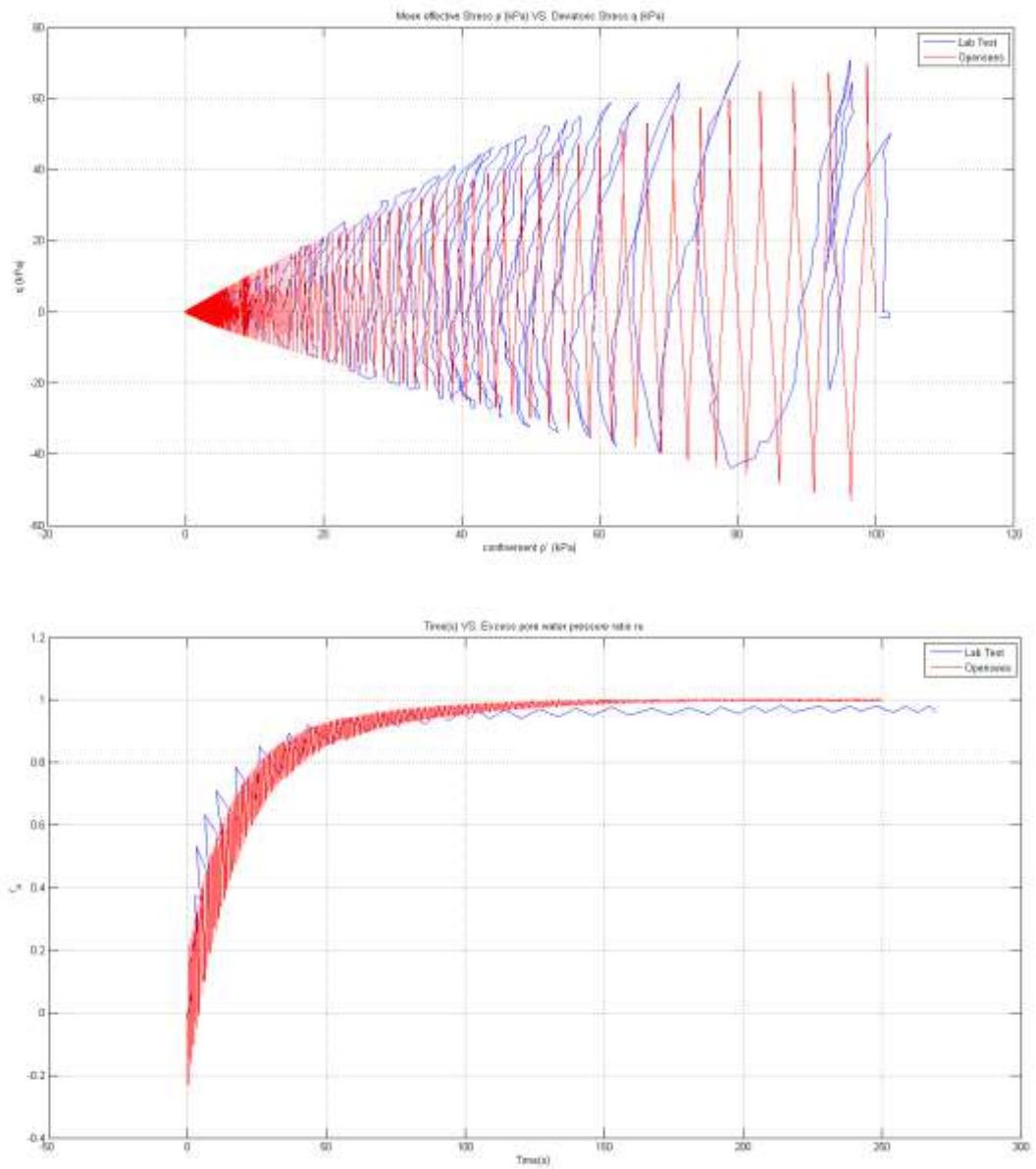


**Figure 3.19 Confinement (kPa) VS Deviatoric Stress (kPa) and ru VS Time (s) respectively Test #4.**

La información presentada en este documento es de exclusiva responsabilidad de los autores y no compromete a la EIA.

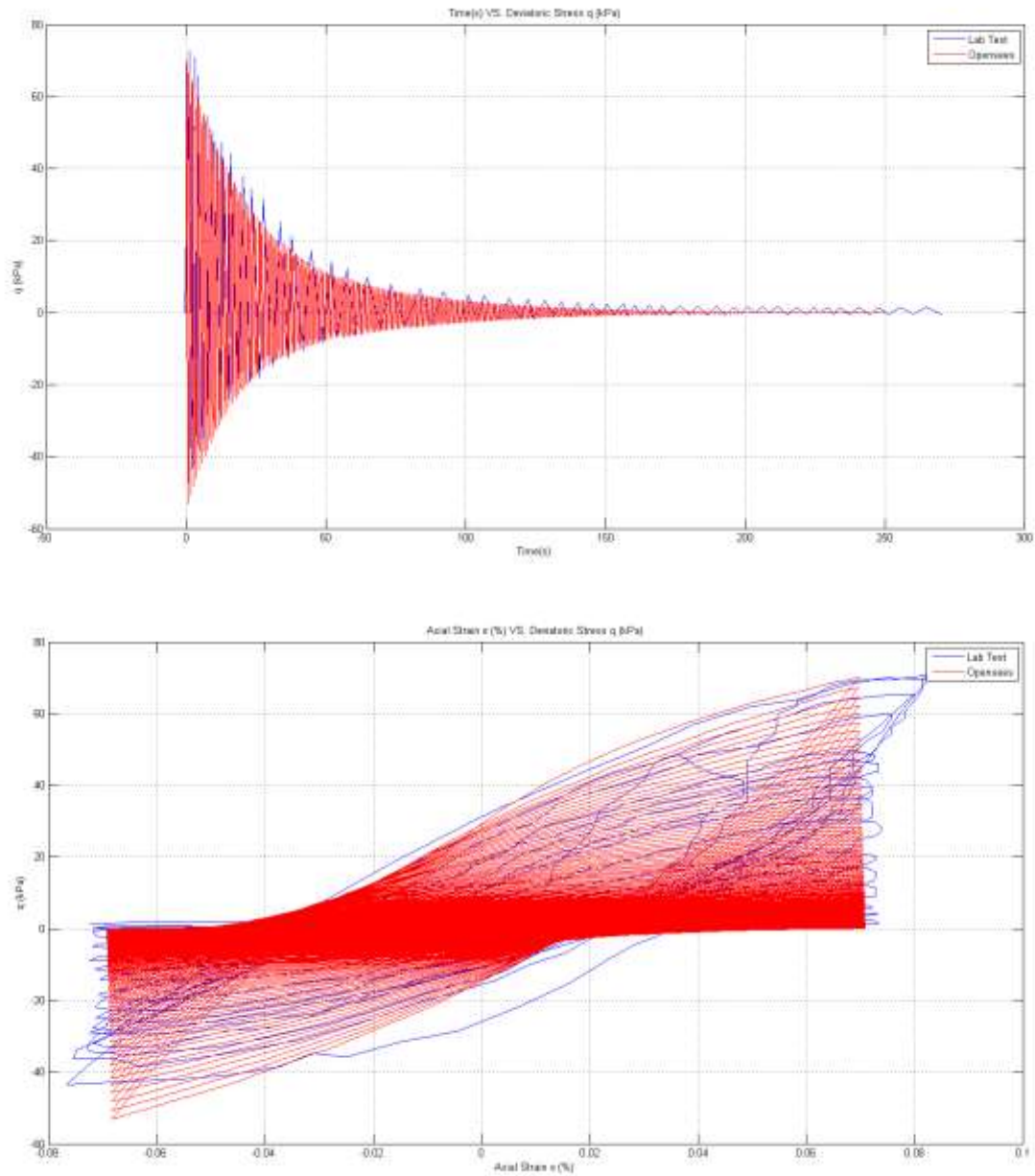


**Figure 3.20 Time (s) VS Deviatoric stress (kPa) and Axial strain (%) VS Deviatoric stress (kPa) respectively Test #4.**

Due to the fact a problem around the digitalization of data, the analysis over this test is done principally with the loss of deviatoric stress in time and generation of excess pore water pressure in time, and in both cases, the simulation can capture the experimental results in a correct way.

- CIU-Cyclic TXC Test #5 strain control ( $\epsilon=0.250\%$ ,  $D_r=84\%$   $p' = 100\text{kPa}$ ).

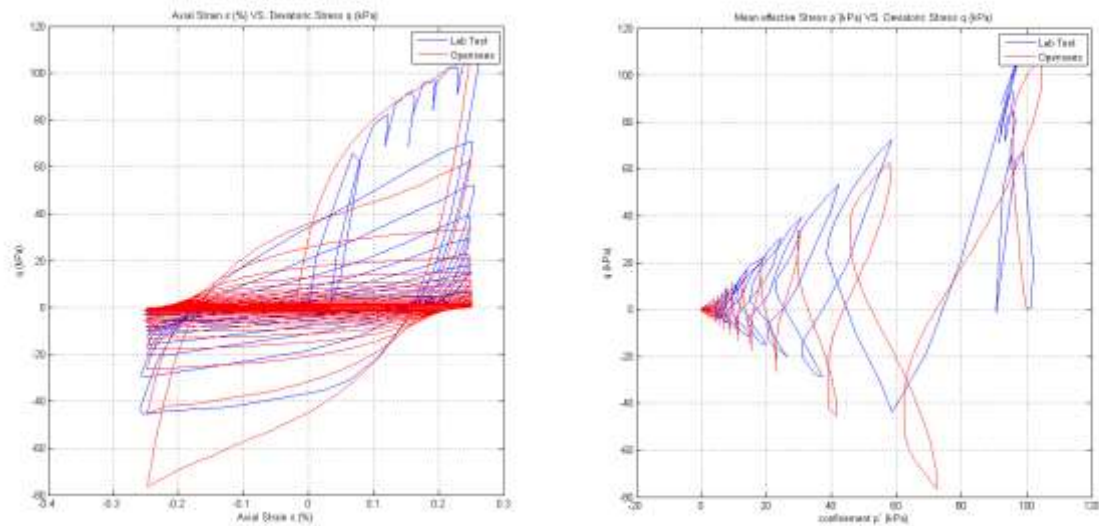


**Figure 3.21 Deviatoric stress (kPa) VS Axial strain (%) and confinement (kPa) respectively Test #5.**

As is show it in the **Figure 3.21**, the overprediction of deviatoric stress occurs in the extension part of cycle, the same pattern that other tests, besides the loss of deviatoric stress is not occurs with the same path in the extension process, something that in the compression part, the match of peaks is more accurate. On the other hand, the presence of “loops”, indicates that a dilatancy process occurs, something that simulation process can recreates just in the compression phase in a more accurate way. In the **Figure 3.22** is show the accurate match in the generation excess of pore water pressure, where the gap between the compression axial strain is due an error from laboratory test execution, that cannot control the magnitude of this strain, something that could explain the better match in a phase of cycle (compression or extension) than the other.

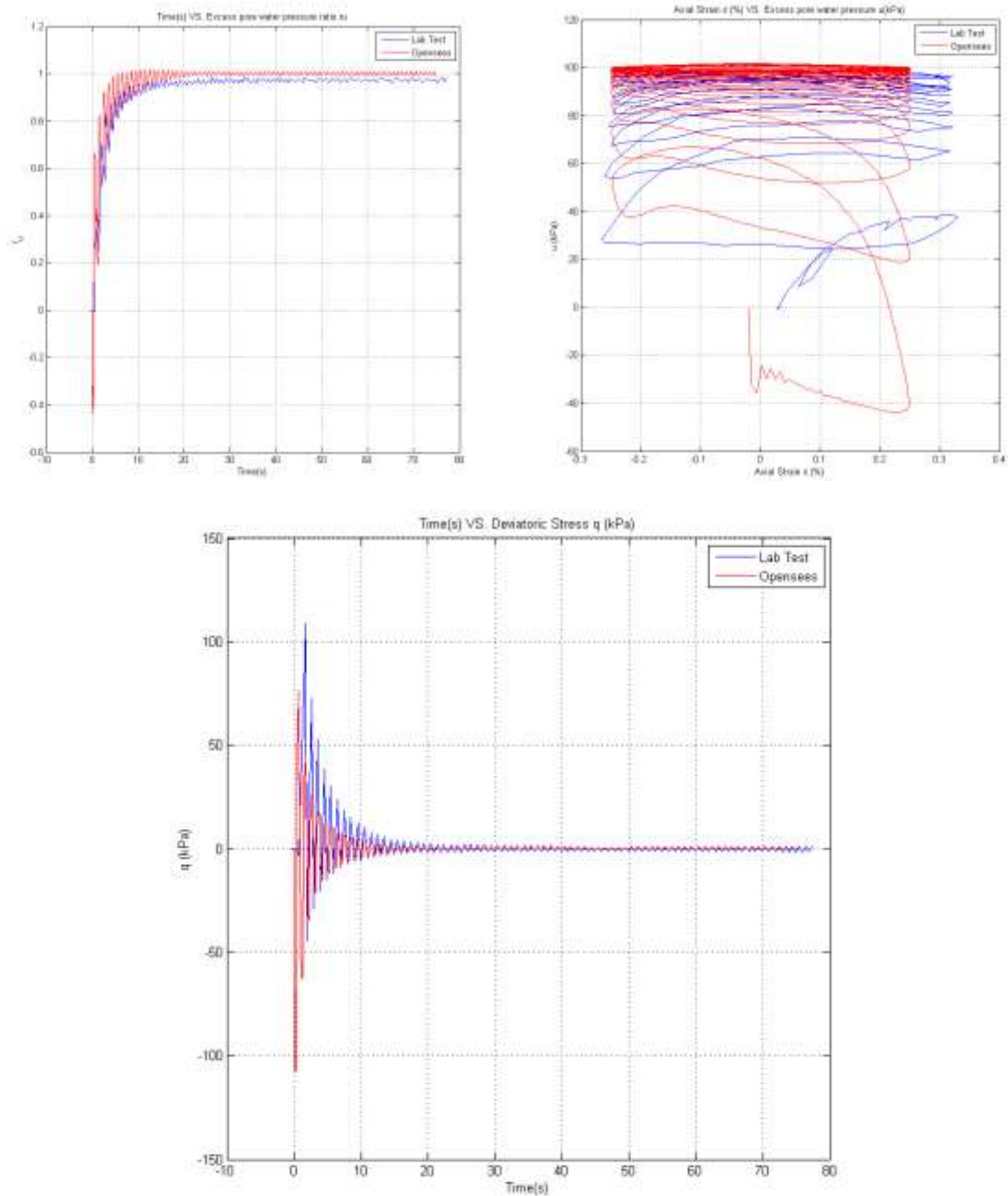


**Figure 3.22  $u$  VS Time (s), Axial Strain (%) VS  $u$  (kPa) and Time (s) VS Deviatoric stress (kPa) respectively Test #5.**

La información presentada en este documento es de exclusiva responsabilidad de los autores y no compromete a la EIA.



- CIU-Cyclic TXC Test #6 strain control ( $\epsilon=0.486\%$ ,  $D_r=86\%$   $p' = 100\text{kPa}$ ).

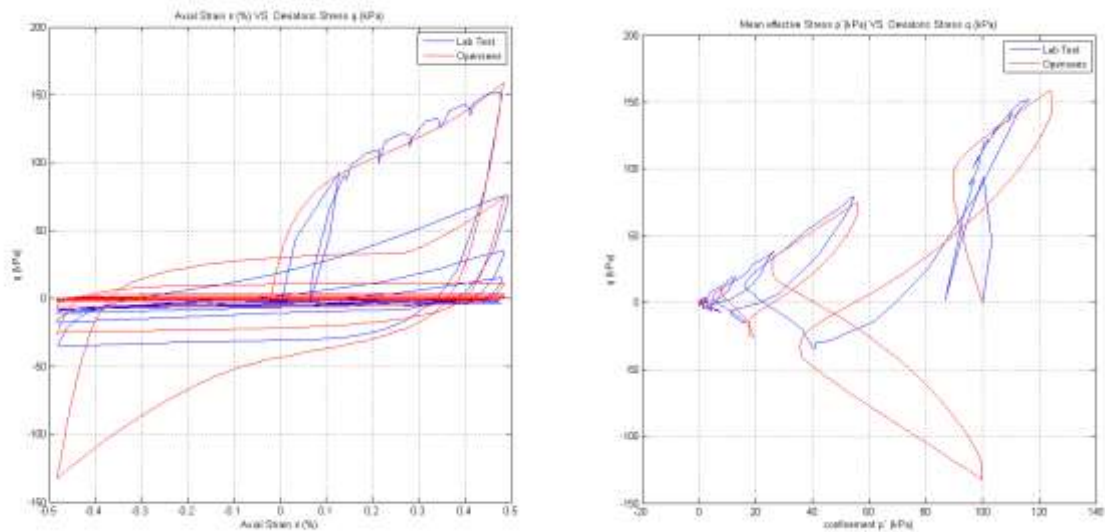


**Figure 3.23 Deviatoric stress (kPa) VS Axial strain (%) and confinement (kPa) respectively Test #6.**

As is shown in the **Figure 3.23**, the overprediction of deviatoric stress occurs in the extension part of cycle, the same pattern that other tests, besides the loss of deviatoric stress is not occurs with the same path in the extension process, something that in the compression part, the match of peaks is more accurate. On the other hand, the presence of “loops”, indicates that a dilatancy process occurs, something that simulation process can recreate just in the compression phase in a more accurate way, and where the loop generate over the extension phase, could indicate that model overpredict dilatancy phenomena's because is not based on critical state criteria. In the **Figure 3.24** is shown the accurate match in the generation excess of pore water pressure.

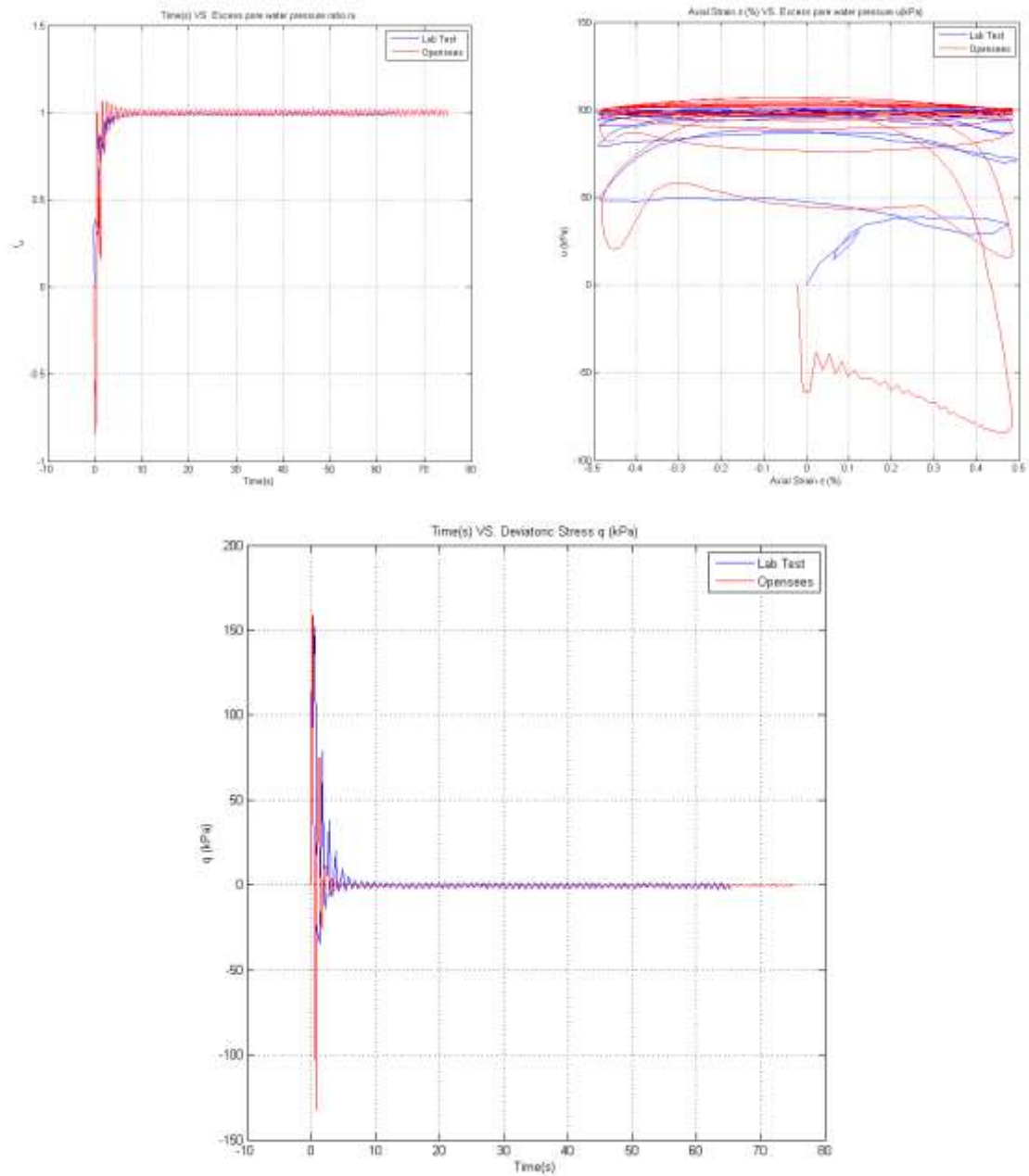


**Figure 3.24  $u$  VS Time (s), Axial Strain (%) VS  $u$  (kPa) and Time (s) VS Deviatoric stress (kPa) respectively Test #6.**

Finally, is presented the resume of parameters per test.

La información presentada en este documento es de exclusiva responsabilidad de los autores y no compromete a la EIA.

**Table 3.5 Resume of sets of parameters per test.**

Parameter	Test #1	Test #2	Test #3	Test #4	Test #5	Test #6
set massDen	1.9	1.9	1.9	1.9	1.9	1.9
set refG (Mpa)	60000	80000	60000	65000	65000	69000
set refB (Mpa)	160000	180000	160000	165000	165000	165000
set frinctionAng (°)	20	23	21	29	31	35
set peakShearStrain (%)	0.15	0.15	0.15	0.15	0.15	0.15
set refPress (kPa)	101	101	101	101	101	101
set pressDependCoe (-)	0.5	0.5	0.5	0.5	0.5	0.5
set phaseTransAng (°)	20	29	27	20	19	25
set contractionParam1 (-)	0.07	0.12	0.07	0.013	0.1	0.16
set contractionParam2 (-)	2	0.5	0.5	1	1	1
set contractionParam3 (-)	0.6	0.6	0.6	0.75	0.9	0.4
set dilationParam1 (-)	0	0.75	0.75	0.1	0.1	0.3
set dilationParam2 (-)	3	3	3	3	3	1
set dilationParam3 (-)	0	0	0	0	0	0.1
set liqParam1 (-)	1	1.3	1.3	1	1	1
set liqParam2 (-)	0	0	0	0	0	0
set noYieldSurf (-)	40	40	40	20	20	20
set void (-)	0.75	0.5	0.5	0.75	0.75	0.75
set cs1 (-)	0.9	0.9	0.9	0.9	0.9	0.9
set cs2 (-)	0.02	0.02	0.02	0.02	0.02	0.02
set cs3 (-)	0	0	0	0	0	0
set pa (kPa)	101	101	101	101	101	101
set c (-)	0.1	0.1	0.1	0.1	0.1	0.1

### 3.5.2 Comparison between each set of parameters

Once all six tests get a set of parameters, a comparison between all of them is done for the sake of determinate a difference between sets for low or high densities. At next is show the results.

La información presentada en este documento es de exclusiva responsabilidad de los autores y no compromete a la EIA.

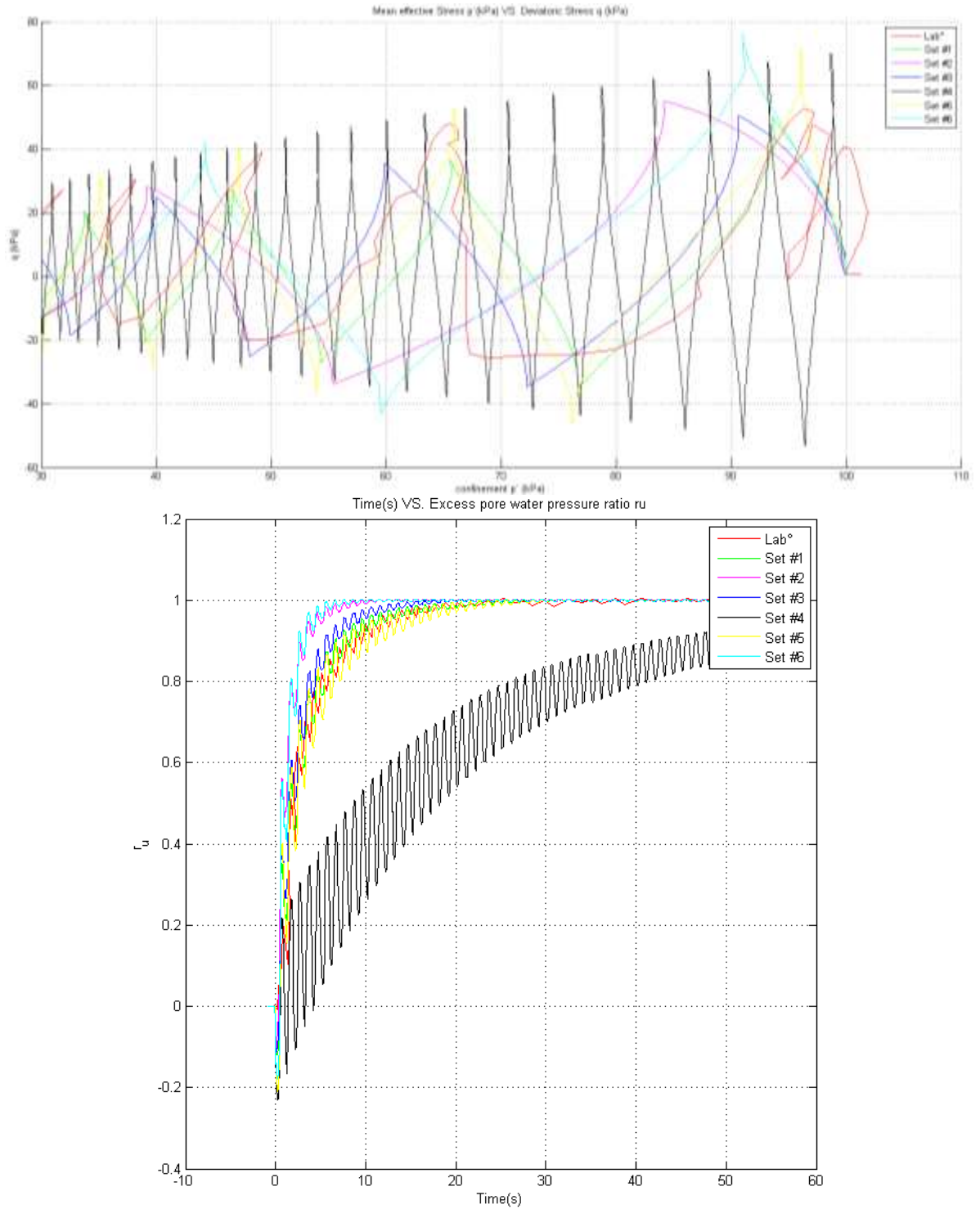


**Figure 3.25 Comparison between all sets of parameters to reproduce test #1 conditions.**

La información presentada en este documento es de exclusiva responsabilidad de los autores y no compromete a la EIA.

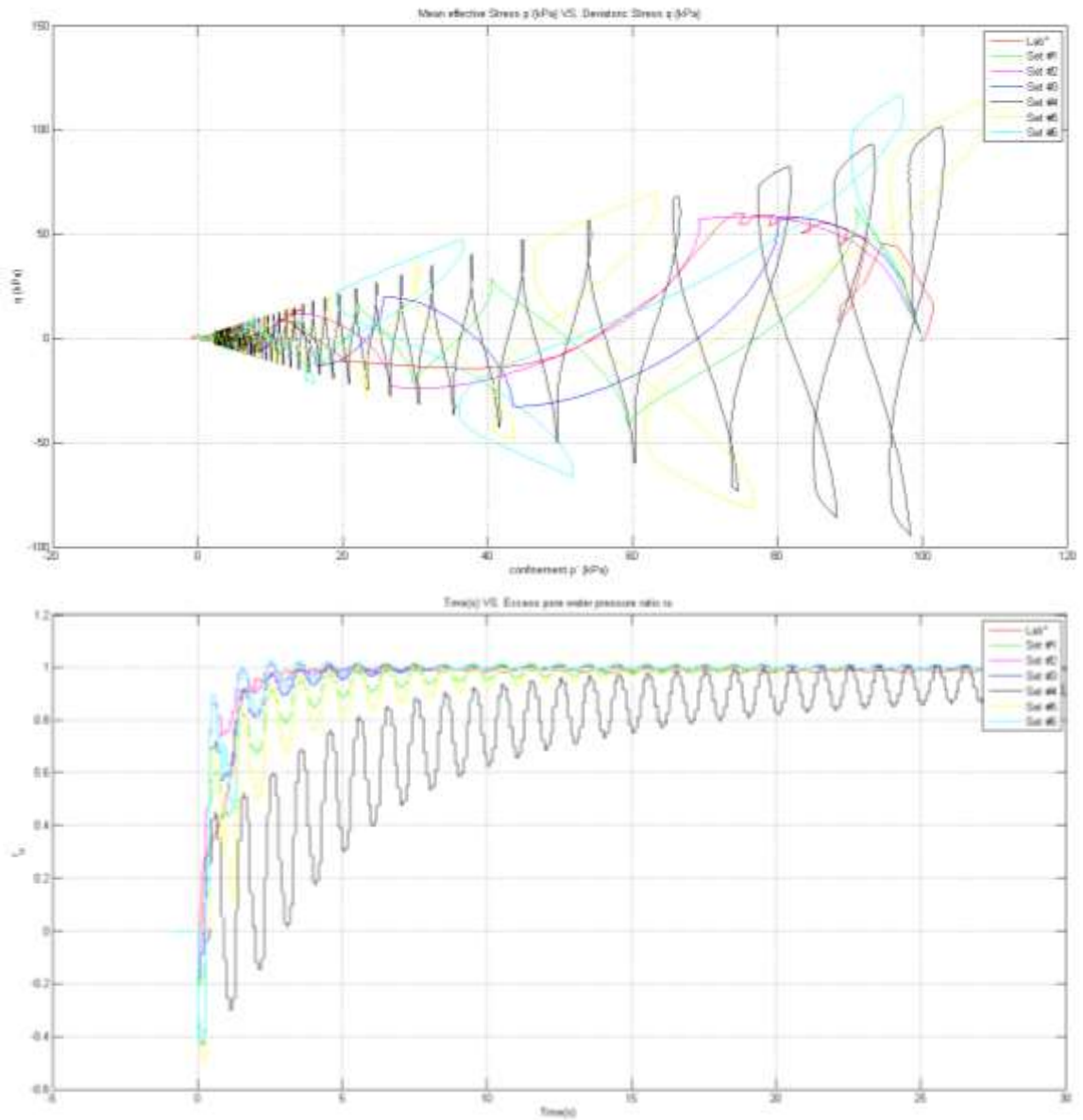


**Figure 3.26 Comparison between all sets of parameters to reproduce test #2 conditions.**

La información presentada en este documento es de exclusiva responsabilidad de los autores y no compromete a la EIA.

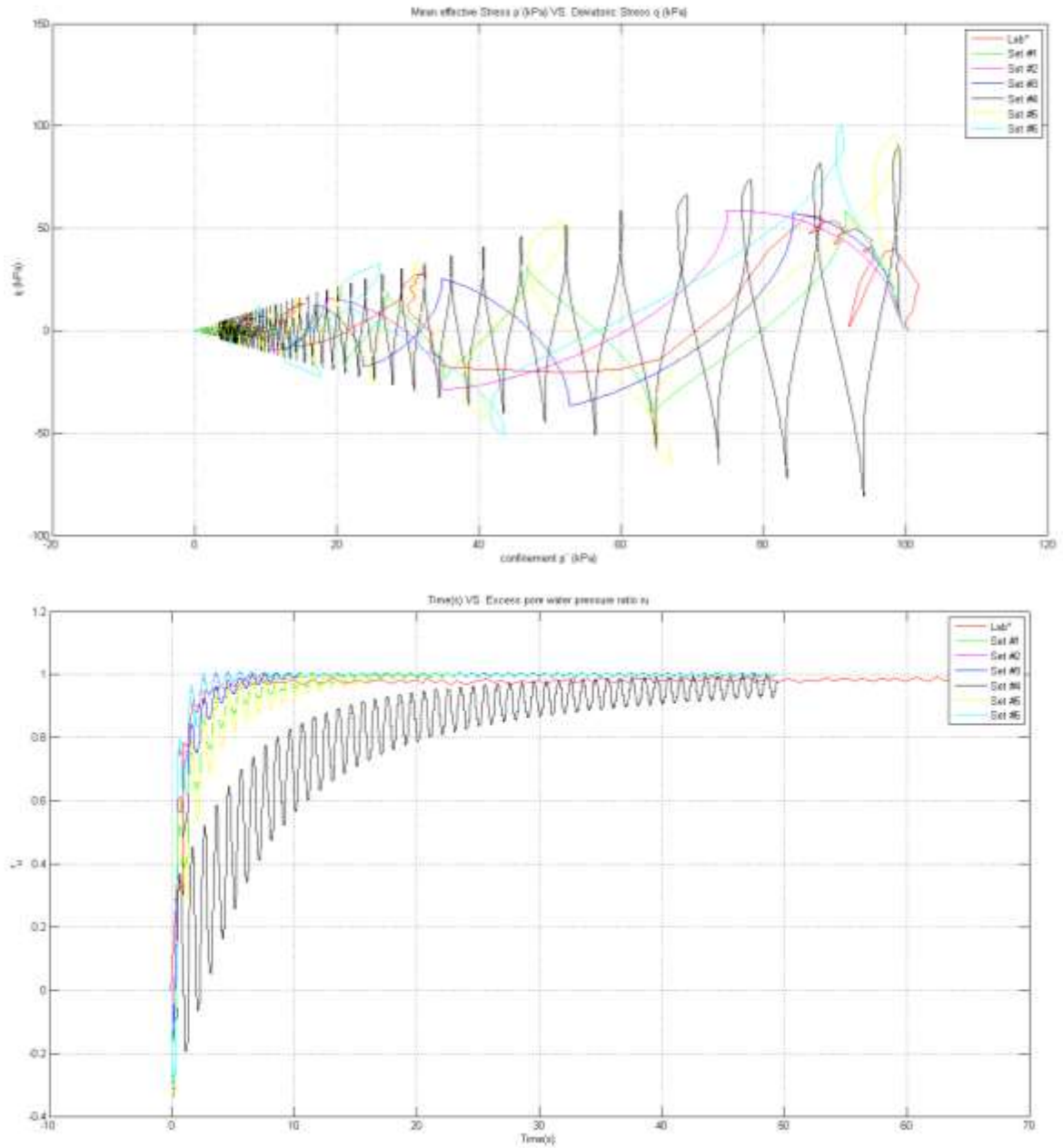


**Figure 3.27 Comparison between all sets of parameters to reproduce test #3 conditions.**

La información presentada en este documento es de exclusiva responsabilidad de los autores y no compromete a la EIA.

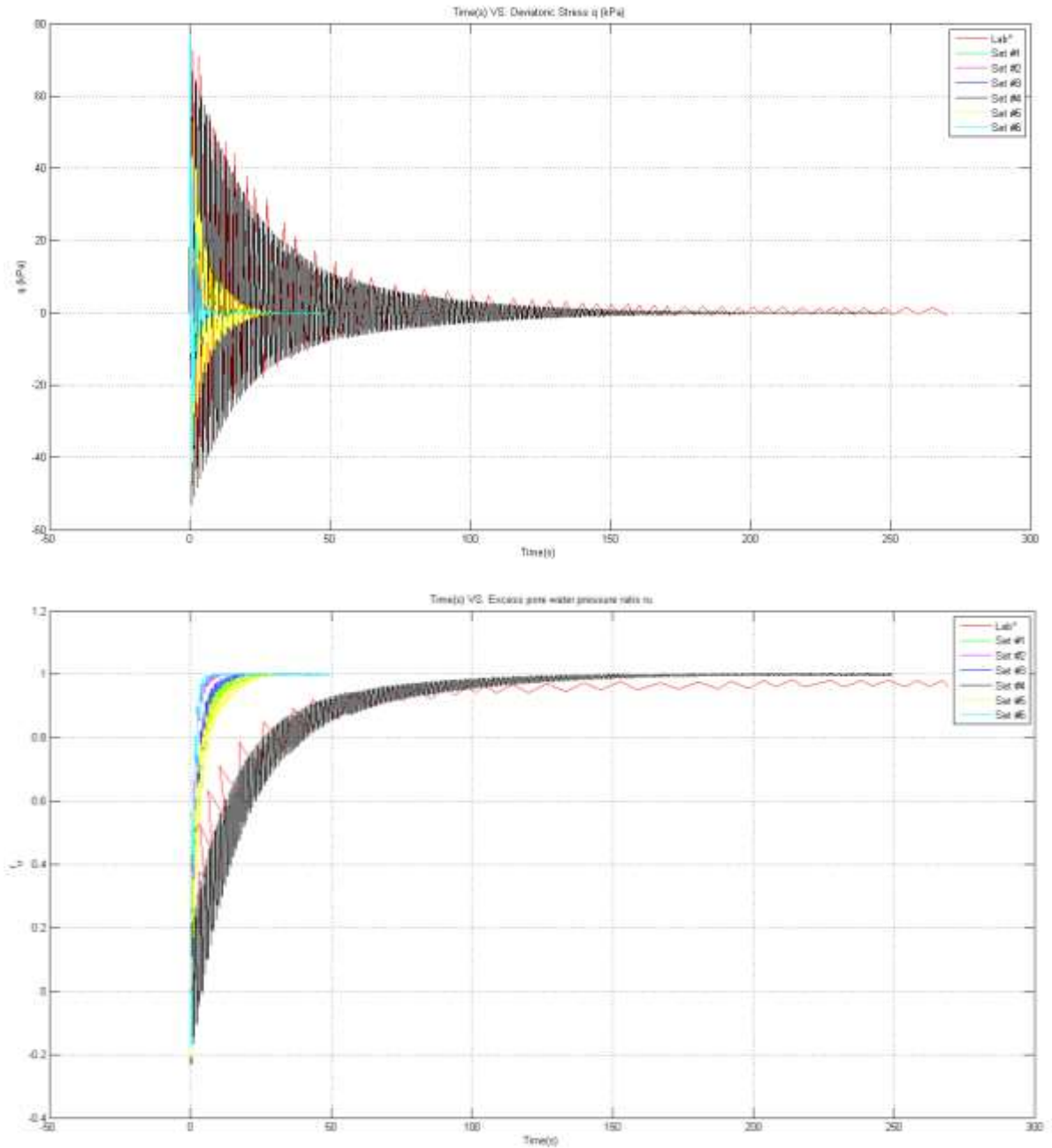


**Figure 3.28 Comparison between all sets of parameters to reproduce test #4 conditions.**

La información presentada en este documento es de exclusiva responsabilidad de los autores y no compromete a la EIA.

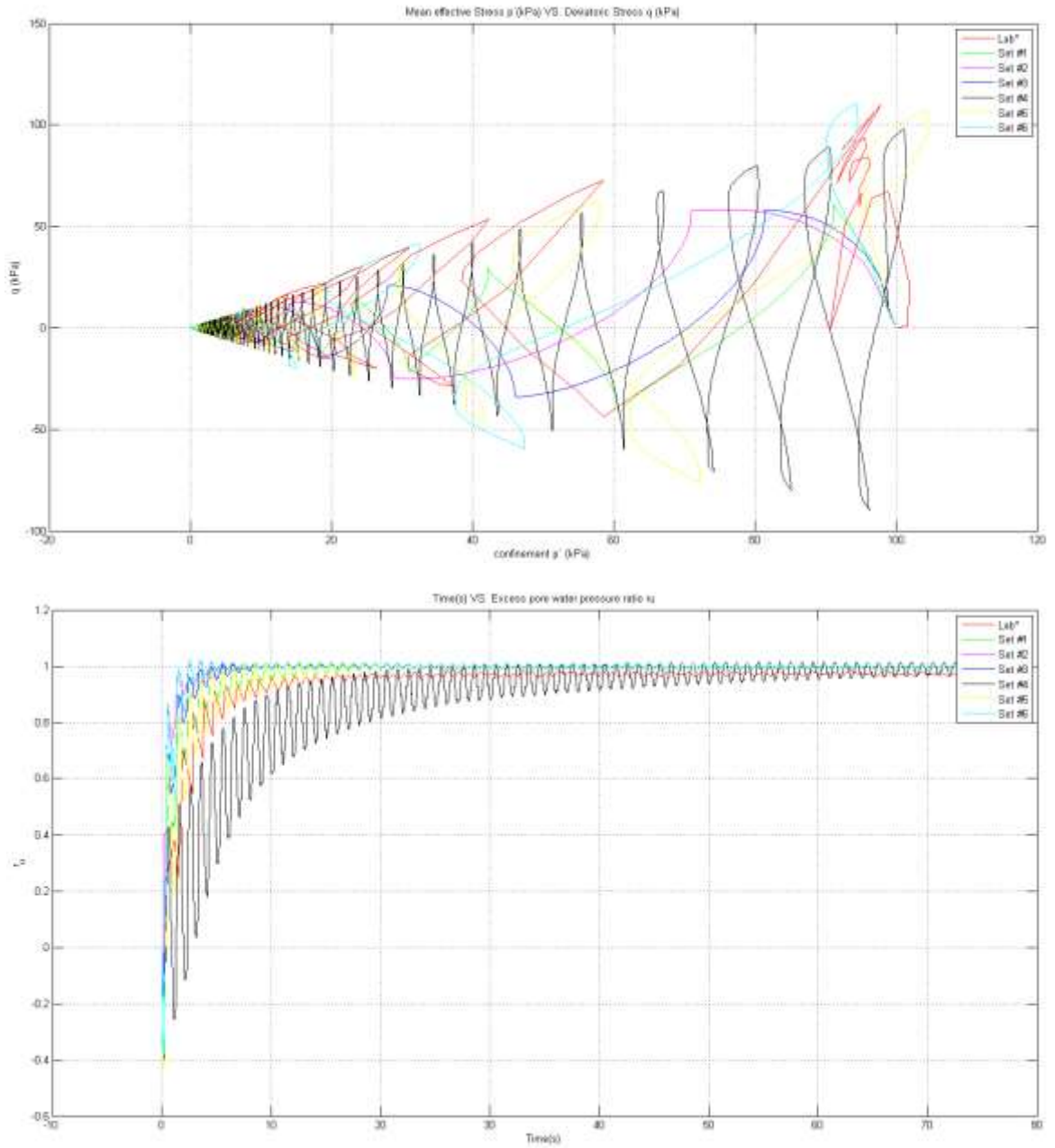


**Figure 3.29 Comparison between all sets of parameters to reproduce test #5 conditions.**

La información presentada en este documento es de exclusiva responsabilidad de los autores y no compromete a la EIA.



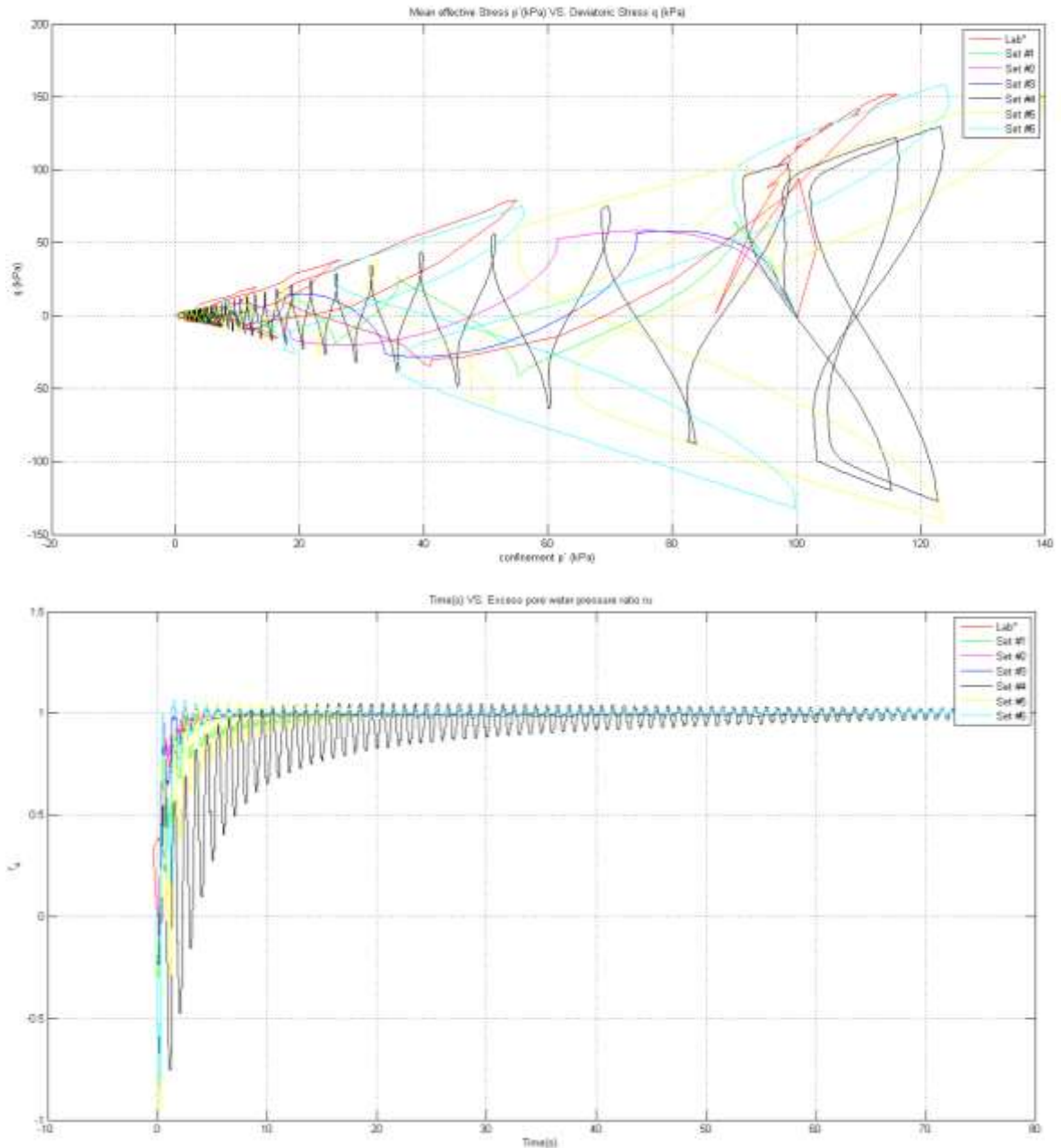


**Figure 3.30 Comparison between all sets of parameters to reproduce test #6 conditions.**

Product of this comparison, is valid to say that is needed two sets of parameters, the first one for low relative densities ( $D_r$  around 35%), and a second for the higher ones ( $D_r$  around 85%), principally because at low densities, the soil have a contractive tendency, something that is just capable to do the model with values of friction angle lower than phase transformation angle, where the plastic potential function is upper the failure, creating a zone where all the volumetric changes is controlled purely by the plastic potential function. At

La información presentada en este documento es de exclusiva responsabilidad de los autores y no compromete a la EIA.

higher values of density, the volumetric and deviatoric process is first controlled by a contraction phase, follow it by a dilatancy phase controlled by a phase transformation angle lower than frictional angle, creating the previously mentioned loops, where not just the plastic potential function dictates the volumetric and deviatoric process, but the failure surface determinates the form as the changes occurs.

### **3.6 DETERMINATION OF SETS PER TYPE OF DR**

Once is evidentiated the necessity of two sets of parameters, the first way of get it is through an average around each parameter, just averaging the values of lower densities and apart the values of higher ones. The results for this assumption are showed at next.

As is see it, the response of an average set of parameters for lower densities tests works, been capable to capture in all three times, the excess pore water pressure and as the individual results, overpredict the deviatoric stress at compression in the first test and the same values at extension in the other two.

On the other hand, the results over higher values of relative density, present a variation majorly with the 4<sup>th</sup> test, which one is the only one who do not achieve a dilation phase, product of a smaller strain than others two tests, who get a representative response with the average set of parameters, principally capturing the excess pore water pressure and loss of deviatoric stress, and continue presenting an overprediction over deviatoric stress in the extension phase.

- Results of averaging process for lower densities modeling the test #1 conditions.

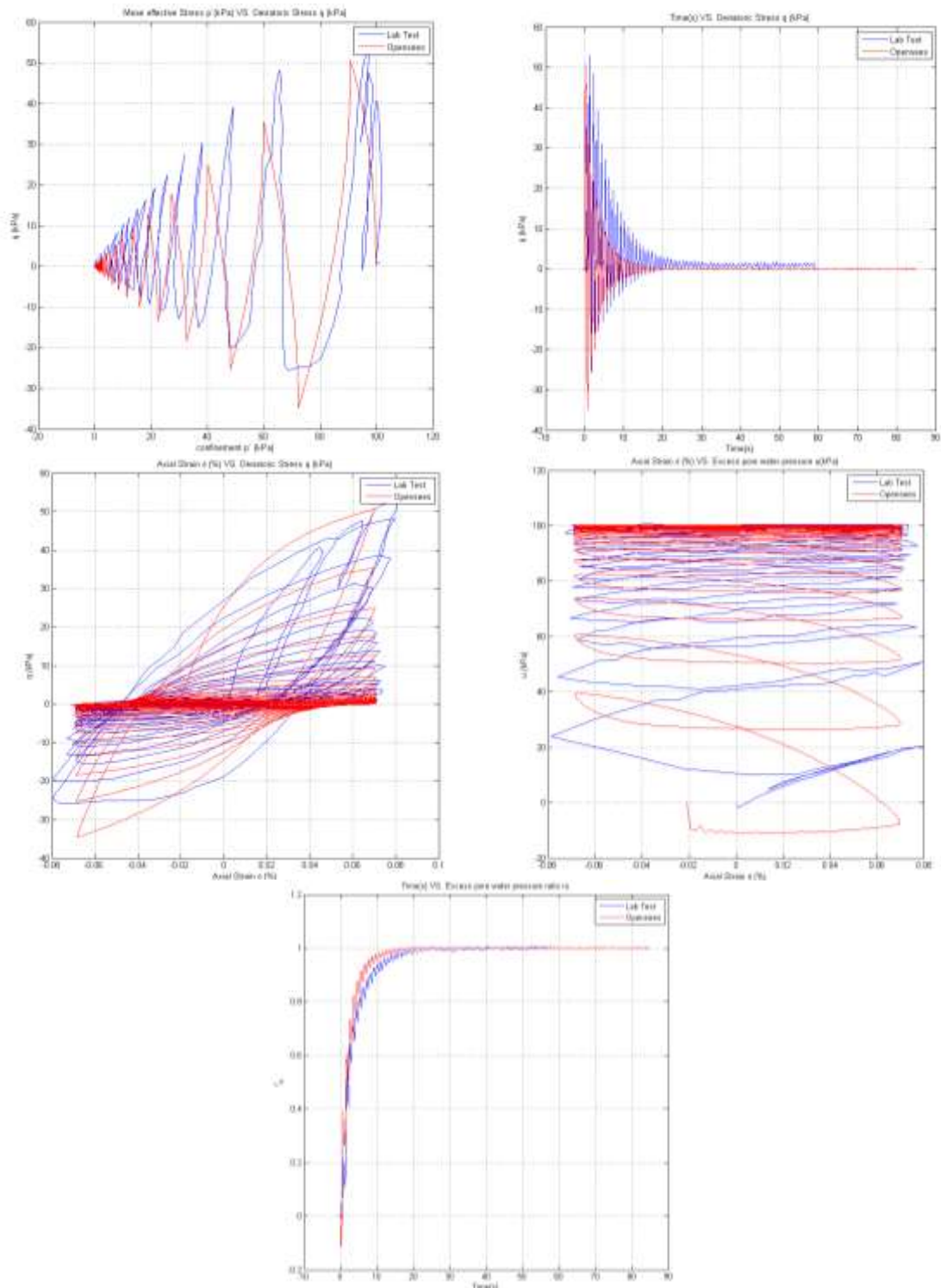


**Figure 3.31 Simulation results of average set modeling test #1 conditions.**

La información presentada en este documento es de exclusiva responsabilidad de los autores y no compromete a la EIA.

- Results of averaging process for lower densities modeling the test #2 conditions.

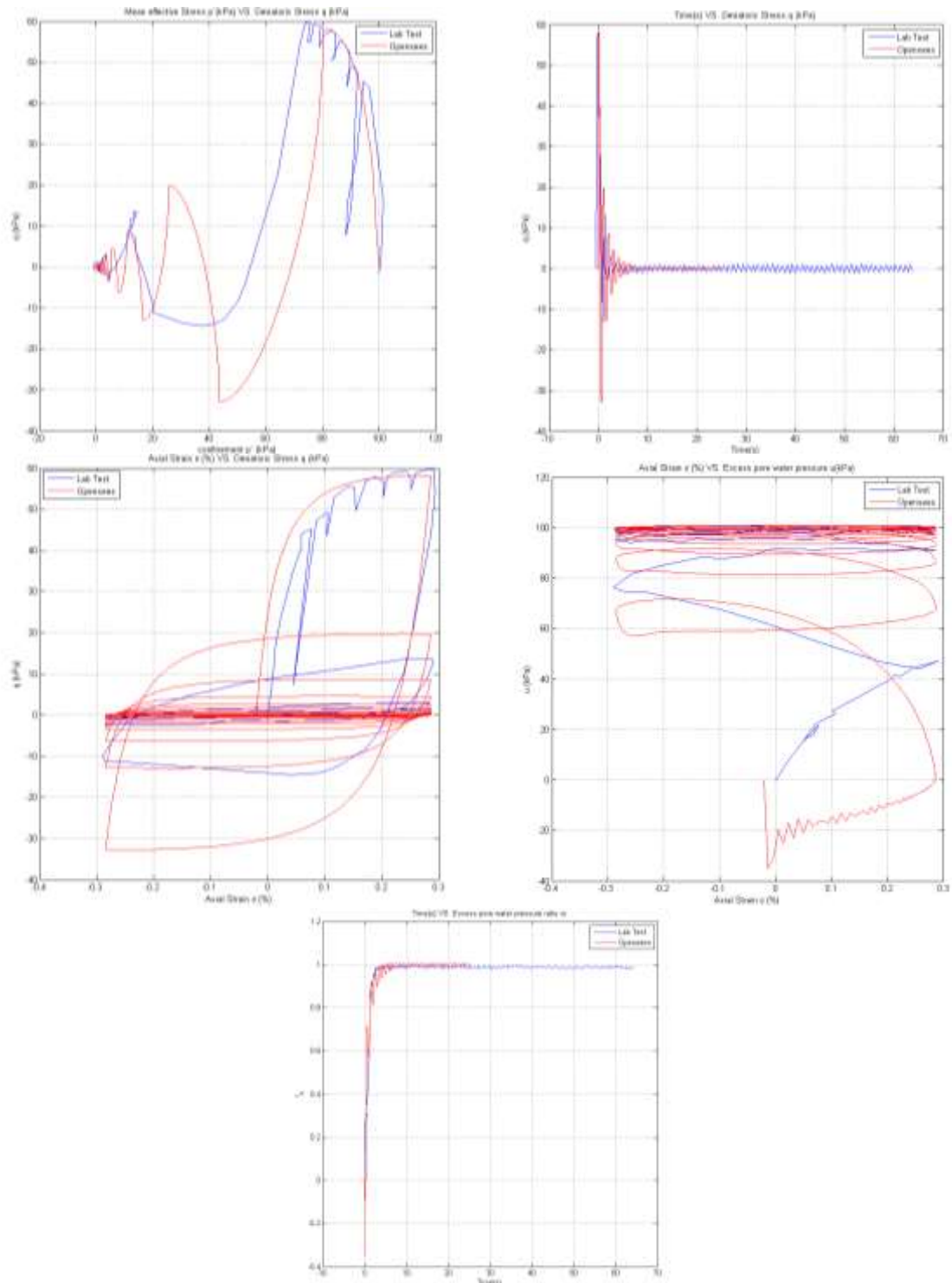


**Figure 3.32 Simulation results of average set modeling test #2 conditions.**

La información presentada en este documento es de exclusiva responsabilidad de los autores y no compromete a la EIA.

- Results of averaging process for lower densities modeling the test #3 conditions.

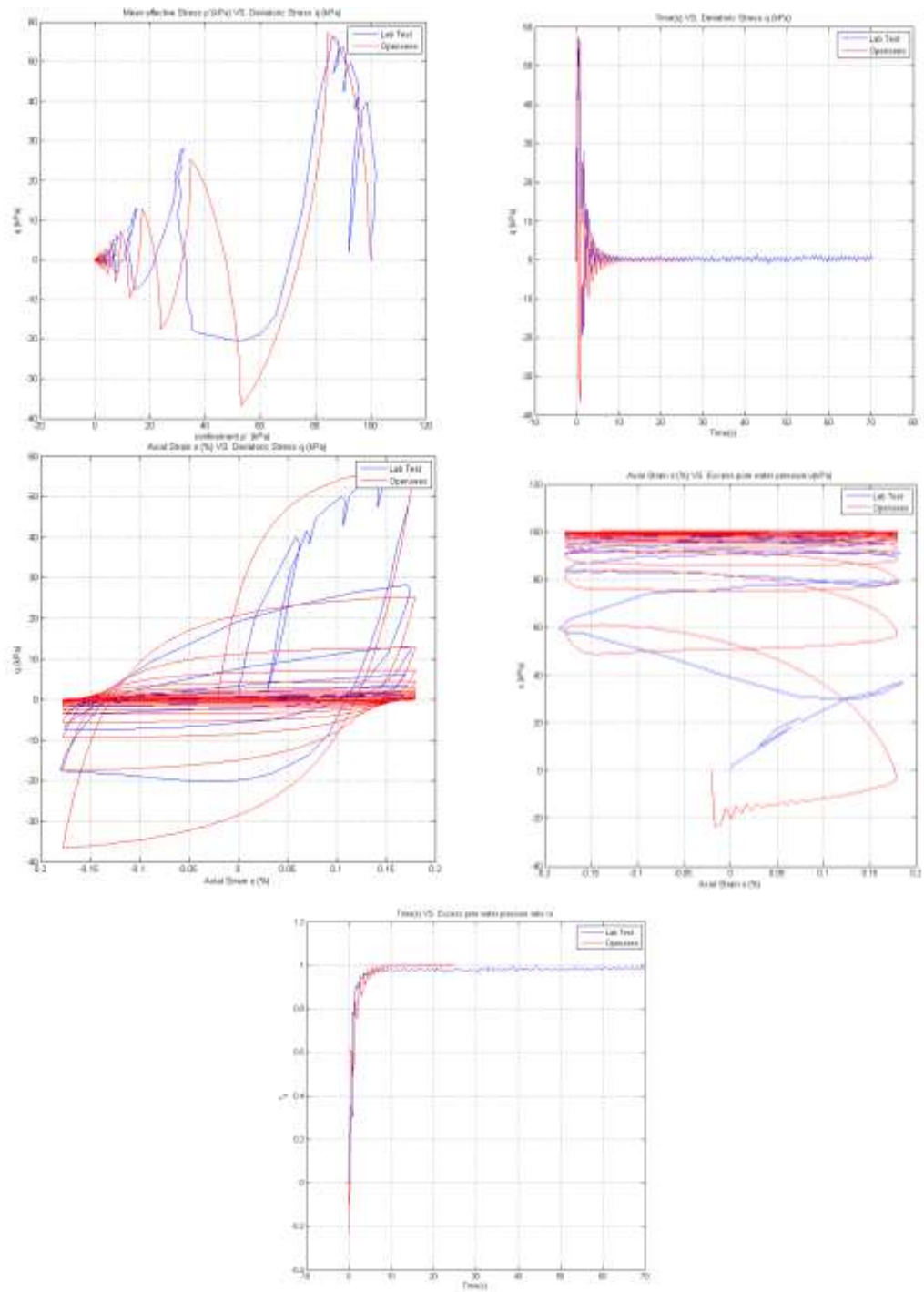


**Figure 3.32 Simulation results of average set modeling test #3 conditions.**

La información presentada en este documento es de exclusiva responsabilidad de los autores y no compromete a la EIA.

- Results of averaging process for higher densities modeling the test #4 conditions.

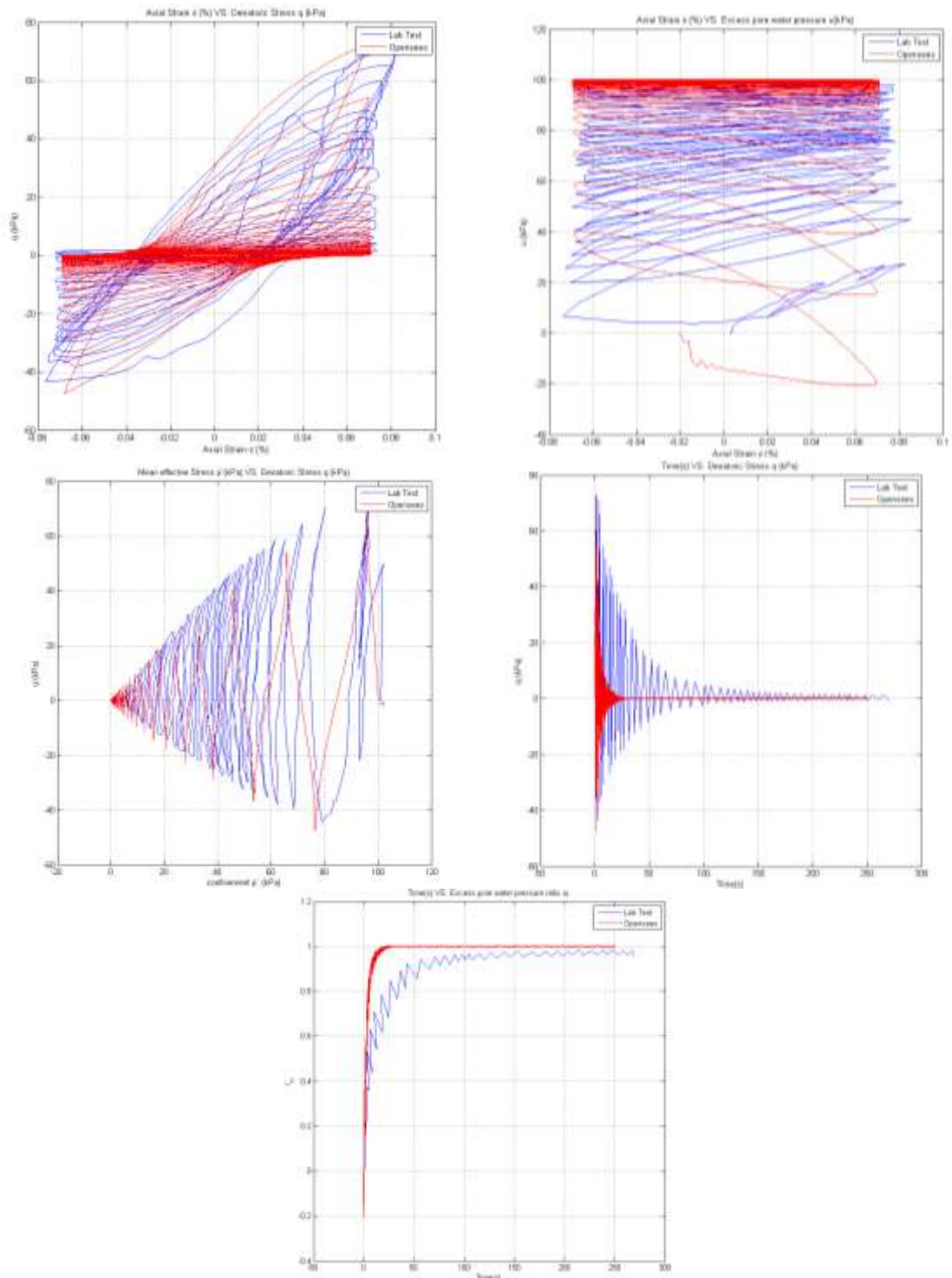


**Figure 1.1** Simulation results of average set modeling test #4 conditions.

La información presentada en este documento es de exclusiva responsabilidad de los autores y no compromete a la EIA.

- Results of averaging process for higher densities modeling the test #5 conditions.

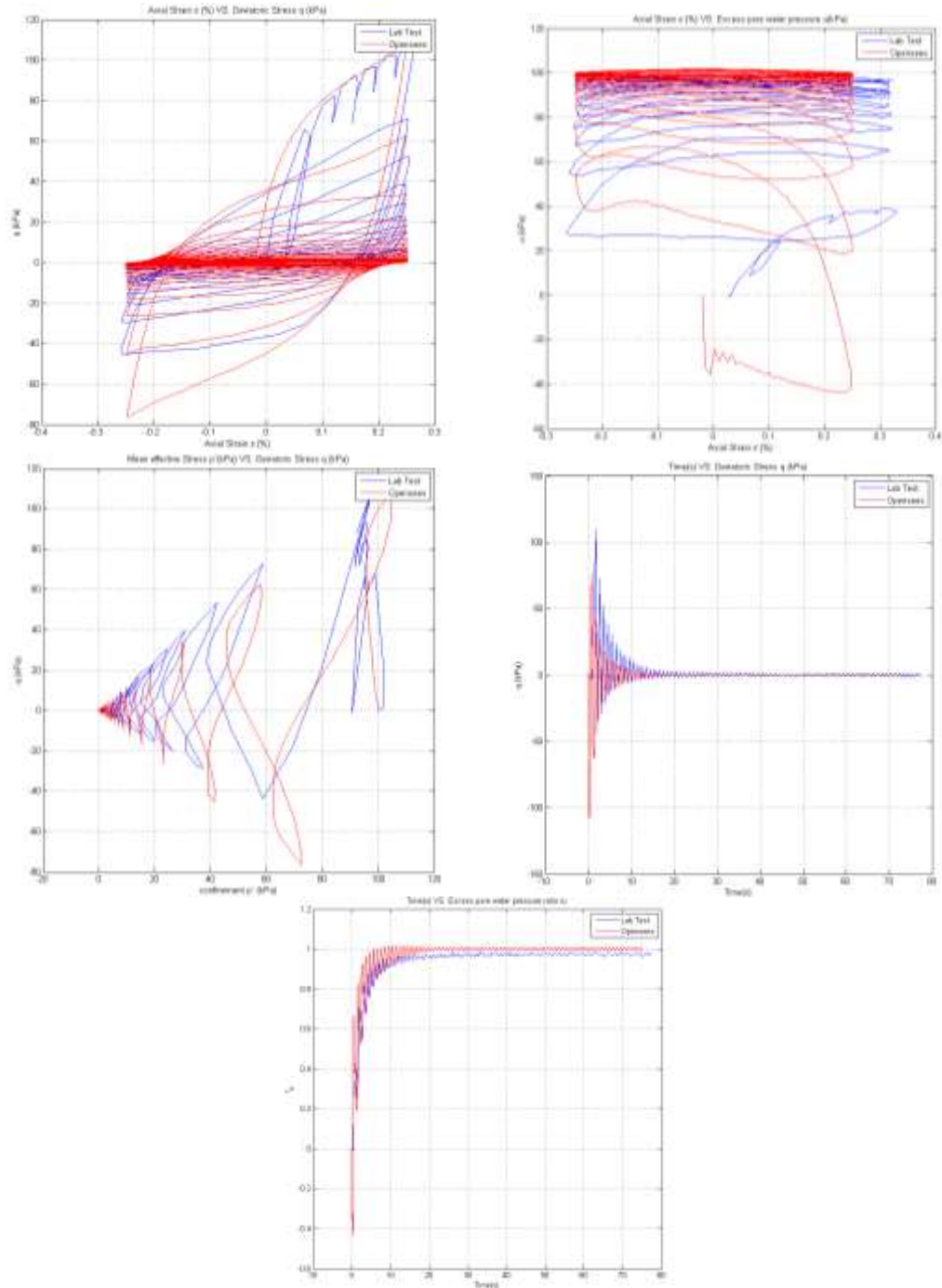


**Figure 1.2 Simulation results of average set modeling test #5 conditions.**

La información presentada en este documento es de exclusiva responsabilidad de los autores y no compromete a la EIA.

- Results of averaging process for higher densities modeling the test #6 conditions.

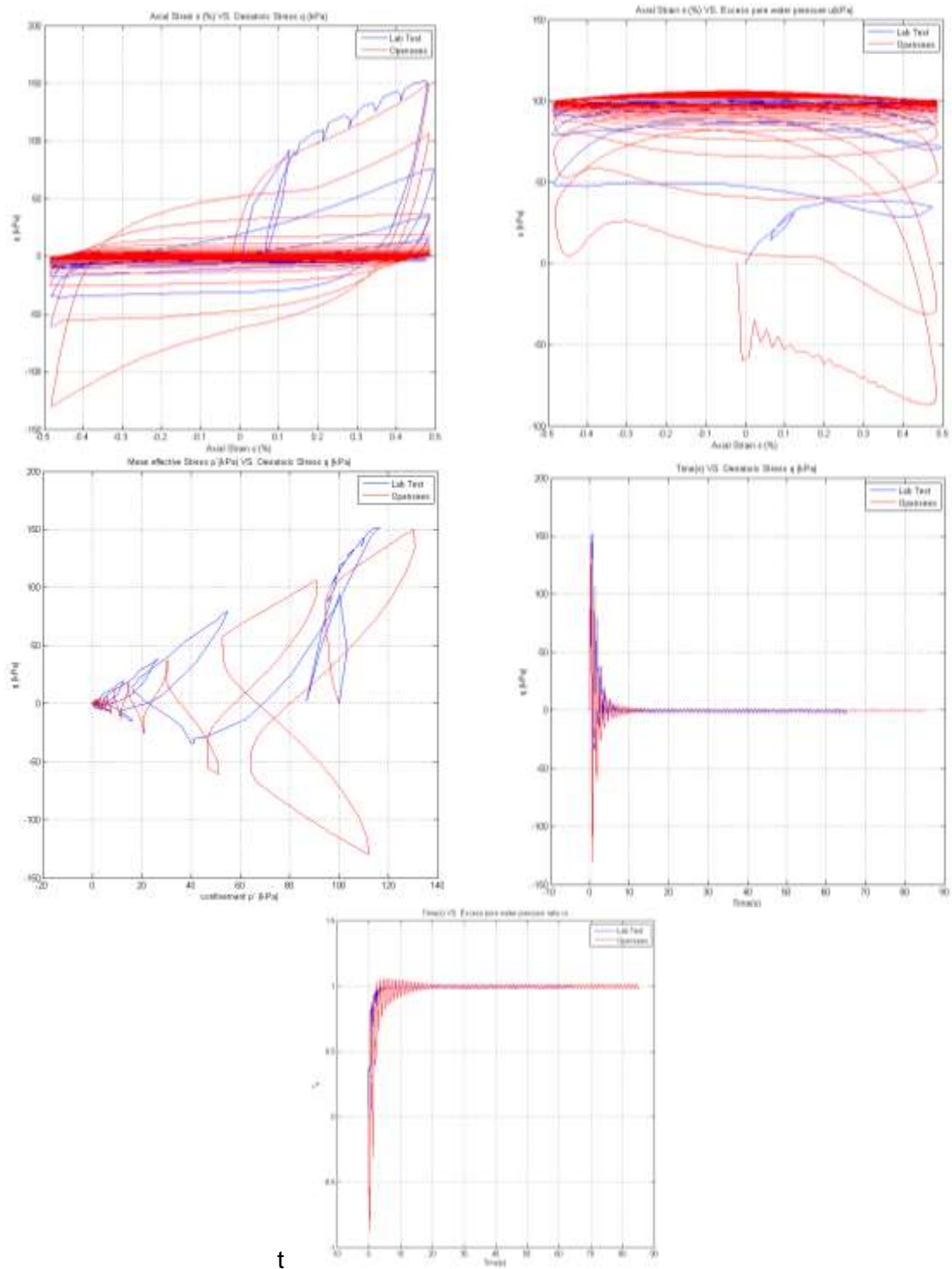


**Figure 1.3 Simulation results of average set modeling test #6 conditions.**

La información presentada en este documento es de exclusiva responsabilidad de los autores y no compromete a la EIA.



In this table is presented the resume of parameters per individual calibration as average sets of parameters (lower and higher relative density sets).

**Table 1.1 Resume of different set of parameters.**

Parameter	Test #1	Test #2	Test #3	Test #4	Test #5	Test #6	Average High Dr	Average Low Dr
set massDen	1.9	1.9	1.9	1.9	1.9	1.9	1.900	1.900
set refG (Mpa)	60000	80000	60000	65000	65000	69000	66333	66667
set refB (Mpa)	160000	180000	160000	165000	165000	165000	165000	166667
set frinctionAng (°)	20.00	23.00	21.00	29.00	31.00	35.00	31.67	21.33
set peakShearStrain (%)	0.15	0.15	0.15	0.15	0.15	0.15	0.15	0.15
set refPress (kPa)	101.00	101.00	101.00	101.00	101.00	101.00	101.00	101.00
set pressDependCoe (-)	0.50	0.50	0.50	0.50	0.50	0.50	0.50	0.50
set phaseTransAng (°)	20.00	29.00	27.00	20.00	19.00	25.00	21.33	25.33
set contractionParam1 (-)	0.07	0.12	0.07	0.01	0.10	0.16	0.09	0.087
set contractionParam2 (-)	2.00	0.50	0.50	1.00	1.00	1.00	1.00	1.00
set contractionParam3 (-)	0.60	0.60	0.60	0.75	0.90	0.40	0.68	0.60
set dilationParam1 (-)	0.00	0.75	0.75	0.10	0.10	0.30	0.17	0.50
set dilationParam2 (-)	3.00	3.00	3.00	3.00	3.00	1.00	2.33	3.00
set dilationParam3 (-)	0.00	0.00	0.00	0.00	0.00	0.10	0.03	0.00
set liqParam1 (-)	1.00	1.30	1.30	1.00	1.00	1.00	1.00	1.20
set liqParam2 (-)	0.00	0.00	0.00	0.00	0.00	0.00	0.00	0.00
set noYieldSurf (-)	40.00	40.00	40.00	20.00	20.00	20.00	20.00	40.00
set void (-)	0.75	0.50	0.50	0.75	0.75	0.75	0.75	0.58
set cs1 (-)	0.90	0.90	0.90	0.90	0.90	0.90	0.90	0.90
set cs2 (-)	0.02	0.02	0.02	0.02	0.02	0.02	0.02	0.02
set cs3 (-)	0.00	0.00	0.00	0.00	0.00	0.00	0.00	0.00
set pa (kPa)	101.00	101.00	101.00	101.00	101.00	101.00	101.00	101.00
set c (-)	0.1	0.1	0.1	0.1	0.1	0.1	0.1	0.1

La información presentada en este documento es de exclusiva responsabilidad de los autores y no compromete a la EIA.

## 4. PRELIMINARY NUMERICAL MODELING OF FREE FIELD CONDITIONS AT MANTA ECUADOR

### 4.1 SEISMICITY OF MANTA ECUADOR

As is mentioned previously, the seismic event of April 16<sup>th</sup> of 2016 affected in a tremendous way not just the transportation infrastructures (highways, bridges and ports) but in a significantly way the residential structures around Manta town (Geoestudios S.A, 2016). The geotechnical and dynamic conditions of ground had been a factor who was a principal role on the behavior and performance of this structures.

Because of the seismicity and geotectonic conditions of the region, plus the fact of be located near an ocean, the hazard over this place is high, just as showed in the **Figure 4.1**, the pacific coast of Ecuador is an over a subduction area between continental and Nazca plate, and because of this, not just the mountains system knows as *Cordillera de los Andes* is product of this, but a high seismic activity is produced.

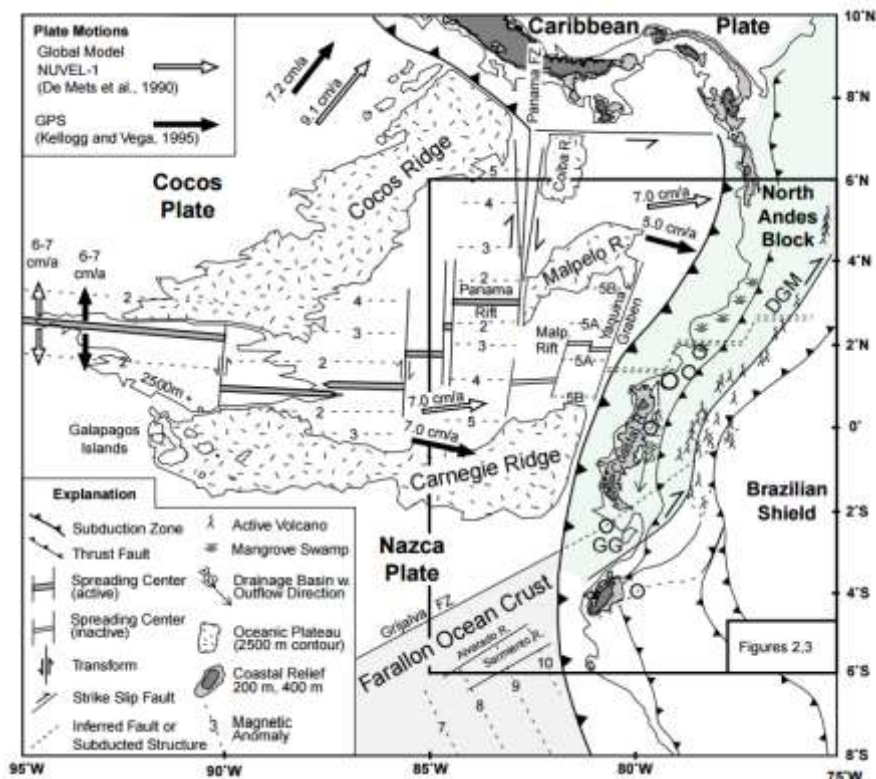


**Figure 4.1 Tectonic condition of study region** (Gutscher, Malavieille, Lallemand, & Collot, 1999).

More precisely in the near region of Manta, two failure zones are identified, knowns as *Falla de Montecristi* and *Falla Rio Salado*, which ones creates over the peninsula a local focus point of potential seismic events.

La información presentada en este documento es de exclusiva responsabilidad de los autores y no compromete a la EIA.

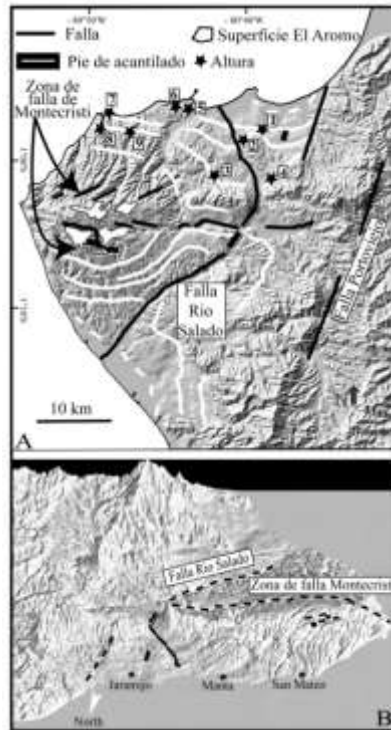


**Figure 4.2 Local tectonic conditions** (Geoestudios S.A, 2016).

#### 4.1.1 Area of study

Manta is a city that limits at north, south and west with Pacific Ocean and at east with *Cantones Montecristi*, where one of most important suburbs of this city is *Barrio Tarqui*, who is going to be the point of study because it behavior of soil and soil – structure interaction once the earthquake happened.



**Figure 4.3 Barrio Tarqui location, Manta Ecuador.**

Over this portion of city, after the seismic event were quantified the structure damages subdividing the area in 9 zones and categorizing the damage in 5 categories in function of cracks (absence or presence and size of them), the presence of expulse dust around the

La información presentada en este documento es de exclusiva responsabilidad de los autores y no compromete a la EIA.

cracks and the possible lateral displacement of structural elements. The results are summarized at next.



**Figure 4.4 Damages over the infrastructure of Tarqui suburb (Geoestudios S.A, 2016).**

After the damage inventory, taking into consideration the distribution of them a series of stratigraphic profiles were defined to obtain the necessary data to understand the soil behavior under the seismic event. The proposal arrangement of profile is presented at next.



**Figure 4.5 Distribution of stratigraphic profiles in Tarqui, Manta (Geoestudios S.A, 2016).**

La información presentada en este documento es de exclusiva responsabilidad de los autores y no compromete a la EIA.

Now, to understand the soil behavior product of the earthquake, an altimetry process had been made to determinate the settlement due this excitation. At next is presented the location of this profile, as the initial topography and the settlement because of event.

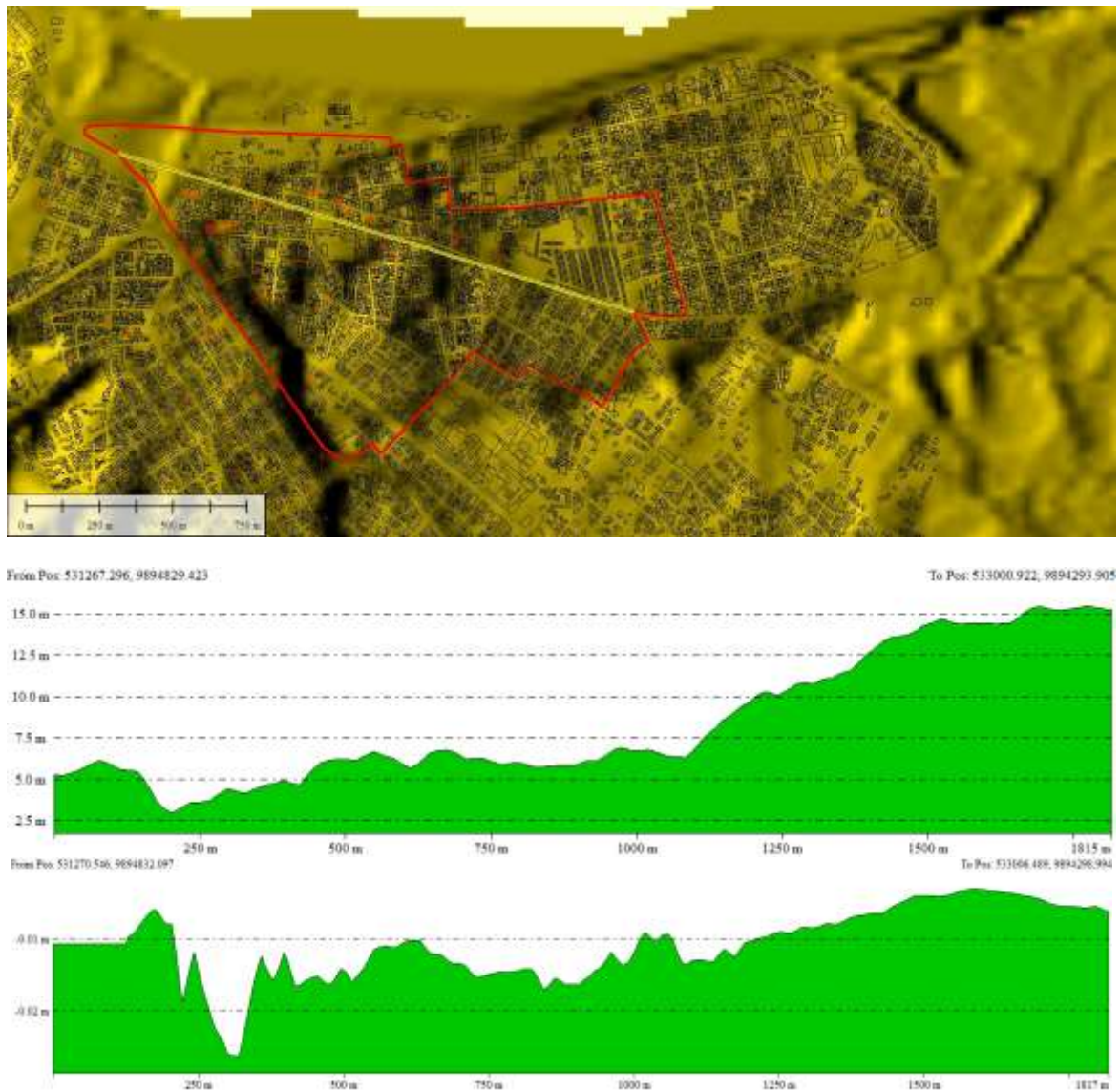


**Figure 4.6 Altimetry data (Geoestudios S.A, 2016).**

Now, due to the sand used to realize all the TXC test comes from *Calicata C7*, and the semiempirical liquefaction analysis is realize over the *Perforación P26*, and this place is near at Profile D and over the abscissa km 0+750, the stratigraphic profile used to this preliminary analysis is the next presented.

La información presentada en este documento es de exclusiva responsabilidad de los autores y no compromete a la EIA.

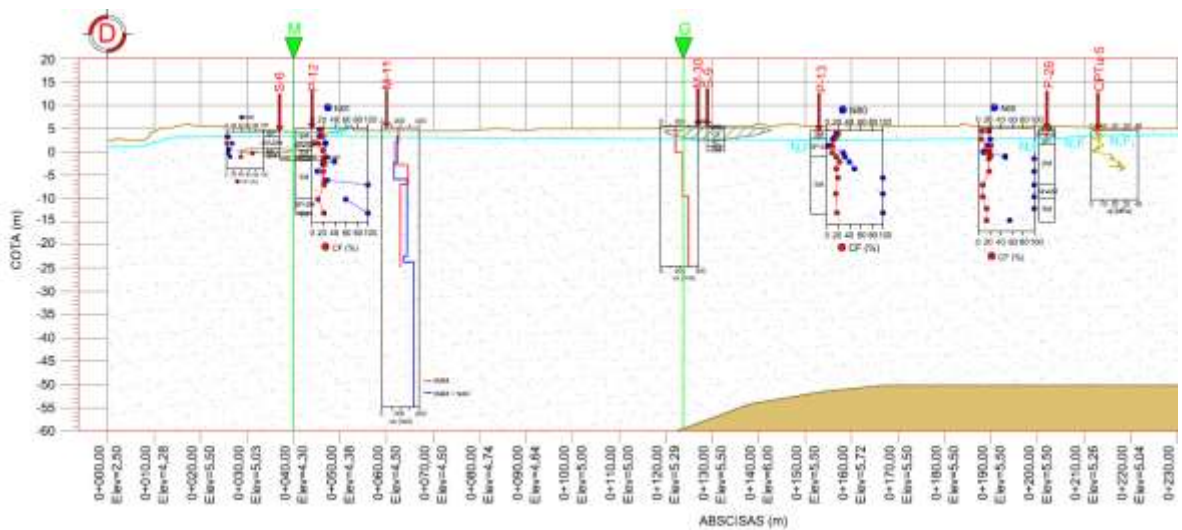


Figure 4.7 Profile D (Geostudios S.A, 2016).

## 4.2 SUBSURFACE CONDITIONS

On April 16<sup>th</sup> of 2016, around 18:58 there was a 7.8 Richter scale magnitude earthquake, with epicenter over the nearest place of *Cantón Pedemales*, that in study location a PGA of 0.94g was reached.

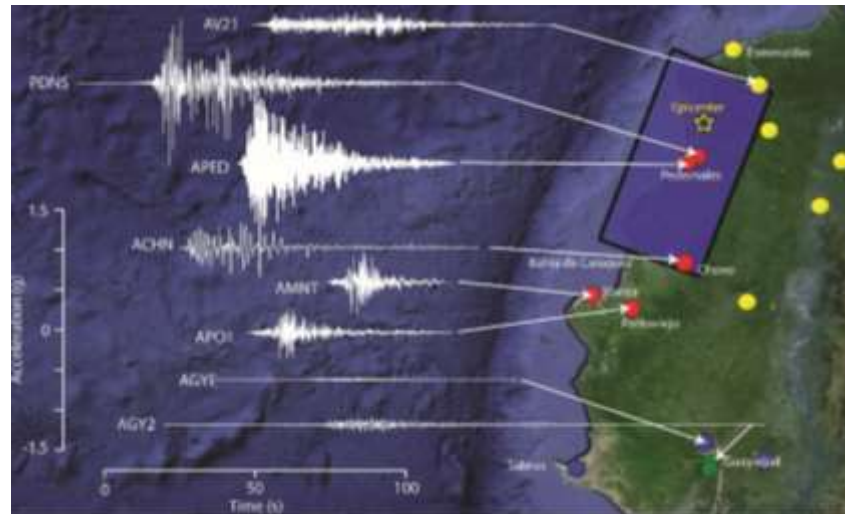
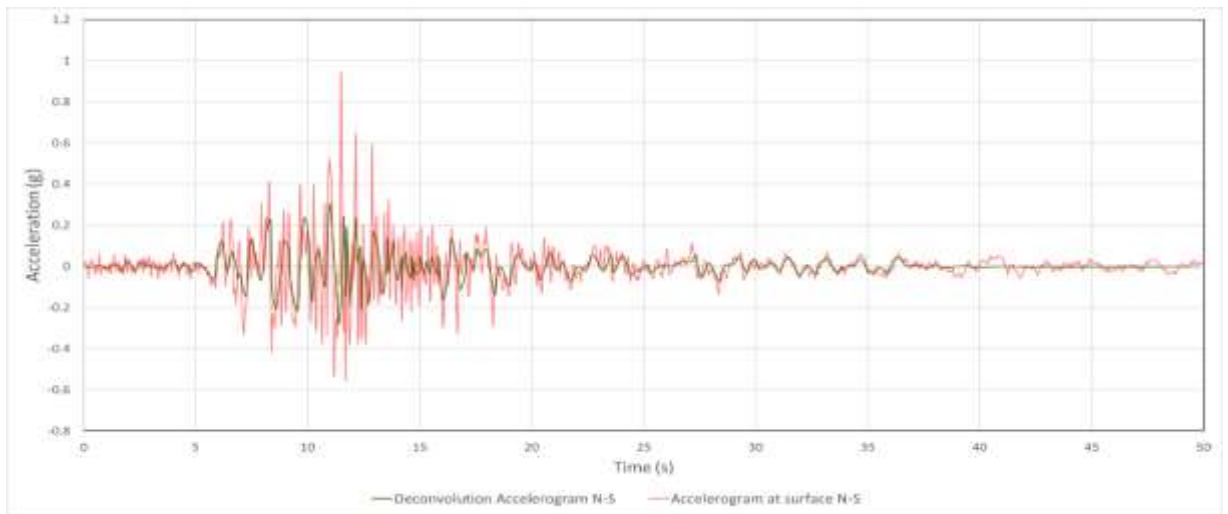


Figure 4.8 Accelerograms at different locations (Geostudios S.A, 2016).

Now, because of Manta data was obtained in surface, a deconvolution process is needed to be done to recreate the seismic condition in a better way. The accelerogram get in surface and through deconvolution process is showed at next.

La información presentada en este documento es de exclusiva responsabilidad de los autores y no compromete a la EIA.



**Figure 4.9 Comparison between field obtained and convolution obtained (15m depth) accelerogram (Geoestudios S.A, 2016).**

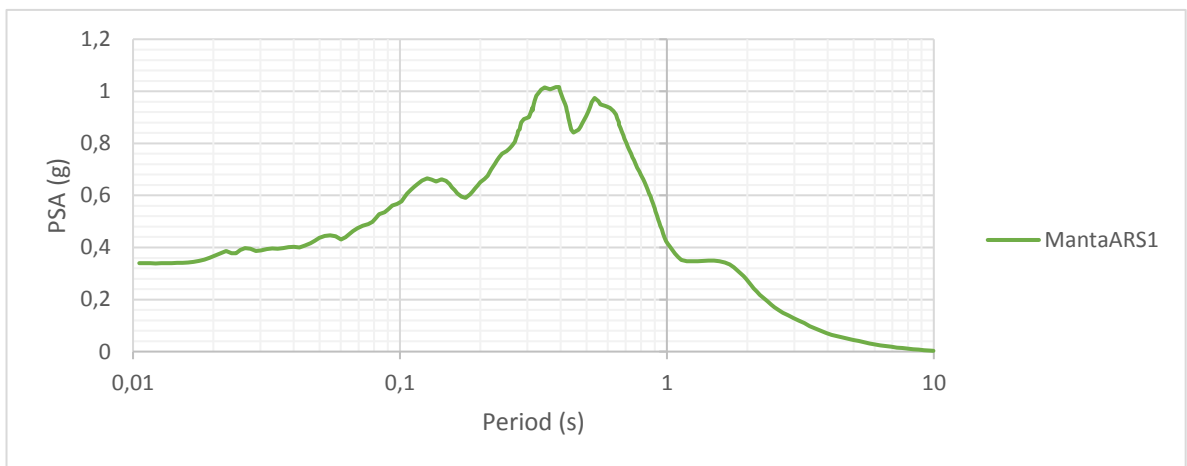


**Figure 4.10 Response spectrum at surface at ARS1 zone.**

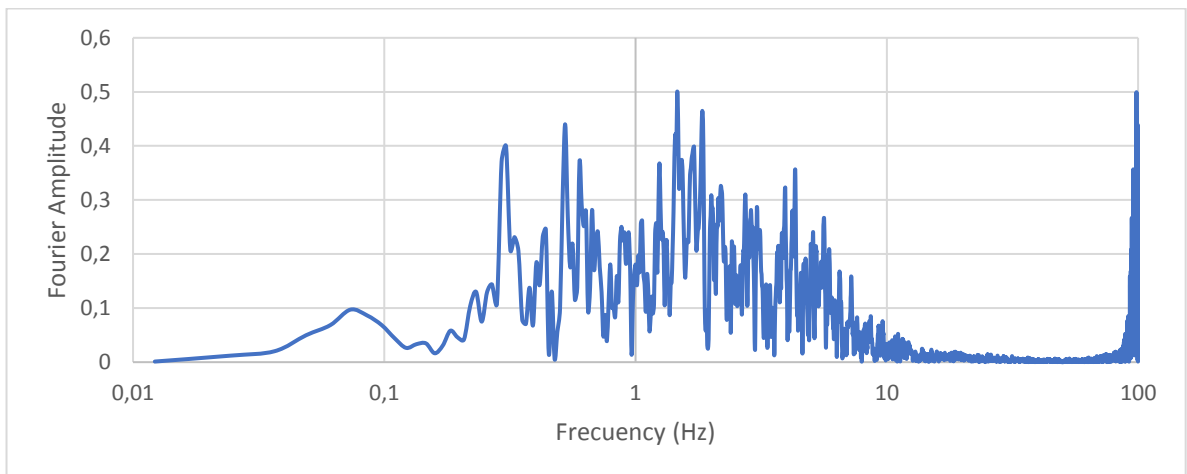


**Figure 4.11 Fourier spectrum.**

La información presentada en este documento es de exclusiva responsabilidad de los autores y no compromete a la EIA.

### 4.3 OPENSEES MODEL

Now, with a stratigraphic condition defined, as the seismic loading and a calibration of parameters for two types of relative densities, an initial process of free field analysis is started to determinate if the constitutive model (PDMY02) is capable to reproduce the conditions of a seismic event, principally around accelerations, settlements and excess of pore water pressure values. With that in mind, a shear beam model is used principally because of the simplicity about coding process. On the other hand, a limitation of this model is because total soil thick is 15m and not 30m as the conventional situation is recommended (this comes from the definition of 30m to determinate the shear wave velocity to characterize the ground surface).

The model starts an initial definition of properties of soil based on 2 units, Unit A and Unit B, product of considerate from **Table 3.2**, two conditions of N<sub>spt</sub> values and liquefaction susceptibility. The first layer (Unit A) will be controlled by lower densities parameters, and the other unit (Unit B) will be controlled by higher densities parameters values. This information is summarized in the next table.

**Tabla 4.1 Soil layer definition.**

Input Data				Liquefaction Susceptibility - Sands	Soil Layer
Layer	Depth (m)	N <sub>SPT</sub>	Clasificati on (USCS)	F <sub>S<sub>liq</sub></sub>	-
1	0.30			-	Unit A
2	0.75	19	SM	-	
3	1.20	15	SP-SM	-	
4	1.65	16	SP-SM	-	
5	2.10	10	SP-SM	0.47	
6	2.55	21	SP	0.82	
7	3.00	23	SP	0.86	
8	3.45	12	SP	0.39	
9	3.90	16	SM	0.59	
10	4.35	14	SM	0.48	
11	4.80	11	SM	0.38	
12	5.25	9	SM	0.32	
13	5.85	10	SM	0.30	
14	6.30	48	SM	>2.00	Unit B
15	9.00	100	SM	>2.00	
16	12.00	100	SM	>2.00	
17	14.50	100	SP-SM	>2.00	
18	17.00	100	SP-SM	>2.00	
19	19.55	100	SM	>2.00	
20	20.00	56	SM	>2.00	

About the definition of mesh, the column has a transversal section of 1mX1m and the thickness of every node is defined in function of a maximum value of this dimension, using

La información presentada en este documento es de exclusiva responsabilidad de los autores y no compromete a la EIA.



the (Lysmer & Kuhlemeyer, 1969) approximation, where they suggest that maximum value can be determinate as follows:

$$Max. Size = \frac{\lambda}{8} = \frac{V_{s min}}{8 * f_{max}}$$

Where  $V_{s min}$  is the lowest wave velocity value of soil.

$V_{s min} = 150 m/s$  from **Figure 4.7 Profile D** (Geoestudios S.A, 2016). and  $f_{max} = 1.46 Hz$  from **Figure 4.11 Fourier spectrum**.

$$Max. Size = \frac{150 m/s}{8 * 1.46 Hz} = 12.84m$$

On the other hand, a suggested mesh is get from Geoestudios report, where 44 elements where used, and the definitions of soil layer differs at used on this analysis, nevertheless this proposal is used because it guaranties a non-convergence problem. To eliminate another possible numerical variation, the same SSP Brick UP element will be use. This mesh is presented at next.

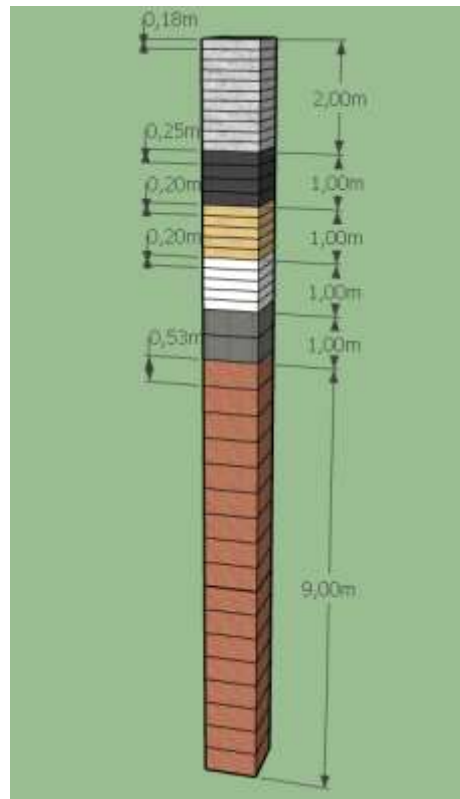


**Figure 4.12 Shear beam test mesh.**

Once the model elements are defined (soil parameters, mesh, loading conditions), this are the results got.

La información presentada en este documento es de exclusiva responsabilidad de los autores y no compromete a la EIA.

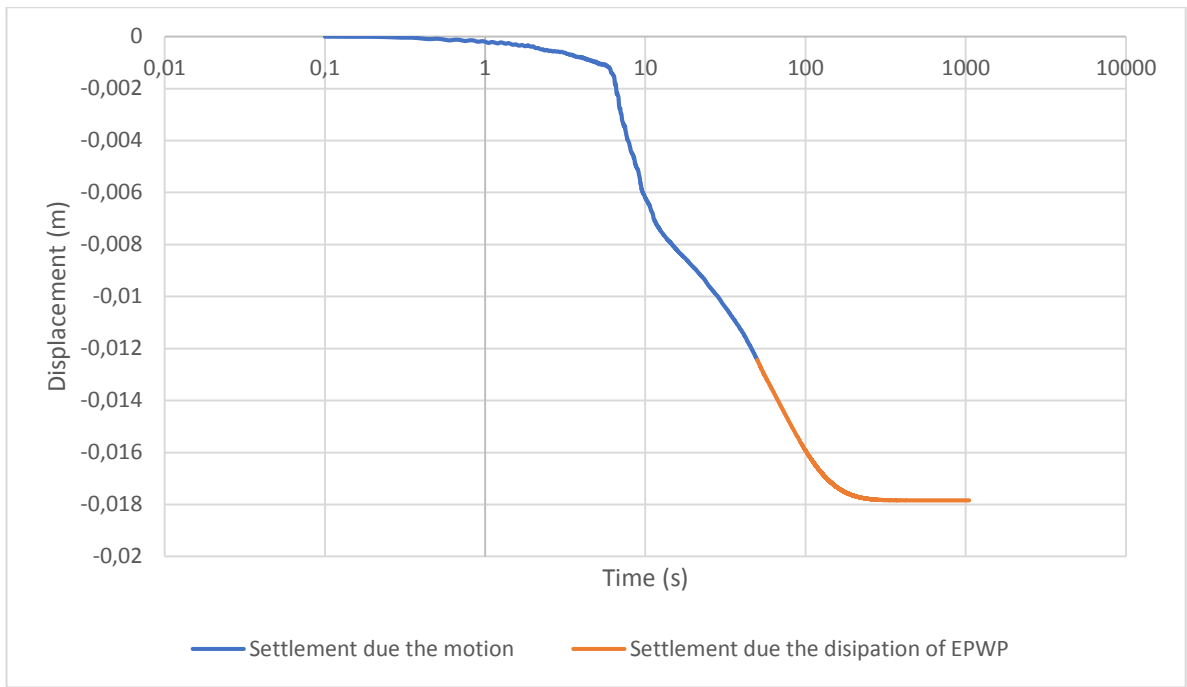


**Figure 4.13 Vertical Displacement (km 0+750)**

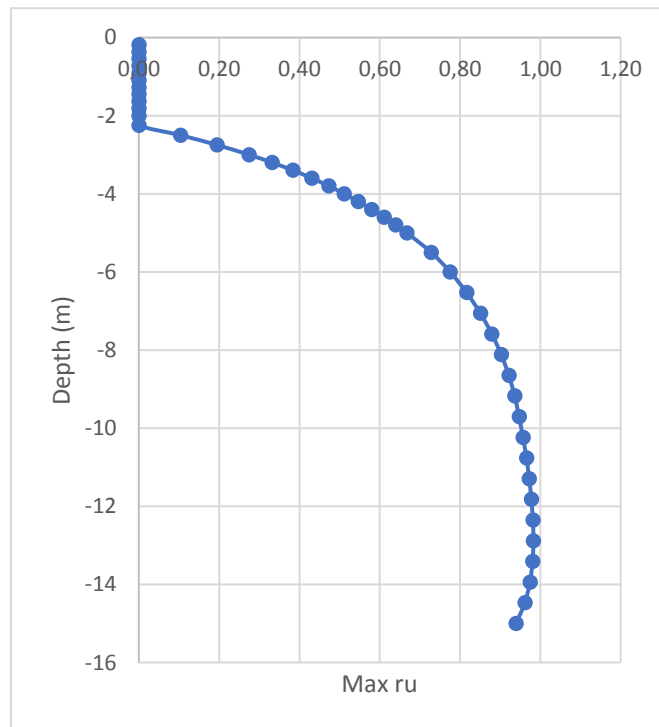


**Figure 4.14 Maximum ru value achieved in different depths.**

As is see it from **Figure 4.6** and **Figure 4.13**, the values of settlement due the seismic condition are similar around 0.015m and 0.018m respectively, and the results of **Figure 4.14** say that not just the initial 6m are susceptible of liquefaction, but even at 15m the excess

La información presentada en este documento es de exclusiva responsabilidad de los autores y no compromete a la EIA.

pore water pressure ratio values could suggest an instability, for a further conclusion is needed a deepest analysis (a larger shear beam column and a refined stratigraphy). The variation of excess pore water pressure ratio in time is presented at next, that says the model is capable to capture excess water pressure under a cyclic loading condition, been stable until 50 seconds (the end of seismic event is around this time), and later is capable to dissipate it.

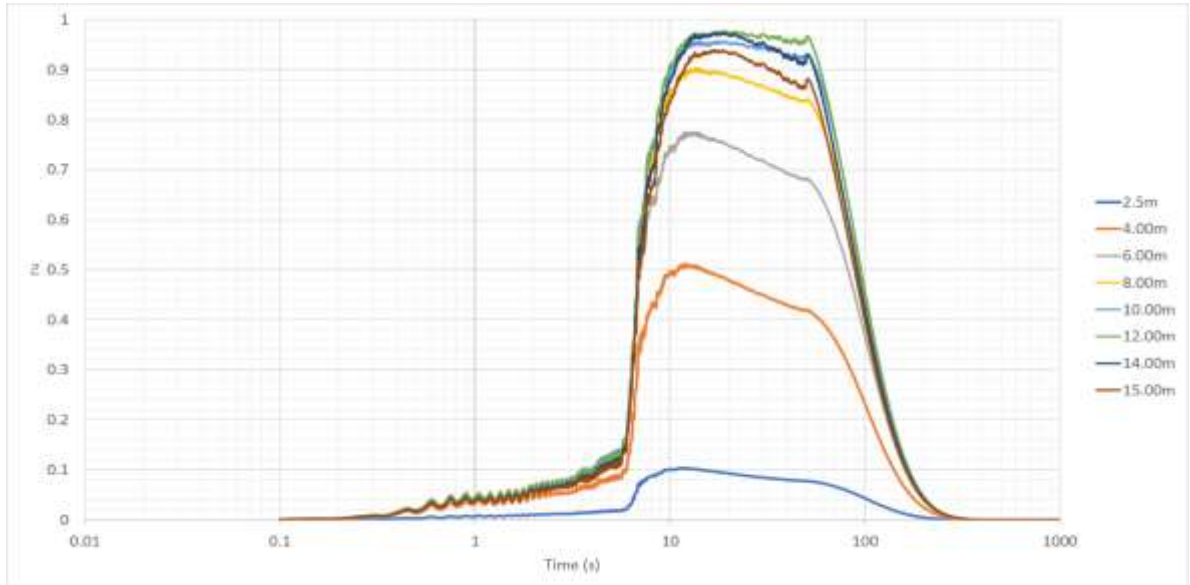


**Figure 4.15 Excess of pore water pressure ratio in time.**

### 4.3.1 VALIDATION AGAINST DEEPSOIL

Another validation of this modeling process is compare the OpenSees results with a DeepSoil simulation where a non-linearity soil model is used, with a General Quadratic/Hyperbolic model (GQ/H model). At next is presented the soil parameters per soil layer, and because is a non-linearity simulation, the stiffness degradation and damping backbone curves are presented.

**Table 4.1 DeepSoil model parameters.**

Layer	Thickness (m)	Soil Weight (kN/m <sup>3</sup> )	Wave Shear Velocity (m/s) <b>Figure 4.7</b>
Layer 1	2	19	120
Layer 2	1	19	135
Layer 3	1	19	145
Layer 4	1	19	145
Layer 5	1	19	155
Layer 6	4	19	260
Layer 7	5	19	260

La información presentada en este documento es de exclusiva responsabilidad de los autores y no compromete a la EIA.

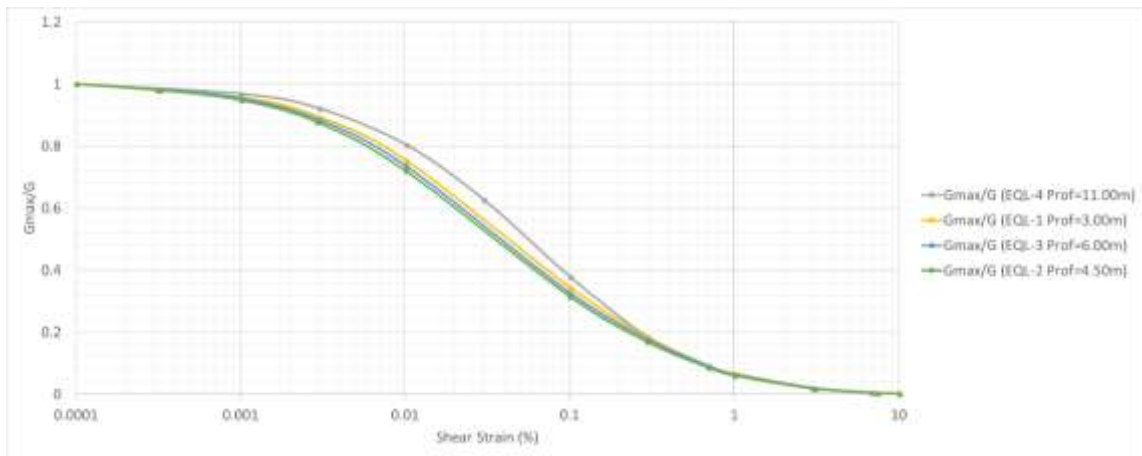


**Figure 4.16 Degradation of stiffness due shear strain at different depths (Geoestudios S.A, 2016).**

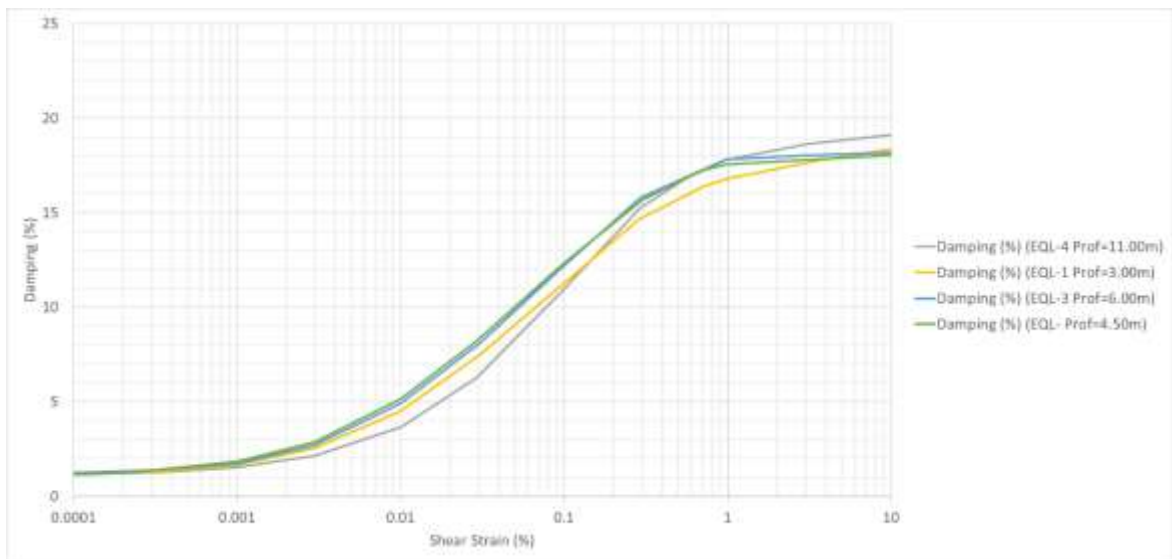


**Figure 4.17 Damping due shear strain at different depths (Geoestudios S.A, 2016).**

Once the model is completed, here are the results over response spectrum and shear strain.

La información presentada en este documento es de exclusiva responsabilidad de los autores y no compromete a la EIA.

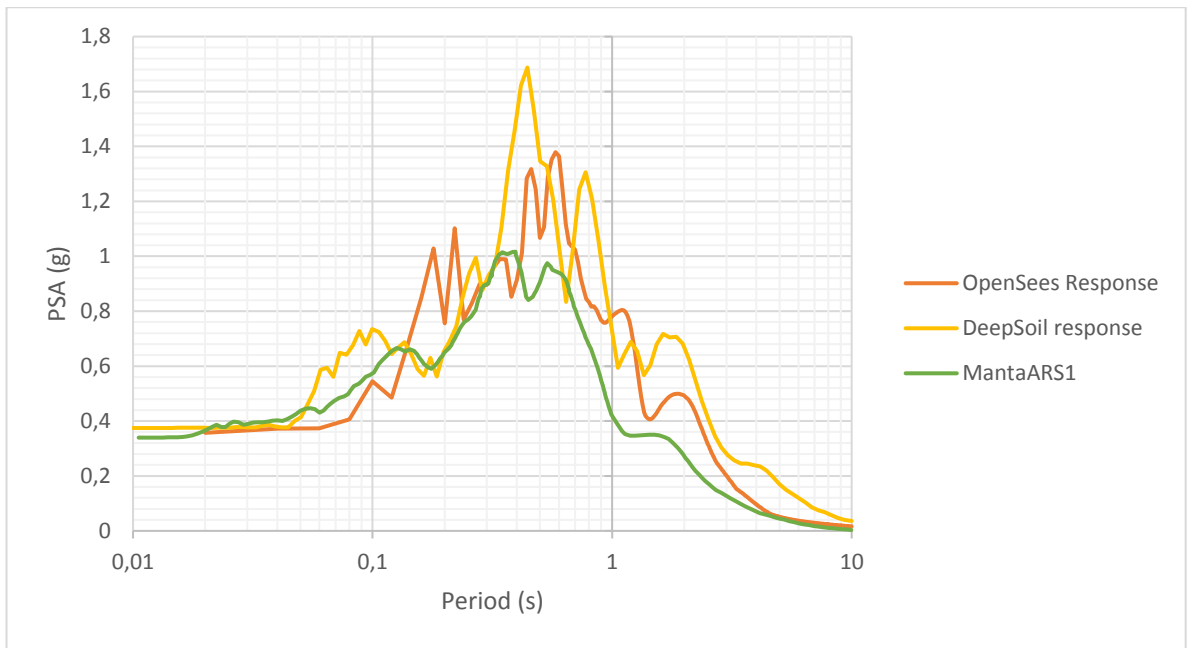


**Figure 4.18 Response spectrum comparison.**

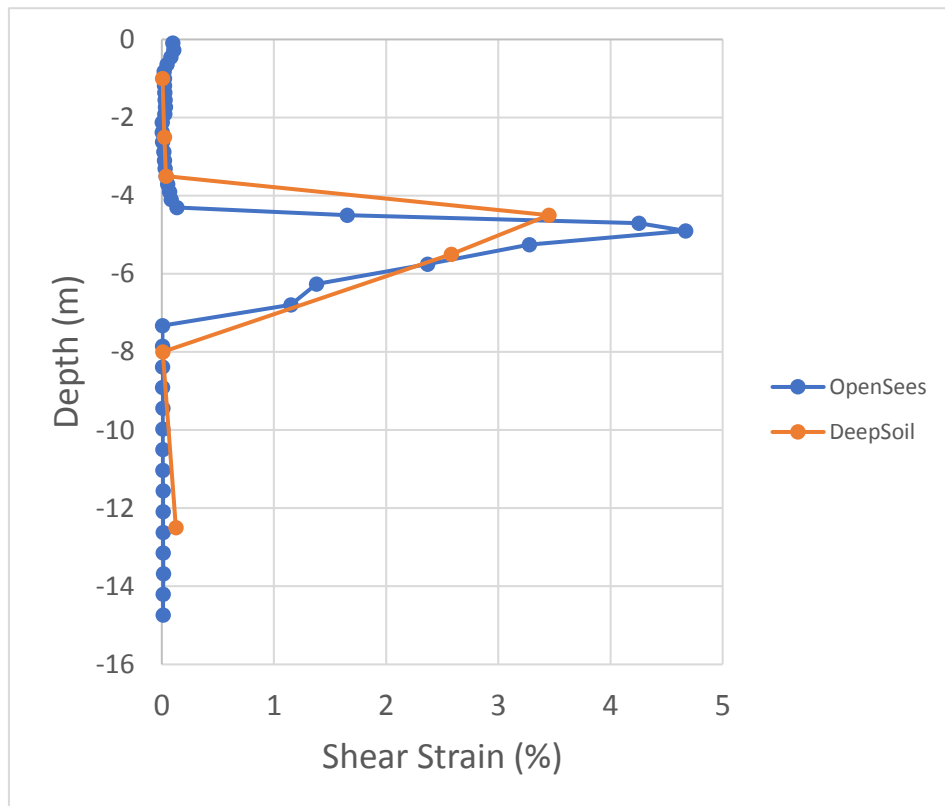


**Figure 4.19 Shear strain comparison.**

La información presentada en este documento es de exclusiva responsabilidad de los autores y no compromete a la EIA.

As is seen in the **Figure 4.18**, the OpenSees and DeepSoil simulation tends to overpredict the acceleration in all range of periods, this could be explained because the poorly stratigraphic definition, where a continuous value of elastic parameters in the first 6m and second 9m is defined, and otherwise in the **Figure 4.19**, the overprediction of shear strain could be explained to poorly calibration of contractive parameters of PDMY02 model ( $c_1, c_2, c_3$  and PT angle).

## 5. SUMMARY AND CONCLUSIONS

Based on the 2 monotonic drained TXC tests, the model is capable of capturing not just the volumetric changes, the stiffness degradation, but also the resistance product of mechanic response without softening, something that is a limitation of the model. About the undrained monotonic tests, at large deformation the model overpredicted the mechanic response on deviatoric and excess pore water pressure level, and underpredicted the degradation of stiffness, even though only the elastic parameters on the first model calibration had been changed, and the tendency around the mechanic response is correct.

On the other hand, the cyclic mechanical response of TXC tests says that under lower relative densities, the soil tends to reproduce a contractive response, where the pore water pressure tries to increase and the instability of soil is reached, indicating a liquefaction potential around this density conditions, and on the TXC tests with higher relative densities, the mechanic response under higher axial strains (0.25% or higher) shows a dilatancy response condition that express a lower potential of liquefaction, because of an increase of volume that tends to create lower excess pore water pressure values, and under lower axial strains (0.07%), the mechanic response tends to a slower process of contraction, something that could express a potential of liquefaction if the excitation tends to create actually lower and constant strain conditions. Both conditions are captured with two sets of parameters, after a manual optimization of model parameters, first a sensibility analysis to identify the role of each parameter, followed by an individual calibration and at the end, after verifying that any of the individual sets were capable to reproduce the other conditions of loadings, an average process over each parameter is considered the best approximation to capture the mechanic response for two conditions with two sets of parameters, one for lower and another for higher densities. Now with a calibration process done, one of the principal limitations of model is due to an overprediction of extension response, and this could be explained because the use of an isotropic definition of multiple yield surface, and isotropic phase transformation angle (responsible of switch the dilatancy of contractive response of soil), which could be managed with an inclusion of back-bone curve for extensive conditions, which are in charge of creating a different distribution of yield surfaces on this loading process.

About the calibration process, the main parameter that actually controls the mechanic response (contractive or dilatancy behavior) is the phase angle, which is the one that defines the most part of the calibration process, the other parameters ( $c_1$ ,  $c_2$ ,  $c_3$ ,  $d_1$ ,  $d_2$  and  $d_3$ ) are just fitting parameters that could allow a better approximation in terms of velocity of bearing loss capacity or accumulation of excess pore water pressure.

Now, once the TXC tests calibration is finished, the use of this information is the first step to reproduce the behavior after an earthquake event produced in April 16<sup>th</sup> of 2016 in Manta Ecuador. First of all, a determination not just the stratigraphy must be defined, but the seismic loading has to be determinated. The soil layers were obtained thanks to Geoestudios works, where after this event a local ground motion studio was done, and different soil profiles where defined. The D-D' profile had to be selected because it is near to the place where the sands samples where obtained for the TXC tests, and because an

La información presentada en este documento es de exclusiva responsabilidad de los autores y no compromete a la EIA.

altimetry line was executed, and for free field simulations this is a good parameter to determine the fitting with experimental results.

The seismic loading was selected because a deconvolution process made by Geoestudios in the ARS1 zone in Tarqui suburb, that shows the limitation of presents the accelerogram at 15m of depth. Once these two conditions were defined, an initial profile definition of layer distribution for a shear beam analysis is proposed, where the first 6 meters of soil were modeled by the first set of parameters of PDMY02 model (lower densities set) and the next 9 meters with the second set. The results presented shows a good fitting in the acceleration and settlement level, besides presenting an instability not just the first 6 meters (as the semiempirical susceptibility of liquefaction says) but the next 9 meters presented an even higher condition of bearing loss capacity. The OpenSees results were comparable with DeepSoil, showing similar responses in terms of accelerations and shear strains.

The OpenSees free field results for the Manta case history were compared to the conventional 1D DeepSoil software and field performance data collected at Manta site. A reasonable agreement between the results was found in terms of acceleration, deformations and shear strains. It shows that the PMYD02 constitutive soil model is promising for capturing post-liquefaction behavior of geo-structures.

Future work must be done tacking into consideration the results presented and developing at minimum 30 meters simulation of shear beam analysis, with a refined stratigraphy that could be calibrated with CPTu test executed in the zone of study. Once the free field is validated with the field measures, a soil - structure interaction simulation must be done to analyze the capability of the model to reproduce the post liquefaction behavior of structures of 1 and 2 floors.



## REFERENCES

- Badanagki, M. (2016). *Isotropically consolidated undrained cyclic triaxial tests: (Vol. 13)*.
- Boulanger, R. W., & Ziotopoulou, K. (2015). PM4SAND (Version 3): A Sand Plasticity Model for Earthquake Engineering Applications, (March), 108.
- Campos Sigüenza, A. (1992). *Ensayo triaxial dinámico*.
- Carrillo, N., & Casagrande, A. (1944). *Shear Failure of Anisotropic Materials*. Cambridge, Massachusetts: Harvard Graduate School of Engineering.
- Elgamal, A., Yang, Z., & Parra, E. (2002). Computational modeling of cyclic mobility and post liquefaction site response. *Soil Dynamics and Earthquake Engineering*, 22(4), 259–271.
- Fayun, L., Haibing, C., & Maosong, H. (2017). Accuracy of three-dimensional seismic ground response analysis in time domain using nonlinear numerical simulations, (July). <https://doi.org/10.1007/s11803-017-0401-1>
- Galavi, V., Petalas, A., & Brinkgreve, R. B. . J. (2013). Finite Element Modelling of Seismic Liquefaction in Soils. *Geotechnical Engineering Journal*, 44(3), 55–64.
- García Núñez, J. R. (2007). *Análisis comparativo del fenómeno de licuación en arenas. Aplicación Tumaco (Colombia)*. Universitat Politècnica de Catalunya. Retrieved from <http://hdl.handle.net/10803/6249>
- GDS. (2013). Part one: Introduction to triaxial testing, 1(Cd), 1–4.
- Geoestudios S.A. (2016). *Estudio geotécnico y de riesgo sísmico de la zona tarqui de la ciudad de manta de acuerdo a la norma ecuatoriana de la construcción 2015 Entregable #2*.
- Grunauer, X. V. (2017). Enseñanzas del Sismo del 16 de Abril de 2016 Temario. In *Comportamiento de Terraplenes y Cimentaciones en el Sismo del 16A16*. Quito.
- Gutscher, M., Malavieille, J., Lallemand, S., & Collot, J. (1999). Tectonic segmentation of the North Andean margin : impact of the Carnegie Ridge collision, 168, 255–270.
- Hill, R. (1950). *The mathematical theory of plasticity*. (Oxford University Press, Ed.). London: Oxford University Press.
- Kamalzare, S., Dove, J. E., Flint, M. M., Green, R. A., & Rodriguez-marek, A. (2016). Performance of Columnar Reinforced Ground during Seismic Excitation.
- Karimi, Z. and dashti, S. (2015). Numerical Simulation of Earthquake Induced Soil

La información presentada en este documento es de exclusiva responsabilidad de los autores y no compromete a la EIA.

Liquefaction : Validation. *Ifcee2015*, 11–20.

- Karimi, Z., & Dashti, S. (2016). Seismic Performance of Shallow Founded Structures on Liquefiable Ground: Validation of Numerical Simulations Using Centrifuge Experiments. *Journal of Geotechnical and Geoenvironmental Engineering*, 142(6), 04016011. [https://doi.org/10.1061/\(ASCE\)GT.1943-5606.0001479](https://doi.org/10.1061/(ASCE)GT.1943-5606.0001479)
- Khosravifar, A. (2013). A note on calibrating PDMY. In *Journal of Chemical Information and Modeling* (Vol. 53, pp. 1689–1699). <https://doi.org/10.1017/CBO9781107415324.004>
- Kramer, S. L. (2008). Performance-Based Earthquake Engineering: Opportunities and Implications for Geotechnical Engineering Practice. In ASCE (Ed.), *Geotechnical Earthquake Engineering and Soil Dynamics IV* (pp. 1–32). Retrieved from <http://ascelibrary.org/doi/book/10.1061/9780784409756>
- Kramer, S. L., Arduino, P., & Shin, H. (2008). Using OpenSees for Performance-Based Evaluation of Bridges on Liquefiable Soils Using OpenSees for Performance-Based Evaluation of Bridges on Liquefiable Soils, (November).
- Ladd, C. (1995). Estimation of design  $S_u$  in practice (p. 29). Boston: MIT Press.
- Larsen, K. A., & Ibsen, L. B. (2006). *Method for Predicting Void Ratio and Triaxial Friction Angle from Laboratory CPT at Shallow Depths*. AAU Geotechnical Engineering Papers. Retrieved from [http://vbn.aau.dk/files/208102277/Method\\_for\\_Predicting\\_Void\\_Ratio\\_and\\_Triaxial\\_Friction\\_Angle\\_from\\_Laboratory\\_CPT\\_at\\_Shallow\\_Depths.pdf](http://vbn.aau.dk/files/208102277/Method_for_Predicting_Void_Ratio_and_Triaxial_Friction_Angle_from_Laboratory_CPT_at_Shallow_Depths.pdf)
- Lopez-caballero, F., & Modaressi, A. (2008). Numerical simulation of liquefaction effects on seismic SSI Fernando Lopez-Caballero , Arezou Modaressi Numerical simulation of liquefaction effects on seismic SSI.
- Lu, J. (2006). Parallel finite element modeling of earthquake ground response and liquefaction, 359.
- Lysmer, J., & Kuhlemeyer, A. M. (1969). Finite dynamic model for infinite media. *Journal of the Engineering Mechanics Division*, 95, 859–877.
- Matter, G., & Jang, E. (2014). How contact stiffness and density determine stress-dependent elastic moduli: A micromechanics approach, (May). <https://doi.org/10.1007/s10035-013-0456-2>
- McManus, K. (2016). Earthquake geotechnical engineering practice. *New Zealand Geotechnical Society INC*, 60. Retrieved from <https://www.building.govt.nz/assets/Uploads/building-code-compliance/b-stability/b1-structure/geotechnical-guidelines/geotech-module-4.pdf>
- Mercado Martínez Aparicio, J. A. (2016). *SIMULATION OF LIQUEFACTION-INDUCED DAMAGE OF THE PORT OF LONG BEACH CALIFORNIA USING THE UBC3D-PLM MODEL*.

La información presentada en este documento es de exclusiva responsabilidad de los autores y no compromete a la EIA.

- Nieto Leal, A., Camacho-Tauta, J. F., & Ruiz Blanco, E. F. (2009). Determinación de parámetros para los modelos elastoplásticos mohr-coulomb y hardening soil en suelos arcillosos. *Revista Ingenierías Universidad de Medellín*, 8(15), 75–91. Retrieved from <http://revistas.udem.edu.co/index.php/ingenierias/article/view/63>
- Nikolaou, S., Vera-Grunauer, X., & Gilsanz, R. (2016). *GEER-ATC earthquake reconnaissance April 16th 2016, Muisne, Ecuador*. Muisne: GEER.
- Petalas, A., & Galavi, V. (2013). UBC3D-PLM.
- Roscoe, K. H., & Burland, J. B. (1970). On the generalized stress-strain behavior of “wet” clay. *Journal of Terramechanics*, 7(2), 107–108. [https://doi.org/10.1016/0022-4898\(70\)90160-6](https://doi.org/10.1016/0022-4898(70)90160-6)
- Seed, H. B. (1987). Design Problems in Soil Liquefaction. *Journal of Geotechnical Engineering*, 113(8). [https://doi.org/https://doi.org/10.1061/\(ASCE\)0733-9410\(1987\)113:8\(827\)](https://doi.org/https://doi.org/10.1061/(ASCE)0733-9410(1987)113:8(827))
- SSPbrickUP Element. (2017). Retrieved October 5, 2018, from [http://opensees.berkeley.edu/wiki/index.php/SSPbrickUP\\_Element](http://opensees.berkeley.edu/wiki/index.php/SSPbrickUP_Element)
- Stark, T., Olson, S., Kramer, S. L., & Youd, L. (1989). Shear strength of liquefied soil, 30(3), 153–158.
- Stark, T., & Vettel, J. (1991). Effective Stress Hyperbolic Stress Strain Parameters for Clay. *Geotechnical Testing Journal*, 14(2), 146–156.
- Ti, K. S. (2014). *A Review of Basic Soil Constitutive Models for Geotechnical Application*.
- Vesic, A. (1969). Experiments with instrumented pile groups in sand. *Performance of Deep Foundations, ASTM Spec*, 444, 177–222.
- Wu, J., Kammerer, A. M., Riemer, M. F., Seed, R. B., & Pestana, J. M. (2004). Laboratory study of liquefaction triggering criteria. In *13th World Conference on Earthquake Engineering*.
- Zienkiewicz, O., & Shiomi, T. (1984). Dynamic behavior of saturated porous media; the generalized Biot formulation and its numerical solution. *International Journal for Numerical Methods in Geomechanics*, 8, 71–96.

## APPENDIX A

OpenSees code for an isotopically consolidated undrained triaxial test (CIU TXC test).

```
#####
# Model with SSPBrick Element and PressureDependentMultiYield02 material #
# By: Jaime A. Mercado April 17th 2018 #
# Version 1 #
#####
wipe
wipe all
set startT [clock seconds]
# -----
# U N I T S
# -----
# Length : m
# Force : kN
# Stress : kPa
# Mass : ton
##### MAIN USER INPUTS #####

set Analysis_case "undrained_cyclic"
# Options:
# undrained_cyclic
# undrained_monotonic: define target max shear strain ($devDisp)
set consolidation_type "isotropic"
# Options:
# isotropic
# ko

set matTag 1; # material Tag
set matType "PDMY02"; # use PDMY02 for sand, or MD for Manzaris
Dafalias
set LoadingMode "StrainC"; # use StrainC for strain-controlled or
StressC for stress-controlled
set vertPress [expr 1.0*100.]; # kPa vertical confining pressure
set ko [expr 0.5*$vertPress]; # kPa lateral confining pressure (this just
works used when ko consolidation is chosen)
set loadbias 0.0; # Alpha = tau_xy/s'vo
set sigmad 100.; # kPa vertical deviator stress (only works for
the monotonic case) THIS IS FOR STRESS CONTROL
set cycDev 100.; # Applied sinusoidal loading amplitude (only
works for the cyclic case) THIS IS FOR STRESS CONTROL
set target_shear_strain [expr 1.0*0.00070]; # Target shear strain (only works for the
cyclic case) THIS IS FOR STRAIN CONTROL
set frequency 1.; # Hz (only works for the cyclic case)
set devDisp -0.18; # Deviatoric strain (This only works for
monotonic case) THIS IS FOR STRAIN CONTROL
# # # # # Average High Dr (3 tests)
# set massDen 1.90
# set refG 66333.33
# set refB 165000.00
# set frinctionAng 31.67
# set peakShearStrain 0.15
# set refPress 101.00
# set pressDependCoe 0.50
# set phaseTransAng 25.33
# set contractionParam1 0.11
# set contractionParam2 1.00
# set contractionParam3 0.7
# set dilationParam1 0.15
```

La información presentada en este documento es de exclusiva responsabilidad de los autores y no compromete a la EIA.

```

# set dilationParam2 2.3
# set dilationParam3 0.025
# set liqParam1 1.00
# set liqParam2 0.00
# set noYieldSurf 20.00
# set void 0.75
# set cs1 0.90
# set cs2 0.02
# set cs3 0.00
# set pa 101.00
# set c 0.10
# Average Test #5 and %#6
# set massDen 1.9
# set refG 67000
# set refB 165000
# set frinctionAng 33
# set peakShearStrain 0.15
# set refPress 101
# set pressDependCoe 0.5
# set phaseTransAng 22
# set contractionParam1 0.13
# set contractionParam2 1
# set contractionParam3 0.65
# set dilationParam1 0.2
# set dilationParam2 2
# set dilationParam3 0.05
# set liqParam1 1
# set liqParam2 0
# set noYieldSurf 20
# set void 0.75
# set cs1 0.9
# set cs2 0.02
# set cs3 0
# set pa 101
# set c 0.1
# # # # # # # # Average Low Dr
set massDen 1.9
set refG 60000
set refB 160000
set frinctionAng 21
set peakShearStrain 0.15
set refPress 101
set pressDependCoe 0.5
set phaseTransAng 27
set contractionParam1 0.07
set contractionParam2 0.5
set contractionParam3 0.6
set dilationParam1 0.75
set dilationParam2 3
set dilationParam3 0
set liqParam1 1.3
set liqParam2 0
set noYieldSurf 40
set void 0.5
set cs1 0.9
set cs2 0.02
set cs3 0
set pa 101
set c 0.1
# Sensibility Analysis over PT C1 C3 D1
# set massDen 1.9; # (ton/m3)
# set refG 8.e4; # (kPa)
# set refB 18.e4; # (kPa)
# set frinctionAng 35.; # (degree)
# set peakShearStrain 0.15;
# set refPress 101.; # (kPa)

```

La información presentada en este documento es de exclusiva responsabilidad de los autores y no compromete a la EIA.

```

# set pressDependCoe      0.5;
# set phaseTransAng      29.; # (degree)
# set contractionParam1   0.12; # Contraction rate.
# set contractionParam2   0.5; # fabric damage
# set contractionParam3   1.6; # k_sigma effect      1.6 1.2 0.8 /0.6/ 0.4
# set dilationParam1     2.0; # 2.0 1.5 1.0 /0.75/ 0.50 0.25
# set dilationParam2     3.0; # As suggested by the manual
# set dilationParam3     0.; #
# set liqParam1          1.3;
# set liqParam2          0.0;
# set noYieldSurf        40;
# set void               0.5;
# set cs1                0.9;
# set cs2                0.02;
# set cs3                0.0;
# set pa                 101.; # (kPa)
# set c                  0.1; # (kPa)
# Constitutive soil model parameters input
# define variables for Sand
# set massDen 1.9
# set refG 7.00E+04
# set refB 1.65E+05
# set frinctionAng 35.
# set peakShearStrain 0.15
# set refPress 101.
# set pressDependCoe 0.5
# set phaseTransAng 28.
# set contractionParam1 0.07
# set contractionParam2 1.
# set contractionParam3 0.2
# set dilationParam1 0.4
# set dilationParam2 0.01
# set dilationParam3 0.1
# set liqParam1 6.
# set liqParam2 0.
# set noYieldSurf 20.
# set void 0.75
# set cs1 0.9
# set cs2 0.02
# set cs3 0.
# set pa 101.
# set c 0.1
# # # # # # # # TEST #1
# set massDen 1.9; # (ton/m3)
# set refG 6.e4; # (kPa)
# set refB 16.e4; # (kPa)
# set frinctionAng 20.; # (degree)
# set peakShearStrain 0.15;
# set refPress 101.; # (kPa)
# set pressDependCoe 0.5;
# set phaseTransAng 20.; # (degree)
# set contractionParam1 0.07; # Contraction rate.
# set contractionParam2 2.0; # fabric damage
# set contractionParam3 0.6; # k_sigma effect
# set dilationParam1 0.;
# set dilationParam2 3.0; # As suggested by the manual
# set dilationParam3 0.; #
# set liqParam1 1.0;
# set liqParam2 0.0;
# set noYieldSurf 20;
# set void 0.75;
# set cs1 0.9;
# set cs2 0.02;
# set cs3 0.0;
# set pa 101.; # (kPa)

```

La información presentada en este documento es de exclusiva responsabilidad de los autores y no compromete a la EIA.

```

# set c 0.1; # (kPa)
# # # # # # # # # # TEST #2
# set massDen 1.9; # (ton/m3)
# set refG 8.e4; # (kPa)
# set refB 18.e4; # (kPa)
# set frinctionAng 23.; # (degree)
# set peakShearStrain 0.15;
# set refPress 101.; # (kPa)
# set pressDependCoe 0.5;
# set phaseTransAng 29.; # (degree)
# set contractionParam1 0.12; # Contraction rate.
# set contractionParam2 0.5; # fabric damage
# set contractionParam3 0.6; # k_sigma effect
# set dilationParam1 0.75;
# set dilationParam2 3.0; # As suggested by the manual
# set dilationParam3 0.; #
# set liqParam1 1.3;
# set liqParam2 0.0;
# set noYieldSurf 40;
# set void 0.5;
# set cs1 0.9;
# set cs2 0.02;
# set cs3 0.0;
# set pa 101.; # (kPa)
# set c 0.1; # (kPa)
# # # # # # # # # # TEST #3
# set massDen 1.9
# set refG 6.00E+04
# set refB 1.60E+05
# set frinctionAng 21
# set peakShearStrain 0.15
# set refPress 101
# set pressDependCoe 0.5
# set phaseTransAng 27
# set contractionParam1 0.07
# set contractionParam2 0.5
# set contractionParam3 0.6
# set dilationParam1 0.75
# set dilationParam2 3
# set dilationParam3 0
# set liqParam1 1.3
# set liqParam2 0
# set noYieldSurf 40
# set void 0.5
# set cs1 0.9
# set cs2 0.02
# set cs3 0
# set pa 101
# set c 0.1
# # # # # # # # # # TEST #4
# set massDen 1.9
# set refG 6.50E+04
# set refB 1.65E+05
# set frinctionAng 29
# set peakShearStrain 0.15
# set refPress 101
# set pressDependCoe 0.5
# set phaseTransAng 20
# set contractionParam1 0.013
# set contractionParam2 1
# set contractionParam3 0.75
# set dilationParam1 0.1
# set dilationParam2 3
# set dilationParam3 0
# set liqParam1 1
# set liqParam2 0

```

La información presentada en este documento es de exclusiva responsabilidad de los autores y no compromete a la EIA.

```

# set noYieldSurf 20
# set void 0.75
# set cs1 0.9
# set cs2 0.02
# set cs3 0
# set pa 101
# set c 0.1
# # # # # # # # # TEST #5

# set massDen 1.9
# set refG 6.50E+04
# set refB 1.65E+05
# set frinctionAng 31
# set peakShearStrain 0.15
# set refPress 101
# set pressDependCoe 0.5
# set phaseTransAng 19
# set contractionParam1 0.1
# set contractionParam2 1
# set contractionParam3 0.9
# set dilationParam1 0.1
# set dilationParam2 3.
# set dilationParam3 0.
# set liqParam1 1.
# set liqParam2 0.
# set noYieldSurf 20
# set void 0.75
# set cs1 0.9
# set cs2 0.02
# set cs3 0
# set pa 101
# set c 0.1
# # # # # # # # # TEST #6

# set massDen 1.9
# set refG 6.90E+04
# set refB 1.65E+05
# set frinctionAng 35
# set peakShearStrain 0.15
# set refPress 101
# set pressDependCoe 0.5
# set phaseTransAng 25
# set contractionParam1 0.16
# set contractionParam2 1
# set contractionParam3 0.4
# set dilationParam1 0.3
# set dilationParam2 1
# set dilationParam3 0.1
# set liqParam1 1
# set liqParam2 0
# set noYieldSurf 20
# set void 0.75
# set cs1 0.9
# set cs2 0.02
# set cs3 0
# set pa 101
# set c 0.1
# Some variables for the ELEMENT
set fluidDen 1.0; # Fluid mass density
set waterbulk 2.2e6; # kPa
set kdrain 1.e1; # permeability for drained loading
set kundrain 1.e-20; # permeability for undrained loading
set alpha 1.0e-5; # alpha = h^2/(4*(Ks + (4/3)*Gs))
##### END OF MAIN USER INPUTS #####
#Directory
set dir Results.$consolidation_type.$Analysis_case
file mkdir $dir

```

La información presentada en este documento es de exclusiva responsabilidad de los autores y no compromete a la EIA.



```

logFile "TRIAXIAL.txt"

# Some loading related variables
if {$Analysis_case == "undrained_cyclic"} {
    set period [expr 1.0/$frequency];
    set kPerm $kundrain
}
if {$Analysis_case == "undrained_monotonic"} {
    set period 1.;
    set deltaT 100;
    set numSteps 10000;
    set kPerm $kundrain
}
puts "Finished creating loading case..."
##### model domain #####
# node $NodeTag $XCoord $Ycoord $Zcoord
model basic -ndm 3 -ndf 4
# node 1 0.15 0.00 0.00
# node 2 0.15 0.15 0.00
# node 3 0.00 0.15 0.00
# node 4 0.00 0.00 0.00
# node 5 0.15 0.00 0.30
# node 6 0.15 0.15 0.30
# node 7 0.00 0.15 0.30
# node 8 0.00 0.00 0.30
node 1 1.0 0.0 0.0
node 2 1.0 1.0 0.0
node 3 0.0 1.0 0.0
node 4 0.0 0.0 0.0
node 5 1.0 0.0 1.0
node 6 1.0 1.0 1.0
node 7 0.0 1.0 1.0
node 8 0.0 0.0 1.0
# fix $NodeTag x-transl y-transl z-transl
fix 1 0 1 1 1
fix 2 0 0 1 1
fix 3 1 0 1 1
fix 4 1 1 1 1
fix 5 0 1 0 1
fix 6 0 0 0 1
fix 7 1 0 0 1
fix 8 1 1 0 1
##### define material ##### (so far only have the
PDMY02 and Manzari Dafalias)
if {$matType == "PDMY02"} {
# SAND (PDMY02)
nDMaterial PressureDependMultiYield02 $matTag 3 $massDen $refG $refB $frinctionAng \
    $peakShearStrain $refPress $pressDependCoe $phaseTransAng \
    $contractionParam1 $contractionParam3 $dilationParam1 $dilationParam3 \
    $noYieldSurf $contractionParam2 $dilationParam2 $liqParam1 $liqParam2 \
    $void $cs1 $cs2 $cs3 $pa $c;
}
if {$matType == "MD"} {
# ManzariDafalias tag G0 nu e_init Mc c lambda_c e0 ksi
P_atm m h0 ch nb A0 nd z_max cz Den
nDMaterial ManzariDafalias 1 125 0.05 $void 1.25 0.712 0.019 0.934 0.7
100 0.01 7.05 0.968 1.1 0.704 3.5 4 600 1.42
}
# nDMaterial InitialStateAnalysisWrapper 2 $matTag 3
#####

# SSPbrickUP tag i j k l m n p q matTag fBulk fDen k1 k2 k3 void alpha
<b1 b2 b3>
element SSPbrickUP 1 1 2 3 4 5 6 7 8 $matTag $waterbulk $fluidDen $kPerm $kPerm $kPerm
$void $alpha
puts "Finished creating model..."

```

La información presentada en este documento es de exclusiva responsabilidad de los autores y no compromete a la EIA.

```

##### RECORDERS #####
# recorder Node -file pressure.out -time -node 6 -dof 4 vel;
# recorder Element -file stress.out -time stress;
# recorder Element -file strain.out -time strain;

# Rayleigh damping parameter
set pi 3.141592654
set damp 0.3
# set omega1 [expr 2*$pi*0.2]
# set omega2 [expr 2*$pi*20]
# set omega1 0.0157
set omega1 25.
# set omega2 64.123
set omega2 1.123
# set a1 [expr 2.0*$damp/($omega1+$omega2)]
# set a0 [expr $a1*$omega1*$omega2]
set a1 0.0250826
set a0 0.00012707
##### ANALYSIS PARAMETERS #####
# Newmark parameters for elastic
# set gammal 0.5
# set betal 0.25

set gammal 0.5
set betal 0.25
numberer RCM
# system ProfileSPD ufmpack
# system BandGeneral
system UmfPack General
test NormDispIncr 5.e-3 50 2
constraints Penalty 3.e6 3.e1
# constraints Plain
integrator Newmark $gammal $betal;
algorithm KrylovNewton
# algorithm Newton
rayleigh $a0 0. $a1 0.01
# rayleigh 0.1 0.005 0.02 0.03
# rayleigh $a0 $a1 0. 0.0
analysis Transient
# -----
# Stage 1 - Consolidation
# -----

set vN [expr -$vertPress/4.0];
set hN [expr -$ko/4.0];
# # turn on the initial state analysis feature
# InitialStateAnalysis on
if {$consolidation_type == "isotropic"} {
    pattern Plain 1 {Series -time {0 10000 1e10} -values {0 1 1} -factor 1} {
        load 1 $vN 0.0 0.0 0.0
        load 2 $vN $vN 0.0 0.0
        load 3 0.0 $vN 0.0 0.0
        load 4 0.0 0.0 0.0 0.0
        load 5 $vN 0.0 $vN 0.0
        load 6 $vN $vN $vN 0.0
        load 7 0.0 $vN $vN 0.0
        load 8 0.0 0.0 $vN 0.0
    }
}
if {$consolidation_type == "ko"} {
    pattern Plain 1 {Series -time {0 10000 1e10} -values {0 1 1} -factor 1} {
        load 1 $hN 0.0 0.0 0.0
        load 2 $hN $hN 0.0 0.0
        load 3 0.0 $hN 0.0 0.0
    }
}

```

La información presentada en este documento es de exclusiva responsabilidad de los autores y no compromete a la EIA.

```

        load 4 0.0 0.0 0.0 0.0
        load 5 $hN 0.0 $vN 0.0
        load 6 $hN $hN $vN 0.0
        load 7 0.0 $hN $vN 0.0
        load 8 0.0 0.0 $vN 0.0
    }
}
if {$Analysis_case == "undrained_monotonic"} {
analyze 100 100
analyze 10 1000
}

if {$Analysis_case == "undrained_cyclic"} {
#analyze 500 1
#analyze 50 1
analyze 100 100
analyze 10 1000
}
puts "Finished with consolidation stage..."
# # turn off the initial state analysis feature
# InitialStateAnalysis off
# -----
# Stage 2 - Deviatoric Loading
# -----
numberer RCM
# system ProfileSPD ufmpack
# system BandGeneral
system UmfPack General
test NormDispIncr 5.e-3 50 2
constraints Penalty 3.e6 3.e1
# constraints Plain
integrator Newmark $gamma1 $beta1;
algorithm KrylovNewton
# algorithm Newton
rayleigh $a0 0. $a1 0.01
# rayleigh 0.1 0.005 0.02 0.03
# rayleigh $a0 $a1 0. 0.0
analysis Transient
recorder Node -file pressurePT4.out -time -node 6 -dof 4 vel;
recorder Element -file stressPT4.out -time stress;
recorder Element -file strainPT4.out -time strain;

#close drainage
for {set i 1} {$i < 9} {incr i} {
    remove sp $i 4
}
if {$Analysis_case == "undrained_monotonic"} {
analyze 5 0.1
#loadConst -time 20001; # keep consolidation stresses
updateMaterialStage -material $matTag -stage 1; # update materials to ensure plastic
behavior
analyze 5 0.1
}
if {$Analysis_case == "undrained_cyclic"} {
#analyze 50 1
analyze 5 0.1
#loadConst -time 600; # keep consolidation stresses
analyze 5 0.1
}
puts "Drainage closed..."
updateMaterialStage -material $matTag -stage 1; # update materials to ensure plastic
behavior
##### STRESS CONTROL #####
set cyclicL [expr $cycDev/4.0]
if {$LoadingMode == "StressC"} {

```

La información presentada en este documento es de exclusiva responsabilidad de los autores y no compromete a la EIA.

```

if {$Analysis_case == "undrained_cyclic"} {
    #set tStart 600
    #set tEnd 670
    set tStart 0
    set tEnd 301
    # sinusoidal loading
    timeSeries Trig 1 $tStart $tEnd $period
    pattern Plain 2 1 {
        load 1 0.0 0.0 0.0 0.0
        load 2 0.0 0.0 0.0 0.0
        load 3 0.0 0.0 0.0 0.0
        load 4 0.0 0.0 0.0 0.0
        load 5 0.0 0.0 $cyclicL 0.0
        load 6 0.0 0.0 $cyclicL 0.0
        load 7 0.0 0.0 $cyclicL 0.0
        load 8 0.0 0.0 $cyclicL 0.0
    }
    analyze 9500 0.007
puts "Finished with cyclic loading..."
}
}

##### STRAINS CONTROL #####

if {$LoadingMode == "StrainC"} {
if {$Analysis_case == "undrained_cyclic"} {
    set tStart 20000.
    set tEnd 20201.
    model basic -ndm 3 -ndf 4
    # Read vertical displacement of top plane
    set vertDisp [nodeDisp 5 3]

    set shift [expr asin($vertDisp/$target_shear_strain)]
    timeSeries Trig 1 $tStart $tEnd $period -factor 1 -shift $shift
    pattern Plain 2 1 {
        sp 5 3 [expr $target_shear_strain]
        sp 6 3 [expr $target_shear_strain]
        sp 7 3 [expr $target_shear_strain]
        sp 8 3 [expr $target_shear_strain]
    }
    analyze 17000 0.005
    #analyze 3000 0.1
puts "Finished with cyclic loading..."
}
if {$Analysis_case == "undrained_monotonic"} {
    # Read vertical displacement of top plane
    set vertDisp [nodeDisp 5 3]
    # Apply deviatoric strain
    set eDisp [expr 1+$devDisp/$vertDisp]
    eval "timeSeries Path 5 -time {0 20001 20301 1e10} -values {0 1 $eDisp $eDisp}"
    pattern Plain 2 5 {
        sp 5 3 $vertDisp
        sp 6 3 $vertDisp
        sp 7 3 $vertDisp
        sp 8 3 $vertDisp
    }
    analyze 3000 0.1
puts "Finished with monotonic loading..."
}
}
set endT [clock seconds]
puts "Execution time: [expr $endT-$startT] seconds."
puts "Done"
wipe; # flush output stream

```

La información presentada en este documento es de exclusiva responsabilidad de los autores y no compromete a la EIA.

## APPENDIX B

Matlab code for plotting graphics and illustrations.

```
clear all;

%p´ (kPa)VS q(kPa) |||AxialStrain(%)VS q(kPa) |||time(s)VS q(kPa) |||time(s)VS ru |||time(s)VS
ShearStrain(%) |||Axial Strain (%)VS u(kPa)

% h = animatedline('Color',[0 .7 .7]);
plo=load('C:\Users\Diego\Desktop\Carpeta\pressure.out');
slo=load('C:\Users\Diego\Desktop\Carpeta\stress.out');
elo=load('C:\Users\Diego\Desktop\Carpeta\strain.out');

%%%%%%%%%%%%%%%%%%%%%%%%%%%%%%%%%%%%%%%%%%%%%%%%%%%%%%%%%%%%%%%%%%%%%%%%

ploMU=load('C:\Users\Diego\Desktop\Carpeta\pressureMU.out');
sloMU=load('C:\Users\Diego\Desktop\Carpeta\stressMU.out');
eloMU=load('C:\Users\Diego\Desktop\Carpeta\strainMU.out');

%%%%%%%%%%%%%%%%%%%%%%%%%%%%%%%%%%%%%%%%%%%%%%%%%%%%%%%%%%%%%%%%%%%%%%%%
ploPT1=load('C:\Users\Diego\Desktop\Carpeta\pressurePT1.out');
sloPT1=load('C:\Users\Diego\Desktop\Carpeta\stressPT1.out');
eloPT1=load('C:\Users\Diego\Desktop\Carpeta\strainPT1.out');

ploPT2=load('C:\Users\Diego\Desktop\Carpeta\pressurePT2.out');
sloPT2=load('C:\Users\Diego\Desktop\Carpeta\stressPT2.out');
eloPT2=load('C:\Users\Diego\Desktop\Carpeta\strainPT2.out');

ploPT3=load('C:\Users\Diego\Desktop\Carpeta\pressurePT3.out');
sloPT3=load('C:\Users\Diego\Desktop\Carpeta\stressPT3.out');
eloPT3=load('C:\Users\Diego\Desktop\Carpeta\strainPT3.out');

ploPT4=load('C:\Users\Diego\Desktop\Carpeta\pressurePT4.out');
sloPT4=load('C:\Users\Diego\Desktop\Carpeta\stressPT4.out');
eloPT4=load('C:\Users\Diego\Desktop\Carpeta\strainPT4.out');

ploPT5=load('C:\Users\Diego\Desktop\Carpeta\pressurePT5.out');
sloPT5=load('C:\Users\Diego\Desktop\Carpeta\stressPT5.out');
eloPT5=load('C:\Users\Diego\Desktop\Carpeta\strainPT5.out');

ploPT6=load('C:\Users\Diego\Desktop\Carpeta\pressurePT6.out');
sloPT6=load('C:\Users\Diego\Desktop\Carpeta\stressPT6.out');
eloPT6=load('C:\Users\Diego\Desktop\Carpeta\strainPT6.out');

[m,n] = size(plo);

for i=1:m-6

%   p1(i,1)=plo(i+119,1);
%   p1(i,2)=plo(i+119,2);
%
%   s1(i,1)=slo(i+119,1);
%   s1(i,2)=slo(i+119,2);
%   s1(i,3)=slo(i+119,3);
%   s1(i,4)=slo(i+119,4);
%   s1(i,5)=slo(i+119,5);
```

La información presentada en este documento es de exclusiva responsabilidad de los autores y no compromete a la EIA.

```

%      s1(i,6)=s1o(i+119,6);
%      s1(i,7)=s1o(i+119,7);
%      s1(i,8)=s1o(i+119,8);
%
%      e1(i,1)=e1o(i+119,1);
%      e1(i,2)=e1o(i+119,2);
%      e1(i,3)=e1o(i+119,3);
%      e1(i,4)=e1o(i+119,4);
%      e1(i,5)=e1o(i+119,5);
%      e1(i,6)=e1o(i+119,6);
%      e1(i,7)=e1o(i+119,7);
%
p1(i,1)=p1o(i+5,1);
p1(i,2)=p1o(i+5,2);

s1(i,1)=s1o(i+5,1);
s1(i,2)=s1o(i+5,2);
s1(i,3)=s1o(i+5,3);
s1(i,4)=s1o(i+5,4);
s1(i,5)=s1o(i+5,5);
s1(i,6)=s1o(i+5,6);
s1(i,7)=s1o(i+5,7);
s1(i,8)=s1o(i+5,8);

e1(i,1)=e1o(i+5,1);
e1(i,2)=e1o(i+5,2);
e1(i,3)=e1o(i+5,3);
e1(i,4)=e1o(i+5,4);
e1(i,5)=e1o(i+5,5);
e1(i,6)=e1o(i+5,6);
e1(i,7)=e1o(i+5,7);

%      p1(i,1)=p1o(i+200,1);
%      p1(i,2)=p1o(i+200,2);
%
%      s1(i,1)=s1o(i+200,1);
%      s1(i,2)=s1o(i+200,2);
%      s1(i,3)=s1o(i+200,3);
%      s1(i,4)=s1o(i+200,4);
%      s1(i,5)=s1o(i+200,5);
%      s1(i,6)=s1o(i+200,6);
%      s1(i,7)=s1o(i+200,7);
%      s1(i,8)=s1o(i+200,8);
%
%      e1(i,1)=e1o(i+200,1);
%      e1(i,2)=e1o(i+200,2);
%      e1(i,3)=e1o(i+200,3);
%      e1(i,4)=e1o(i+200,4);
%      e1(i,5)=e1o(i+200,5);
%      e1(i,6)=e1o(i+200,6);
%      e1(i,7)=e1o(i+200,7);

end

%%%%%%%%%%%%%%%%%%%%%%%%%%%%%%%%%%%%%%%%%%%%%%%%%%%%%%%%%%%%%%%%%%%%%%%%

[m,n] = size(p1oMU);

```

La información presentada en este documento es de exclusiva responsabilidad de los autores y no compromete a la EIA.

```

for i=1:m-6
    p1oMU(i,1)=p1oMU(i+5,1);
    p1oMU(i,2)=p1oMU(i+5,2);

    s1oMU(i,1)=s1oMU(i+5,1);
    s1oMU(i,2)=s1oMU(i+5,2);
    s1oMU(i,3)=s1oMU(i+5,3);
    s1oMU(i,4)=s1oMU(i+5,4);
    s1oMU(i,5)=s1oMU(i+5,5);
    s1oMU(i,6)=s1oMU(i+5,6);
    s1oMU(i,7)=s1oMU(i+5,7);
    s1oMU(i,8)=s1oMU(i+5,8);

    e1oMU(i,1)=e1oMU(i+5,1);
    e1oMU(i,2)=e1oMU(i+5,2);
    e1oMU(i,3)=e1oMU(i+5,3);
    e1oMU(i,4)=e1oMU(i+5,4);
    e1oMU(i,5)=e1oMU(i+5,5);
    e1oMU(i,6)=e1oMU(i+5,6);
    e1oMU(i,7)=e1oMU(i+5,7);

end

[m,n] = size(p1oMU);
for i=120:m-121
    E(i-119,1)=((-s1oMU(i,4)+s1oMU(i,2)))/((-e1oMU(i,4)))/1000;
    E(i-119,2)=e1oMU(i,4);

end

%%%%%%%%%%%%%%%%%%%%%%%%%%%%%%%%%%%%%%%%%%%%%%%%%%%%%%%%%%%%%%%%%%%%%%%%

[m,n] = size(p1oPT4);
% [m,n] = size(2000);
for i=1:m-121

%     p1PT1(i,1)=p1oPT1(i+119,1);
%     p1PT1(i,2)=p1oPT1(i+119,2);
%
%     s1PT1(i,1)=s1oPT1(i+119,1);
%     s1PT1(i,2)=s1oPT1(i+119,2);
%     s1PT1(i,3)=s1oPT1(i+119,3);
%     s1PT1(i,4)=s1oPT1(i+119,4);
%     s1PT1(i,5)=s1oPT1(i+119,5);
%     s1PT1(i,6)=s1oPT1(i+119,6);
%     s1PT1(i,7)=s1oPT1(i+119,7);
%     s1PT1(i,8)=s1oPT1(i+119,8);
%
%     e1PT1(i,1)=e1oPT1(i+119,1);
%     e1PT1(i,2)=e1oPT1(i+119,2);
%     e1PT1(i,3)=e1oPT1(i+119,3);
%     e1PT1(i,4)=e1oPT1(i+119,4);
%     e1PT1(i,5)=e1oPT1(i+119,5);
%     e1PT1(i,6)=e1oPT1(i+119,6);
%     e1PT1(i,7)=e1oPT1(i+119,7);
%
%
%
%     p1PT2(i,1)=p1oPT2(i+119,1);
%     p1PT2(i,2)=p1oPT2(i+119,2);
%
%
```

La información presentada en este documento es de exclusiva responsabilidad de los autores y no compromete a la EIA.

```

%      s1PT2(i,1)=s1oPT2(i+119,1);
%      s1PT2(i,2)=s1oPT2(i+119,2);
%      s1PT2(i,3)=s1oPT2(i+119,3);
%      s1PT2(i,4)=s1oPT2(i+119,4);
%      s1PT2(i,5)=s1oPT2(i+119,5);
%      s1PT2(i,6)=s1oPT2(i+119,6);
%      s1PT2(i,7)=s1oPT2(i+119,7);
%      s1PT2(i,8)=s1oPT2(i+119,8);
%
%      e1PT2(i,1)=e1oPT2(i+119,1);
%      e1PT2(i,2)=e1oPT2(i+119,2);
%      e1PT2(i,3)=e1oPT2(i+119,3);
%      e1PT2(i,4)=e1oPT2(i+119,4);
%      e1PT2(i,5)=e1oPT2(i+119,5);
%      e1PT2(i,6)=e1oPT2(i+119,6);
%      e1PT2(i,7)=e1oPT2(i+119,7);
%
%
%      p1PT3(i,1)=p1oPT3(i+119,1);
%      p1PT3(i,2)=p1oPT3(i+119,2);
%
%      s1PT3(i,1)=s1oPT3(i+119,1);
%      s1PT3(i,2)=s1oPT3(i+119,2);
%      s1PT3(i,3)=s1oPT3(i+119,3);
%      s1PT3(i,4)=s1oPT3(i+119,4);
%      s1PT3(i,5)=s1oPT3(i+119,5);
%      s1PT3(i,6)=s1oPT3(i+119,6);
%      s1PT3(i,7)=s1oPT3(i+119,7);
%      s1PT3(i,8)=s1oPT3(i+119,8);
%
%      e1PT3(i,1)=e1oPT3(i+119,1);
%      e1PT3(i,2)=e1oPT3(i+119,2);
%      e1PT3(i,3)=e1oPT3(i+119,3);
%      e1PT3(i,4)=e1oPT3(i+119,4);
%      e1PT3(i,5)=e1oPT3(i+119,5);
%      e1PT3(i,6)=e1oPT3(i+119,6);
%      e1PT3(i,7)=e1oPT3(i+119,7);
%
%
%      p1PT4(i,1)=p1oPT4(i+119,1);
%      p1PT4(i,2)=p1oPT4(i+119,2);
%
%      s1PT4(i,1)=s1oPT4(i+119,1);
%      s1PT4(i,2)=s1oPT4(i+119,2);
%      s1PT4(i,3)=s1oPT4(i+119,3);
%      s1PT4(i,4)=s1oPT4(i+119,4);
%      s1PT4(i,5)=s1oPT4(i+119,5);
%      s1PT4(i,6)=s1oPT4(i+119,6);
%      s1PT4(i,7)=s1oPT4(i+119,7);
%      s1PT4(i,8)=s1oPT4(i+119,8);
%
%      e1PT4(i,1)=e1oPT4(i+119,1);
%      e1PT4(i,2)=e1oPT4(i+119,2);
%      e1PT4(i,3)=e1oPT4(i+119,3);
%      e1PT4(i,4)=e1oPT4(i+119,4);
%      e1PT4(i,5)=e1oPT4(i+119,5);
%      e1PT4(i,6)=e1oPT4(i+119,6);
%      e1PT4(i,7)=e1oPT4(i+119,7);
%
%
%      p1PT5(i,1)=p1oPT5(i+119,1);
%      p1PT5(i,2)=p1oPT5(i+119,2);
%
%      s1PT5(i,1)=s1oPT5(i+119,1);
%      s1PT5(i,2)=s1oPT5(i+119,2);
%      s1PT5(i,3)=s1oPT5(i+119,3);

```

La información presentada en este documento es de exclusiva responsabilidad de los autores y no compromete a la EIA.



```

%      s1PT5(i,4)=s1oPT5(i+119,4);
%      s1PT5(i,5)=s1oPT5(i+119,5);
%      s1PT5(i,6)=s1oPT5(i+119,6);
%      s1PT5(i,7)=s1oPT5(i+119,7);
%      s1PT5(i,8)=s1oPT5(i+119,8);
%
%      e1PT5(i,1)=e1oPT5(i+119,1);
%      e1PT5(i,2)=e1oPT5(i+119,2);
%      e1PT5(i,3)=e1oPT5(i+119,3);
%      e1PT5(i,4)=e1oPT5(i+119,4);
%      e1PT5(i,5)=e1oPT5(i+119,5);
%      e1PT5(i,6)=e1oPT5(i+119,6);
%      e1PT5(i,7)=e1oPT5(i+119,7);
%
%
%      p1PT6(i,1)=p1oPT6(i+119,1);
%      p1PT6(i,2)=p1oPT6(i+119,2);
%
%      s1PT6(i,1)=s1oPT6(i+119,1);
%      s1PT6(i,2)=s1oPT6(i+119,2);
%      s1PT6(i,3)=s1oPT6(i+119,3);
%      s1PT6(i,4)=s1oPT6(i+119,4);
%      s1PT6(i,5)=s1oPT6(i+119,5);
%      s1PT6(i,6)=s1oPT6(i+119,6);
%      s1PT6(i,7)=s1oPT6(i+119,7);
%      s1PT6(i,8)=s1oPT6(i+119,8);
%
%      e1PT6(i,1)=e1oPT6(i+119,1);
%      e1PT6(i,2)=e1oPT6(i+119,2);
%      e1PT6(i,3)=e1oPT6(i+119,3);
%      e1PT6(i,4)=e1oPT6(i+119,4);
%      e1PT6(i,5)=e1oPT6(i+119,5);
%      e1PT6(i,6)=e1oPT6(i+119,6);
%      e1PT6(i,7)=e1oPT6(i+119,7);
%
%
%      p1PT1(i,1)=p1oPT1(i+1,1);
%      p1PT1(i,2)=p1oPT1(i+1,2);
%
%      s1PT1(i,1)=s1oPT1(i+1,1);
%      s1PT1(i,2)=s1oPT1(i+1,2);
%      s1PT1(i,3)=s1oPT1(i+1,3);
%      s1PT1(i,4)=s1oPT1(i+1,4);
%      s1PT1(i,5)=s1oPT1(i+1,5);
%      s1PT1(i,6)=s1oPT1(i+1,6);
%      s1PT1(i,7)=s1oPT1(i+1,7);
%      s1PT1(i,8)=s1oPT1(i+1,8);
%
%      e1PT1(i,1)=e1oPT1(i+1,1);
%      e1PT1(i,2)=e1oPT1(i+1,2);
%      e1PT1(i,3)=e1oPT1(i+1,3);
%      e1PT1(i,4)=e1oPT1(i+1,4);
%      e1PT1(i,5)=e1oPT1(i+1,5);
%      e1PT1(i,6)=e1oPT1(i+1,6);
%      e1PT1(i,7)=e1oPT1(i+1,7);
%
%
%      p1PT2(i,1)=p1oPT2(i+1,1);
%      p1PT2(i,2)=p1oPT2(i+1,2);
%
%      s1PT2(i,1)=s1oPT2(i+1,1);
%      s1PT2(i,2)=s1oPT2(i+1,2);
%      s1PT2(i,3)=s1oPT2(i+1,3);
%      s1PT2(i,4)=s1oPT2(i+1,4);

```

La información presentada en este documento es de exclusiva responsabilidad de los autores y no compromete a la EIA.





```

%
%
%
%
% end

%%%%%%%%%%%%%%%%%%%%%%%%%%%%%%%%%%%%%%%%%%%%%%%%%%%%%%%%%%%%%%%%%%%%%%%%

num_test=input('Ingrese el número del ensayo')

fs=[0.5, 0.2, 4, 6];
fs2=[0.5, 0.2, 4, 3];

if num_test==0
hold on
grid on
ASu1=load('C:\Users\Diego\Desktop\Ingeniería Civil\Tesis\Manta-Ecuador\MUAxial
Strain(%)VSu(kPa).txt');
ASq1=load('C:\Users\Diego\Desktop\Ingeniería Civil\Tesis\Manta-
Ecuador\MUAxialStrain(%)VSq(kPa).txt');
pql=load('C:\Users\Diego\Desktop\Ingeniería Civil\Tesis\Manta-
Ecuador\MUp´(kPa)VSq(kPa).txt');
AEq1=load('C:\Users\Diego\Desktop\Ingeniería Civil\Tesis\Manta-
Ecuador\MUAxialStrain(%)VS E undrained(kPa).txt');

% x=ASu1(:,1);
% y=ASu1(:,2);

fs=[0.5, 0.2, 4, 6];
fs2=[0.5, 0.2, 4, 3];
accMul = 2;

figure(1); close 1; figure(1);
plot(ASu1(:,1),ASu1(:,2), '-');
hold on
plot(-e1MU(:,4)*100,p1MU(:,2), 'r');
legend('Lab Test', 'Opensees')
hold off
title ('Axial Strain \epsilon (%) VS. Excess pore water pressure u(kPa)');
xlabel('Axial Strain \epsilon (%)');
ylabel('u (kPa)');
set(gcf, 'paperposition', fs);
grid on

% pause(0.001);

% for i=1:5
% % addpoints (h,x(i),y(i));
% % drawnow
% % % plot(ASu1(:,1),ASu1(:,2), '-');
% % % plot(x(i),y(i), '-');
% % pause(0.001);
% comet(x,y,0.001)
%
% end

figure(2); close 2; figure(2);
plot(ASq1(:,1),ASq1(:,2), '-');
hold on
plot(-e1MU(:,4)*100,-s1MU(:,4)+s1MU(:,2), 'r');
legend('Lab Test', 'Opensees')

```

La información presentada en este documento es de exclusiva responsabilidad de los autores y no compromete a la EIA.

```

hold off
title ('Axial Strain \epsilon (%) VS. Deviatoric Stress q (kPa)');
xlabel('Axial Strain \epsilon (%)');
ylabel('q (kPa)');
set(gcf,'paperposition',fs);
grid on

figure(3); close 3; figure(3);
plot(pq1(:,1),pq1(:,2),'-');
hold on
plot(-(s1MU(:,2)+s1MU(:,3)+s1MU(:,4))/3,-s1MU(:,4)+s1MU(:,2),'r');
legend('Lab Test','Opensees')
hold off
title ('Mean effective Stress p' (kPa) VS. Deviatoric Stress q (kPa)');
xlabel('confinement p' (kPa)');
ylabel('q (kPa)');
set(gcf,'paperposition',fs);
grid on

figure(4); close 4; figure(4);
plot(AEq1(:,1),AEq1(:,2),'-');
hold on
plot(-E(:,2)*100,E(:,1),'r');
legend('Lab Test','Opensees')
hold off
title ('Axial Strain \epsilon (%) VS. Undrained Elastic Modulus Eu (MPa)');
xlabel('Axial Strain \epsilon (%)');
ylabel('Undrained Elastic Modulus Eu (MPa)');
set(gcf,'paperposition',fs);
grid on

end

if num_test==1
hold on
grid on
ASu1=load('C:\Users\Diego\Desktop\Ingeniería Civil\Tesis\Manta-Ecuador\1Axial
Strain(\epsilon)VSu(kPa).txt');
ASq1=load('C:\Users\Diego\Desktop\Ingeniería Civil\Tesis\Manta-
Ecuador\1AxialStrain(\epsilon)VSq(kPa).txt');
pq1=load('C:\Users\Diego\Desktop\Ingeniería Civil\Tesis\Manta-
Ecuador\lp'(kPa)VSq(kPa).txt');
tq1=load('C:\Users\Diego\Desktop\Ingeniería Civil\Tesis\Manta-
Ecuador\ltime(s)VSq(kPa).txt');
tru1=load('C:\Users\Diego\Desktop\Ingeniería Civil\Tesis\Manta-
Ecuador\ltime(s)VSru.txt');
tSS1=load('C:\Users\Diego\Desktop\Ingeniería Civil\Tesis\Manta-
Ecuador\ltime(s)VSShearStrain(\epsilon).txt');
% x=ASu1(:,1);
% y=ASu1(:,2);

fs=[0.5, 0.2, 4, 6];
fs2=[0.5, 0.2, 4, 3];
accMul = 2;

figure(1); close 1; figure(1);
plot(ASu1(:,1),ASu1(:,2),'-');

```

La información presentada en este documento es de exclusiva responsabilidad de los autores y no compromete a la EIA.

```

hold on
plot(e1(:,4)*100,p1(:,2),'r');
legend('Lab Test','Opensees')
hold off
title ('Axial Strain \epsilon (%) VS. Excess pore water pressure u(kPa)');
xlabel('Axial Strain \epsilon (%)');
ylabel('u (kPa)');
set(gcf,'paperposition',fs);
grid on

% pause(0.001);

% for i=1:5
% % addpoints (h,x(i),y(i));
% % drawnow
% % % plot(ASu1(:,1),ASu1(:,2),'-');
% % % plot(x(i),y(i),'-');
% % pause(0.001);
% comet(x,y,0.001)
%
% end

figure(2); close 2; figure(2);
plot(ASq1(:,1),ASq1(:,2),'-');
hold on
plot(e1(:,4)*100,s1(:,4)-s1(:,2),'r');
legend('Lab Test','Opensees')
hold off
title ('Axial Strain \epsilon (%) VS. Deviatoric Stress q (kPa)');
xlabel('Axial Strain \epsilon (%)');
ylabel('q (kPa)');
set(gcf,'paperposition',fs);
grid on

figure(3); close 3; figure(3);
plot(pq1(:,1),pq1(:,2),'-');
hold on
plot(-(s1(:,2)+s1(:,3)+s1(:,4))/3,s1(:,4)-s1(:,2),'r');
legend('Lab Test','Opensees')
hold off
title ('Mean effective Stress p´ (kPa) VS. Deviatoric Stress q (kPa)');
xlabel('confinement p´ (kPa)');
ylabel('q (kPa)');
set(gcf,'paperposition',fs);
grid on

figure(4); close 4; figure(4);
plot(tq1(:,1),tq1(:,2),'-');
hold on
plot((s1(:,1))-20001,s1(:,4)-s1(:,2),'r');
legend('Lab Test','Opensees')
hold off
title ('Time(s) VS. Deviatoric Stress q (kPa)');
xlabel('Time(s)');
ylabel('q (kPa)');
set(gcf,'paperposition',fs);
grid on

figure(5); close 5; figure(5);
plot(tru1(:,1),tru1(:,2),'-');
hold on
plot(p1(:,1)-20001,p1(:,2)/100,'r');

```

La información presentada en este documento es de exclusiva responsabilidad de los autores y no compromete a la EIA.

```

legend('Lab Test','Opensees')
hold off
title ('Time(s) VS. Excess pore water pressure ratio ru');
xlabel('Time(s)');
ylabel('r_u');
set(gcf,'paperposition',fs);
grid on

figure(6); close 6; figure(6);
plot(tSS1(:,1),tSS1(:,2),'-');
title ('Time(s) VS. Shear Strain \gamma (%)');
xlabel('Time(s)');
ylabel('Shear Strain \gamma (%)');
grid on

elseif num_test==2
    hold on
    grid on
    ASul=load('C:\Users\Diego\Desktop\Ingenieria Civil\Tesis\Manta-Ecuador\2Axial
Strain(%)VSu(kPa).txt');
    ASql=load('C:\Users\Diego\Desktop\Ingenieria Civil\Tesis\Manta-
Ecuador\2AxialStrain(%)VSq(kPa).txt');
    pql=load('C:\Users\Diego\Desktop\Ingenieria Civil\Tesis\Manta-
Ecuador\2p(kPa)VSq(kPa).txt');
    tq1=load('C:\Users\Diego\Desktop\Ingenieria Civil\Tesis\Manta-
Ecuador\2time(s)VSq(kPa).txt');
    trul=load('C:\Users\Diego\Desktop\Ingenieria Civil\Tesis\Manta-
Ecuador\2time(s)VSru.txt');
    tSS1=load('C:\Users\Diego\Desktop\Ingenieria Civil\Tesis\Manta-
Ecuador\2time(s)VSShearStrain(%) .txt');
    % x=ASul(:,1);
    % y=ASul(:,2);

    fs=[0.5, 0.2, 4, 6];
    fs2=[0.5, 0.2, 4, 3];
    accMul = 2;

    figure(1); close 1; figure(1);
    plot(ASul(:,1),ASul(:,2),'-');
    hold on
    plot(e1(:,4)*100,p1(:,2),'r');
    legend('Lab Test','Opensees')
    hold off
    title ('Axial Strain \epsilon (%) VS. Excess pore water pressure u(kPa)');
    xlabel('Axial Strain \epsilon (%)');
    ylabel('u (kPa)');
    set(gcf,'paperposition',fs);
    grid on

    % pause(0.001);

    % for i=1:5
    % % addpoints (h,x(i),y(i));
    % % drawnow
    % % % plot(ASul(:,1),ASul(:,2),'-');
    % % % plot(x(i),y(i),'-');
    % % pause(0.001);
    % comet(x,y,0.001)
    %
    % end

```

La información presentada en este documento es de exclusiva responsabilidad de los autores y no compromete a la EIA.

```

figure(2); close 2; figure(2);
plot(ASq1(:,1),ASq1(:,2),'-');
hold on
plot(e1(:,4)*100,s1(:,4)-s1(:,2),'r');
legend('Lab Test','Opensees')
hold off
title ('Axial Strain \epsilon (%) VS. Deviatoric Stress q (kPa)');
xlabel('Axial Strain \epsilon (%)');
ylabel('q (kPa)');
set(gcf,'paperposition',fs);
grid on

figure(3); close 3; figure(3);
plot(pq1(:,1),pq1(:,2),'-');
hold on
plot(-(s1(:,2)+s1(:,3)+s1(:,4))/3,s1(:,4)-s1(:,2),'r');
legend('Lab Test','Opensees')
hold off
title ('Mean effective Stress p' (kPa) VS. Deviatoric Stress q (kPa)');
xlabel('confinement p' (kPa)');
ylabel('q (kPa)');
set(gcf,'paperposition',fs);
grid on

figure(4); close 4; figure(4);
plot(tq1(:,1),tq1(:,2),'-');
hold on
plot((s1(:,1))-20001,s1(:,4)-s1(:,2),'r');
legend('Lab Test','Opensees')
hold off
title ('Time(s) VS. Deviatoric Stress q (kPa)');
xlabel('Time(s)');
ylabel('q (kPa)');
set(gcf,'paperposition',fs);
grid on

figure(5); close 5; figure(5);
plot(tru1(:,1),tru1(:,2),'-');
hold on
plot(p1(:,1)-20001,p1(:,2)/100,'r');
legend('Lab Test','Opensees')
hold off
title ('Time(s) VS. Excess pore water pressure ratio ru');
xlabel('Time(s)');
ylabel('r_u');
set(gcf,'paperposition',fs);
grid on

figure(6); close 6; figure(6);
plot(tSS1(:,1),tSS1(:,2),'-');
title ('Time(s) VS. Shear Strain \gamma (%)');
xlabel('Time(s)');
ylabel('Shear Strain \gamma (%)');
grid on

elseif num_test==3
hold on
grid on
ASu1=load('C:\Users\Diego\Desktop\Ingenieria Civil\Tesis\Manta-Ecuador\3Axial
Strain(\%)VSu(kPa).txt');
ASq1=load('C:\Users\Diego\Desktop\Ingenieria Civil\Tesis\Manta-
Ecuador\3AxialStrain(\%)VSq(kPa).txt');
pq1=load('C:\Users\Diego\Desktop\Ingenieria Civil\Tesis\Manta-
Ecuador\3p'(kPa)VSq(kPa).txt');

```

La información presentada en este documento es de exclusiva responsabilidad de los autores y no compromete a la EIA.



```

tq1=load('C:\Users\Diego\Desktop\Ingeniería Civil\Tesis\Manta-
Ecuador\3time(s)VSq(kPa).txt');
trul=load('C:\Users\Diego\Desktop\Ingeniería Civil\Tesis\Manta-
Ecuador\3time(s)VSru.txt');
tSS1=load('C:\Users\Diego\Desktop\Ingeniería Civil\Tesis\Manta-
Ecuador\3time(s)VSShearStrain(%) .txt');
% x=ASul(:,1);
% y=ASul(:,2);

fs=[0.5, 0.2, 4, 6];
fs2=[0.5, 0.2, 4, 3];
accMul = 2;

figure(1); close 1; figure(1);
plot(ASul(:,1),ASul(:,2), '-');
hold on
plot(e1(:,4)*100,p1(:,2), 'r');
legend('Lab Test', 'Opensees')
hold off
title ('Axial Strain \epsilon (%) VS. Excess pore water pressure u(kPa)');
xlabel('Axial Strain \epsilon (%)');
ylabel('u (kPa)');
set(gcf, 'paperposition', fs);
grid on

% pause(0.001);

% for i=1:5
% % addpoints (h,x(i),y(i));
% % drawnow
% % plot(ASul(:,1),ASul(:,2), '-');
% % plot(x(i),y(i), '-');
% % pause(0.001);
% comet(x,y,0.001)
%
% end

figure(2); close 2; figure(2);
plot(ASq1(:,1),ASq1(:,2), '-');
hold on
plot(e1(:,4)*100,s1(:,4)-s1(:,2), 'r');
legend('Lab Test', 'Opensees')
hold off
title ('Axial Strain \epsilon (%) VS. Deviatoric Stress q (kPa)');
xlabel('Axial Strain \epsilon (%)');
ylabel('q (kPa)');
set(gcf, 'paperposition', fs);
grid on

figure(3); close 3; figure(3);
plot(pq1(:,1),pq1(:,2), '-');
hold on
plot(-(s1(:,2)+s1(:,3)+s1(:,4))/3,s1(:,4)-s1(:,2), 'r');
legend('Lab Test', 'Opensees')
hold off
title ('Mean effective Stress p' (kPa) VS. Deviatoric Stress q (kPa)');
xlabel('confinement p' (kPa)');
ylabel('q (kPa)');
set(gcf, 'paperposition', fs);
grid on

```

La información presentada en este documento es de exclusiva responsabilidad de los autores y no compromete a la EIA.

```

figure(4); close 4; figure(4);
plot(tq1(:,1),tq1(:,2),'-');
hold on
plot((s1(:,1))-20001,s1(:,4)-s1(:,2),'r');
legend('Lab Test','Opensees')
hold off
title ('Time(s) VS. Deviatoric Stress q (kPa)');
xlabel('Time(s)');
ylabel('q (kPa)');
set(gcf,'paperposition',fs);
grid on

figure(5); close 5; figure(5);
plot(tru1(:,1),tru1(:,2),'-');
hold on
plot(pl(:,1)-20001,pl(:,2)/100,'r');
legend('Lab Test','Opensees')
hold off
title ('Time(s) VS. Excess pore water pressure ratio ru');
xlabel('Time(s)');
ylabel('r_u');
set(gcf,'paperposition',fs);
grid on

figure(6); close 6; figure(6);
plot(tSS1(:,1),tSS1(:,2),'-');
title ('Time(s) VS. Shear Strain \gamma (%)');
xlabel('Time(s)');
ylabel('Shear Strain \gamma (%)');
grid on

elseif num_test==4
hold on
grid on
ASu1=load('C:\Users\Diego\Desktop\Ingeniería Civil\Tesis\Manta-Ecuador\4Axial
Strain(\%)VSu(kPa).txt');
ASq1=load('C:\Users\Diego\Desktop\Ingeniería Civil\Tesis\Manta-
Ecuador\4AxialStrain(\%)VSq(kPa).txt');
pq1=load('C:\Users\Diego\Desktop\Ingeniería Civil\Tesis\Manta-
Ecuador\4p´(kPa)VSq(kPa).txt');
tq1=load('C:\Users\Diego\Desktop\Ingeniería Civil\Tesis\Manta-
Ecuador\4time(s)VSq(kPa).txt');
tru1=load('C:\Users\Diego\Desktop\Ingeniería Civil\Tesis\Manta-
Ecuador\4time(s)VSru.txt');
tSS1=load('C:\Users\Diego\Desktop\Ingeniería Civil\Tesis\Manta-
Ecuador\4time(s)VSShearStrain(\%).txt');
% x=ASu1(:,1);
% y=ASu1(:,2);

fs=[0.5, 0.2, 4, 6];
fs2=[0.5, 0.2, 4, 3];
accMul = 2;

figure(1); close 1; figure(1);
plot(ASu1(:,1),ASu1(:,2),'-');
hold on
plot(e1(:,4)*100,pl(:,2),'r');
legend('Lab Test','Opensees')
hold off
title ('Axial Strain \epsilon (%) VS. Excess pore water pressure u(kPa)');
xlabel('Axial Strain \epsilon (%)');
ylabel('u (kPa)');
set(gcf,'paperposition',fs);

```

La información presentada en este documento es de exclusiva responsabilidad de los autores y no compromete a la EIA.

```

grid on

% pause(0.001);

% for i=1:5
% % addpoints (h,x(i),y(i));
% % drawnow
% % % plot(ASu1(:,1),ASu1(:,2),'-');
% % % plot(x(i),y(i),'-');
% % pause(0.001);
% comet(x,y,0.001)
%
% end

figure(2); close 2; figure(2);
plot(ASq1(:,1),ASq1(:,2),'-');
hold on
plot(e1(:,4)*100,s1(:,4)-s1(:,2),'r');
legend('Lab Test','Opensees')
hold off
title ('Axial Strain \epsilon (%) VS. Deviatoric Stress q (kPa)');
xlabel('Axial Strain \epsilon (%)');
ylabel('q (kPa)');
set(gcf,'paperposition',fs);
grid on

figure(3); close 3; figure(3);
plot(pq1(:,1),pq1(:,2),'-');
hold on
plot(-(s1(:,2)+s1(:,3)+s1(:,4))/3,s1(:,4)-s1(:,2),'r');
legend('Lab Test','Opensees')
hold off
title ('Mean effective Stress p´ (kPa) VS. Deviatoric Stress q (kPa)');
xlabel('confinement p´ (kPa)');
ylabel('q (kPa)');
set(gcf,'paperposition',fs);
grid on

figure(4); close 4; figure(4);
plot(tq1(:,1),tq1(:,2),'-');
hold on
plot((s1(:,1))-20001,s1(:,4)-s1(:,2),'r');
legend('Lab Test','Opensees')
hold off
title ('Time(s) VS. Deviatoric Stress q (kPa)');
xlabel('Time(s)');
ylabel('q (kPa)');
set(gcf,'paperposition',fs);
grid on

figure(5); close 5; figure(5);
plot(tru1(:,1),tru1(:,2),'-');
hold on
plot(p1(:,1)-20001,p1(:,2)/100,'r');
legend('Lab Test','Opensees')
hold off
title ('Time(s) VS. Excess pore water pressure ratio ru');
xlabel('Time(s)');
ylabel('r_u');
set(gcf,'paperposition',fs);
grid on

```

La información presentada en este documento es de exclusiva responsabilidad de los autores y no compromete a la EIA.

```

figure(6); close 6; figure(6);
plot(tSS1(:,1),tSS1(:,2),'-');
title ('Time(s) VS. Shear Strain \gamma (%)');
xlabel('Time(s)');
ylabel('Shear Strain \gamma (%)');
grid on

elseif num_test==5
hold on
grid on
ASu1=load('C:\Users\Diego\Desktop\Ingeniería Civil\Tesis\Manta-Ecuador\5Axial
Strain(%)VSu(kPa).txt');
ASq1=load('C:\Users\Diego\Desktop\Ingeniería Civil\Tesis\Manta-
Ecuador\5AxialStrain(%)VSq(kPa).txt');
pql=load('C:\Users\Diego\Desktop\Ingeniería Civil\Tesis\Manta-
Ecuador\5p´(kPa)VSq(kPa).txt');
tql=load('C:\Users\Diego\Desktop\Ingeniería Civil\Tesis\Manta-
Ecuador\5time(s)VSq(kPa).txt');
tru1=load('C:\Users\Diego\Desktop\Ingeniería Civil\Tesis\Manta-
Ecuador\5time(s)VSru.txt');
tSS1=load('C:\Users\Diego\Desktop\Ingenieria Civil\Tesis\Manta-
Ecuador\5time(s)VSShearStrain(%.txt');
% x=ASu1(:,1);
% y=ASu1(:,2);

fs=[0.5, 0.2, 4, 6];
fs2=[0.5, 0.2, 4, 3];
accMul = 2;

figure(1); close 1; figure(1);
plot(ASu1(:,1),ASu1(:,2),'-');
hold on
plot(e1(:,4)*100,p1(:,2),'r');
legend('Lab Test','Opensees')
hold off
title ('Axial Strain \epsilon (%) VS. Excess pore water pressure u(kPa)');
xlabel('Axial Strain \epsilon (%)');
ylabel('u (kPa)');
set(gcf,'paperposition',fs);
grid on

% pause(0.001);

% for i=1:5
% % addpoints (h,x(i),y(i));
% % drawnow
% % % plot(ASu1(:,1),ASu1(:,2),'-');
% % % plot(x(i),y(i),'-');
% % pause(0.001);
% comet(x,y,0.001)
%
% end

figure(2); close 2; figure(2);
plot(ASq1(:,1),ASq1(:,2),'-');
hold on
plot(e1(:,4)*100,s1(:,4)-s1(:,2),'r');
legend('Lab Test','Opensees')
hold off
title ('Axial Strain \epsilon (%) VS. Deviatoric Stress q (kPa)');

```

La información presentada en este documento es de exclusiva responsabilidad de los autores y no compromete a la EIA.

```

xlabel('Axial Strain \epsilon (%)');
ylabel('q (kPa)');
set(gcf,'paperposition',fs);
grid on

figure(3); close 3; figure(3);
plot(pq1(:,1),pq1(:,2),'-');
hold on
plot(-(s1(:,2)+s1(:,3)+s1(:,4))/3,s1(:,4)-s1(:,2),'r');
legend('Lab Test','Opensees')
hold off
title ('Mean effective Stress p' (kPa) VS. Deviatoric Stress q (kPa)');
xlabel('confinement p' (kPa)');
ylabel('q (kPa)');
set(gcf,'paperposition',fs);
grid on

figure(4); close 4; figure(4);
plot(tq1(:,1),tq1(:,2),'-');
hold on
plot((s1(:,1))-20001,s1(:,4)-s1(:,2),'r');
legend('Lab Test','Opensees')
hold off
title ('Time(s) VS. Deviatoric Stress q (kPa)');
xlabel('Time(s)');
ylabel('q (kPa)');
set(gcf,'paperposition',fs);
grid on

figure(5); close 5; figure(5);
plot(tru1(:,1),tru1(:,2),'-');
hold on
plot(pl(:,1)-20001,pl(:,2)/100,'r');
legend('Lab Test','Opensees')
hold off
title ('Time(s) VS. Excess pore water pressure ratio ru');
xlabel('Time(s)');
ylabel('r_u');
set(gcf,'paperposition',fs);
grid on

figure(6); close 6; figure(6);
plot(tSS1(:,1),tSS1(:,2),'-');
title ('Time(s) VS. Shear Strain \gamma (%)');
xlabel('Time(s)');
ylabel('Shear Strain \gamma (%)');
grid on

elseif num_test==6
hold on
grid on
ASul=load('C:\Users\Diego\Desktop\Ingeniería Civil\Tesis\Manta-Ecuador\6Axial Strain(%)VSu(kPa).txt');
ASq1=load('C:\Users\Diego\Desktop\Ingeniería Civil\Tesis\Manta-Ecuador\6AxialStrain(%)VSq(kPa).txt');
pq1=load('C:\Users\Diego\Desktop\Ingeniería Civil\Tesis\Manta-Ecuador\6p' (kPa)VSq(kPa).txt');
tq1=load('C:\Users\Diego\Desktop\Ingeniería Civil\Tesis\Manta-Ecuador\6time(s)VSq(kPa).txt');
tru1=load('C:\Users\Diego\Desktop\Ingeniería Civil\Tesis\Manta-Ecuador\6time(s)VSru.txt');
tSS1=load('C:\Users\Diego\Desktop\Ingeniería Civil\Tesis\Manta-Ecuador\6time(s)VSShearStrain(%) .txt');
% x=ASul(:,1);

```

La información presentada en este documento es de exclusiva responsabilidad de los autores y no compromete a la EIA.

```

% y=ASul(:,2);

fs=[0.5, 0.2, 4, 6];
fs2=[0.5, 0.2, 4, 3];
accMul = 2;

figure(1); close 1; figure(1);
plot(ASul(:,1),ASul(:,2),'-');
hold on
plot(e1(:,4)*100,p1(:,2),'r');
legend('Lab Test','Opensees')
hold off
title ('Axial Strain \epsilon (%) VS. Excess pore water pressure u(kPa)');
xlabel('Axial Strain \epsilon (%)');
ylabel('u (kPa)');
set(gcf,'paperposition',fs);
grid on

% pause(0.001);

% for i=1:5
% % addpoints (h,x(i),y(i));
% % drawnow
% % % plot(ASul(:,1),ASul(:,2),'-');
% % % plot(x(i),y(i),'-');
% % pause(0.001);
% comet(x,y,0.001)
%
% end

figure(2); close 2; figure(2);
plot(ASq1(:,1),ASq1(:,2),'-');
hold on
plot(e1(:,4)*100,s1(:,4)-s1(:,2),'r');
legend('Lab Test','Opensees')
hold off
title ('Axial Strain \epsilon (%) VS. Deviatoric Stress q (kPa)');
xlabel('Axial Strain \epsilon (%)');
ylabel('q (kPa)');
set(gcf,'paperposition',fs);
grid on

figure(3); close 3; figure(3);
plot(pq1(:,1),pq1(:,2),'-');
hold on
plot(-(s1(:,2)+s1(:,3)+s1(:,4))/3,s1(:,4)-s1(:,2),'r');
legend('Lab Test','Opensees')
hold off
title ('Mean effective Stress p' (kPa) VS. Deviatoric Stress q (kPa)');
xlabel('confinement p' (kPa)');
ylabel('q (kPa)');
set(gcf,'paperposition',fs);
grid on

figure(4); close 4; figure(4);
plot(tq1(:,1),tq1(:,2),'-');
hold on
plot((s1(:,1))-20001,s1(:,4)-s1(:,2),'r');
legend('Lab Test','Opensees')
hold off
title ('Time(s) VS. Deviatoric Stress q (kPa)');

```

La información presentada en este documento es de exclusiva responsabilidad de los autores y no compromete a la EIA.

```

xlabel('Time (s)');
ylabel('q (kPa)');
set(gcf, 'paperposition', fs);
grid on

figure(5); close 5; figure(5);
plot(tru1(:,1),tru1(:,2), '-');
hold on
plot(p1(:,1)-20001,p1(:,2)/100, 'r');
legend('Lab Test', 'Opensees')
hold off
title ('Time (s) VS. Excess pore water pressure ratio ru');
xlabel('Time (s)');
ylabel('r_u');
set(gcf, 'paperposition', fs);
grid on

figure(6); close 6; figure(6);
plot(tSS1(:,1),tSS1(:,2), '-');
title ('Time (s) VS. Shear Strain \gamma (%)');
xlabel('Time (s)');
ylabel('Shear Strain \gamma (%)');
grid on

elseif num_test==7
hold on
grid on
ASu1=load('C:\Users\Diego\Desktop\Ingeniería Civil\Tesis\Manta-Ecuador\6Axial
Strain(%)VSu(kPa).txt');
ASq1=load('C:\Users\Diego\Desktop\Ingeniería Civil\Tesis\Manta-
Ecuador\6AxialStrain(%)VSq(kPa).txt');
pq1=load('C:\Users\Diego\Desktop\Ingeniería Civil\Tesis\Manta-
Ecuador\6p´(kPa)VSq(kPa).txt');
tq1=load('C:\Users\Diego\Desktop\Ingeniería Civil\Tesis\Manta-
Ecuador\6time(s)VSq(kPa).txt');
tru1=load('C:\Users\Diego\Desktop\Ingeniería Civil\Tesis\Manta-
Ecuador\6time(s)VSru.txt');
tSS1=load('C:\Users\Diego\Desktop\Ingeniería Civil\Tesis\Manta-
Ecuador\6time(s)VSShearStrain(%) .txt');
% x=ASu1(:,1);
% y=ASu1(:,2);

fs=[0.5, 0.2, 4, 6];
fs2=[0.5, 0.2, 4, 3];
accMul = 2;

figure(1); close 1; figure(1);
plot(ASu1(:,1),ASu1(:,2), '-');
hold on
plot(-e1(:,4)*100,p1(:,2), 'r');
legend('Lab Test', 'Opensees')
hold off
title ('Axial Strain \epsilon (%) VS. Excess pore water pressure u (kPa)');
xlabel('Axial Strain \epsilon (%)');
ylabel('u (kPa)');
set(gcf, 'paperposition', fs);
grid on

% pause(0.001);

% for i=1:5

```

La información presentada en este documento es de exclusiva responsabilidad de los autores y no compromete a la EIA.

```

%% % addpoints (h,x(i),y(i));
%% % drawnow
%% % plot(ASu1(:,1),ASu1(:,2),'-');
%% % plot(x(i),y(i),'-');
%% % pause(0.001);
%% comet(x,y,0.001)
%
% end

figure(2); close 2; figure(2);
plot(ASq1(:,1),ASq1(:,2),'-');
hold on
plot(-e1(:,4)*100,-s1(:,4)+s1(:,2),'r');
legend('Lab Test','Opensees')
hold off
title ('Axial Strain \epsilon (%) VS. Deviatoric Stress q (kPa)');
xlabel('Axial Strain \epsilon (%)');
ylabel('q (kPa)');
set(gcf,'paperposition',fs);
grid on

figure(3); close 3; figure(3);
plot(pq1(:,1),pq1(:,2),'-');
hold on
plot(-(s1(:,2)+s1(:,3)+s1(:,4))/3,-s1(:,4)+s1(:,2),'r');
legend('Lab Test','Opensees')
hold off
title ('Mean effective Stress p' (kPa) VS. Deviatoric Stress q (kPa)');
xlabel('confinement p' (kPa)');
ylabel('q (kPa)');
set(gcf,'paperposition',fs);
grid on

figure(4); close 4; figure(4);
plot(tq1(:,1),tq1(:,2),'-');
hold on
plot((s1(:,1))-20001,-s1(:,4)+s1(:,2),'r');
legend('Lab Test','Opensees')
hold off
title ('Time(s) VS. Deviatoric Stress q (kPa)');
xlabel('Time(s)');
ylabel('q (kPa)');
set(gcf,'paperposition',fs);
grid on

figure(5); close 5; figure(5);
plot(tru1(:,1),tru1(:,2),'-');
hold on
plot(p1(:,1)-20001,p1(:,2)/100,'r');
legend('Lab Test','Opensees')
hold off
title ('Time(s) VS. Excess pore water pressure ratio ru');
xlabel('Time(s)');
ylabel('r_u');
set(gcf,'paperposition',fs);
grid on

figure(6); close 6; figure(6);
plot(tSS1(:,1),tSS1(:,2),'-');
title ('Time(s) VS. Shear Strain \gamma (%)');
xlabel('Time(s)');
ylabel('Shear Strain \gamma (%)');
grid on

```

La información presentada en este documento es de exclusiva responsabilidad de los autores y no compromete a la EIA.



```

end

if num_test==123
    hold on
    grid on

    ASu4=load('C:\Users\Diego\Desktop\Ingeniería Civil\Tesis\Manta-Ecuador\4Axial
Strain(%)VSu(kPa).txt');
    ASq4=load('C:\Users\Diego\Desktop\Ingeniería Civil\Tesis\Manta-
Ecuador\4AxialStrain(%)VSq(kPa).txt');
    pq4=load('C:\Users\Diego\Desktop\Ingeniería Civil\Tesis\Manta-
Ecuador\4p´(kPa)VSq(kPa).txt');
    tq4=load('C:\Users\Diego\Desktop\Ingeniería Civil\Tesis\Manta-
Ecuador\4time(s)VSq(kPa).txt');
    tru4=load('C:\Users\Diego\Desktop\Ingeniería Civil\Tesis\Manta-
Ecuador\4time(s)VSru.txt');
    tSS4=load('C:\Users\Diego\Desktop\Ingeniería Civil\Tesis\Manta-
Ecuador\4time(s)VSShearStrain(%) .txt');

    ASu5=load('C:\Users\Diego\Desktop\Ingeniería Civil\Tesis\Manta-Ecuador\5Axial
Strain(%)VSu(kPa).txt');
    ASq5=load('C:\Users\Diego\Desktop\Ingeniería Civil\Tesis\Manta-
Ecuador\5AxialStrain(%)VSq(kPa).txt');
    pq5=load('C:\Users\Diego\Desktop\Ingeniería Civil\Tesis\Manta-
Ecuador\5p´(kPa)VSq(kPa).txt');
    tq5=load('C:\Users\Diego\Desktop\Ingeniería Civil\Tesis\Manta-
Ecuador\5time(s)VSq(kPa).txt');
    tru5=load('C:\Users\Diego\Desktop\Ingeniería Civil\Tesis\Manta-
Ecuador\5time(s)VSru.txt');
    tSS5=load('C:\Users\Diego\Desktop\Ingeniería Civil\Tesis\Manta-
Ecuador\5time(s)VSShearStrain(%) .txt');

    ASu6=load('C:\Users\Diego\Desktop\Ingeniería Civil\Tesis\Manta-Ecuador\6Axial
Strain(%)VSu(kPa).txt');
    ASq6=load('C:\Users\Diego\Desktop\Ingeniería Civil\Tesis\Manta-
Ecuador\6AxialStrain(%)VSq(kPa).txt');
    pq6=load('C:\Users\Diego\Desktop\Ingeniería Civil\Tesis\Manta-
Ecuador\6p´(kPa)VSq(kPa).txt');
    tq6=load('C:\Users\Diego\Desktop\Ingeniería Civil\Tesis\Manta-
Ecuador\6time(s)VSq(kPa).txt');
    tru6=load('C:\Users\Diego\Desktop\Ingeniería Civil\Tesis\Manta-
Ecuador\6time(s)VSru.txt');
    tSS6=load('C:\Users\Diego\Desktop\Ingeniería Civil\Tesis\Manta-
Ecuador\6time(s)VSShearStrain(%) .txt');
    % x=ASu6(:,1);
    % y=ASu6(:,2);

    fs=[0.5, 0.2, 4, 6];
    fs2=[0.5, 0.2, 4, 3];
    accMul = 2;

    figure(1); close 1; figure(1);
    subplot(1,3,1),plot(ASu6(:,1),ASu6(:,2),'-');

```

La información presentada en este documento es de exclusiva responsabilidad de los autores y no compromete a la EIA.

```

hold on
plot(e1PT6(:,4)*100,p1PT6(:,2),'r');
legend('Lab Test#6','Opensees')
hold off
title ('Axial Strain \epsilon (%) VS. Excess pore water pressure u(kPa)');
xlabel('Axial Strain \epsilon (%)');
ylabel('u (kPa)');
set(gcf,'paperposition',fs);
grid on

subplot(1,3,2),plot(ASu5(:,1),ASu5(:,2),'-');
hold on
plot(e1PT5(:,4)*100,p1PT5(:,2),'r');
legend('Lab Test#5','Opensees')
hold off
title ('Axial Strain \epsilon (%) VS. Excess pore water pressure u(kPa)');
xlabel('Axial Strain \epsilon (%)');
ylabel('u (kPa)');
set(gcf,'paperposition',fs);
grid on

subplot(1,3,3),plot(ASu4(:,1),ASu4(:,2),'-');
hold on
plot(e1PT4(:,4)*100,p1PT4(:,2),'r');
legend('Lab Test#4','Opensees')
hold off
title ('Axial Strain \epsilon (%) VS. Excess pore water pressure u(kPa)');
xlabel('Axial Strain \epsilon (%)');
ylabel('u (kPa)');
set(gcf,'paperposition',fs);
grid on

% pause(0.001);

% for i=1:5
% % addpoints (h,x(i),y(i));
% % drawnow
% % % plot(ASu6(:,1),ASu6(:,2),'-');
% % % plot(x(i),y(i),'-');
% % pause(0.001);
% comet(x,y,0.001)
%
% end

figure(2); close 2; figure(2);
subplot(1,3,1),plot(ASq6(:,1),ASq6(:,2),'-');
hold on
plot(e1PT6(:,4)*100,s1PT6(:,4)-s1PT6(:,2),'r');
legend('Lab Test#6','Opensees')
hold off
title ('Axial Strain \epsilon (%) VS. Deviatoric Stress q (kPa)');
xlabel('Axial Strain \epsilon (%)');
ylabel('q (kPa)');
set(gcf,'paperposition',fs);
grid on
subplot(1,3,2),plot(ASq5(:,1),ASq5(:,2),'-');
hold on
plot(e1PT5(:,4)*100,s1PT5(:,4)-s1PT5(:,2),'r');
legend('Lab Test#5','Opensees')
hold off
title ('Axial Strain \epsilon (%) VS. Deviatoric Stress q (kPa)');
xlabel('Axial Strain \epsilon (%)');

```

La información presentada en este documento es de exclusiva responsabilidad de los autores y no compromete a la EIA.

```

ylabel('q (kPa)');
set(gcf, 'paperposition', fs);
grid on

subplot(1,3,3),plot(ASq4(:,1),ASq4(:,2), '-');
hold on
plot(e1PT4(:,4)*100,s1PT4(:,4)-s1PT4(:,2), 'r');
legend('Lab Test#4', 'Opensees')
hold off
title ('Axial Strain \epsilon (%) VS. Deviatoric Stress q (kPa)');
xlabel('Axial Strain \epsilon (%)');
ylabel('q (kPa)');
set(gcf, 'paperposition', fs);
grid on

figure(3); close 3; figure(3);
subplot(1,3,1),plot(pq6(:,1),pq6(:,2), '-');
hold on
plot(-(s1PT6(:,2)+s1PT6(:,3)+s1PT6(:,4))/3,s1PT6(:,4)-s1PT6(:,2), 'r');
legend('Lab Test#6', 'Opensees')
hold off
title ('Mean effective Stress p' (kPa) VS. Deviatoric Stress q (kPa)');
xlabel('confinement p' (kPa)');
ylabel('q (kPa)');
set(gcf, 'paperposition', fs);
grid on

subplot(1,3,2),plot(pq5(:,1),pq5(:,2), '-');
hold on
plot(-(s1PT5(:,2)+s1PT5(:,3)+s1PT5(:,4))/3,s1PT5(:,4)-s1PT5(:,2), 'r');
legend('Lab Test#5', 'Opensees')
hold off
title ('Mean effective Stress p' (kPa) VS. Deviatoric Stress q (kPa)');
xlabel('confinement p' (kPa)');
ylabel('q (kPa)');
set(gcf, 'paperposition', fs);
grid on

subplot(1,3,3),plot(pq4(:,1),pq4(:,2), '-');
hold on
plot(-(s1PT4(:,2)+s1PT4(:,3)+s1PT4(:,4))/3,s1PT4(:,4)-s1PT4(:,2), 'r');
legend('Lab Test#4', 'Opensees')
hold off
title ('Mean effective Stress p' (kPa) VS. Deviatoric Stress q (kPa)');
xlabel('confinement p' (kPa)');
ylabel('q (kPa)');
set(gcf, 'paperposition', fs);
grid on

figure(4); close 4; figure(4);
subplot(1,3,1),plot(tq6(:,1),tq6(:,2), '-');
hold on
plot((s1PT6(:,1))-20001,s1PT6(:,4)-s1PT6(:,2), 'r');
legend('Lab Test#6', 'Opensees')
hold off
title ('Time(s) VS. Deviatoric Stress q (kPa)');
xlabel('Time(s)');
ylabel('q (kPa)');
set(gcf, 'paperposition', fs);
grid on

subplot(1,3,2),plot(tq5(:,1),tq5(:,2), '-');

```

La información presentada en este documento es de exclusiva responsabilidad de los autores y no compromete a la EIA.

```

hold on
plot((s1PT5(:,1))-20001,s1PT5(:,4)-s1PT5(:,2),'r');
legend('Lab Test#5','Opensees')
hold off
title ('Time(s) VS. Deviatoric Stress q (kPa)');
xlabel('Time(s)');
ylabel('q (kPa)');
set(gcf,'paperposition',fs);
grid on

subplot(1,3,3),plot(tq4(:,1),tq4(:,2),'-');
hold on
plot((s1PT5(:,1))-20001,s1PT5(:,4)-s1PT5(:,2),'r');
legend('Lab Test#4','Opensees')
hold off
title ('Time(s) VS. Deviatoric Stress q (kPa)');
xlabel('Time(s)');
ylabel('q (kPa)');
set(gcf,'paperposition',fs);
grid on

figure(5); close 5; figure(5);
subplot(1,3,1),plot(tru6(:,1),tru6(:,2),'-');
hold on
plot(p1PT6(:,1)-20001,p1PT6(:,2)/100,'r');
legend('Lab Test#6','Opensees')
hold off
title ('Time(s) VS. Excess pore water pressure ratio ru');
xlabel('Time(s)');
ylabel('r_u');
set(gcf,'paperposition',fs);
grid on

subplot(1,3,2),plot(tru5(:,1),tru5(:,2),'-');
hold on
plot(p1PT5(:,1)-20001,p1PT5(:,2)/100,'r');
legend('Lab Test#5','Opensees')
hold off
title ('Time(s) VS. Excess pore water pressure ratio ru');
xlabel('Time(s)');
ylabel('r_u');
set(gcf,'paperposition',fs);
grid on

subplot(1,3,3),plot(tru4(:,1),tru4(:,2),'-');
hold on
plot(p1PT4(:,1)-20001,p1PT4(:,2)/100,'r');
legend('Lab Test#4','Opensees')
hold off
title ('Time(s) VS. Excess pore water pressure ratio ru');
xlabel('Time(s)');
ylabel('r_u');
set(gcf,'paperposition',fs);
grid on

figure(6); close 6; figure(6);
plot(tSS6(:,1),tSS6(:,2),'-');
title ('Time(s) VS. Shear Strain \gamma (%)');
xlabel('Time(s)');
ylabel('Shear Strain \gamma (%)');
grid on

```

La información presentada en este documento es de exclusiva responsabilidad de los autores y no compromete a la EIA.

```

end

if num_test==101
    figure(1); close 1; figure(1);
    plot(e1(:,4)*100,p1(:,2), 'r');
    hold on
    plot(e1PT1(:,4)*100,p1PT1(:,2), 'g'); %%%%%%%%%%%%%%%
    hold on
    plot(e1PT2(:,4)*100,p1PT2(:,2), 'm');
    hold on
    plot(e1PT3(:,4)*100,p1PT3(:,2), 'b');
    hold on
    plot(e1PT4(:,4)*100,p1PT4(:,2), 'k');
    legend('PT=23°', 'PT=29°', 'PT=33°', 'PT=25°', 'PT=18°')
    hold off
    title ('Axial Strain \epsilon (%) VS. Excess pore water pressure u(kPa)');
    xlabel('Axial Strain \epsilon (%)');
    ylabel('u (kPa)');
    set(gcf, 'paperposition', fs);
    grid on

    figure(2); close 2; figure(2);
    plot(e1(:,4)*100,s1(:,4)-s1(:,2), 'r');
    hold on
    plot(e1PT1(:,4)*100,s1PT1(:,4)-s1PT1(:,2), 'g');
    hold on
    plot(e1PT2(:,4)*100,s1PT2(:,4)-s1PT2(:,2), 'm');
    hold on
    plot(e1PT3(:,4)*100,s1PT3(:,4)-s1PT3(:,2), 'b');
    hold on
    plot(e1PT4(:,4)*100,s1PT4(:,4)-s1PT4(:,2), 'k');
    legend('PT=23°', 'PT=29°', 'PT=33°', 'PT=25°', 'PT=18°')
    hold off
    title ('Axial Strain \epsilon (%) VS. Deviatoric Stress q (kPa)');
    xlabel('Axial Strain \epsilon (%)');
    ylabel('q (kPa)');
    set(gcf, 'paperposition', fs);
    grid on

    figure(3); close 3; figure(3);
    plot(-(s1(:,2)+s1(:,3)+s1(:,4))/3,s1(:,4)-s1(:,2), 'r');
    hold on
    plot(-(s1PT1(:,2)+s1PT1(:,3)+s1PT1(:,4))/3,s1PT1(:,4)-s1PT1(:,2), 'g');
    hold on
    plot(-(s1PT2(:,2)+s1PT2(:,3)+s1PT2(:,4))/3,s1PT2(:,4)-s1PT2(:,2), 'm');
    hold on
    plot(-(s1PT3(:,2)+s1PT3(:,3)+s1PT3(:,4))/3,s1PT3(:,4)-s1PT3(:,2), 'b');
    hold on
    plot(-(s1PT4(:,2)+s1PT4(:,3)+s1PT4(:,4))/3,s1PT4(:,4)-s1PT4(:,2), 'k');
    legend('PT=23°', 'PT=29°', 'PT=33°', 'PT=25°', 'PT=18°')
    hold off
    title ('Mean effective Stress p' (kPa) VS. Deviatoric Stress q (kPa)');
    xlabel('confinement p' (kPa)');
    ylabel('q (kPa)');
    set(gcf, 'paperposition', fs);
    grid on

    figure(4); close 4; figure(4);
    plot((s1(:,1))-20001,s1(:,4)-s1(:,2), 'r');
    hold on
    plot((s1PT1(:,1))-20001,s1PT1(:,4)-s1PT1(:,2), 'g');

```

La información presentada en este documento es de exclusiva responsabilidad de los autores y no compromete a la EIA.

```

hold on
plot((s1PT2(:,1))-20001,s1PT2(:,4)-s1PT2(:,2),'m');
hold on
plot((s1PT3(:,1))-20001,s1PT3(:,4)-s1PT3(:,2),'b');
hold on
plot((s1PT4(:,1))-20001,s1PT4(:,4)-s1PT4(:,2),'k');
legend('PT=23°','PT=29°','PT=33°','PT=25°','PT=18°')
hold off
title ('Time(s) VS. Deviatoric Stress q (kPa)');
xlabel('Time(s)');
ylabel('q (kPa)');
set(gcf,'paperposition',fs);
grid on

figure(5); close 5; figure(5);
plot(p1(:,1)-20001,p1(:,2)/100,'r');
hold on
plot(p1PT1(:,1)-20001,p1PT1(:,2)/100,'g');
hold on
plot(p1PT2(:,1)-20001,p1PT2(:,2)/100,'m');
hold on
plot(p1PT3(:,1)-20001,p1PT3(:,2)/100,'b');
hold on
plot(p1PT4(:,1)-20001,p1PT4(:,2)/100,'k');
legend('PT=23°','PT=29°','PT=33°','PT=25°','PT=18°')
hold off
title ('Time(s) VS. Excess pore water pressure ratio ru');
xlabel('Time(s)');
ylabel('r_u');
set(gcf,'paperposition',fs);
grid on

```

end

```

if num_test==1000
    ASu1=load('C:\Users\Diego\Desktop\Ingeniería Civil\Tesis\Manta-Ecuador\6Axial Strain(%)VSu(kPa).txt');
    ASq1=load('C:\Users\Diego\Desktop\Ingeniería Civil\Tesis\Manta-Ecuador\6AxialStrain(%)VSq(kPa).txt');
    pql=load('C:\Users\Diego\Desktop\Ingeniería Civil\Tesis\Manta-Ecuador\6p´(kPa)VSq(kPa).txt');
    tq1=load('C:\Users\Diego\Desktop\Ingeniería Civil\Tesis\Manta-Ecuador\6time(s)VSq(kPa).txt');
    trul=load('C:\Users\Diego\Desktop\Ingeniería Civil\Tesis\Manta-Ecuador\6time(s)VSru.txt');
    tSS1=load('C:\Users\Diego\Desktop\Ingeniería Civil\Tesis\Manta-Ecuador\6time(s)VSShearStrain(%) .txt');

```

```

figure(1); close 1; figure(1);
plot(ASu1(:,1),ASu1(:,2),'r');
hold on
plot(e1PT1(:,4)*100,p1PT1(:,2),'g');%%%%%%%%%%
hold on
plot(e1PT2(:,4)*100,p1PT2(:,2),'m');
hold on
plot(e1PT3(:,4)*100,p1PT3(:,2),'b');
hold on
plot(e1PT4(:,4)*100,p1PT4(:,2),'k');

```

La información presentada en este documento es de exclusiva responsabilidad de los autores y no compromete a la EIA.

```

hold on
plot(e1PT5(:,4)*100,p1PT5(:,2),'y');
hold on
plot(e1PT6(:,4)*100,p1PT6(:,2),'c');
legend('Lab°','Set #1','Set #2','Set #3','Set #4','Set #5','Set #6')
hold off
title ('Axial Strain \epsilon (%) VS. Excess pore water pressure u(kPa)');
xlabel('Axial Strain \epsilon (%)');
ylabel('u (kPa)');
set(gcf,'paperposition',fs);
grid on

figure(2); close 2; figure(2);
plot(ASq1(:,1),ASq1(:,2),'r');
hold on
plot(e1PT1(:,4)*100,s1PT1(:,4)-s1PT1(:,2),'g');
hold on
plot(e1PT2(:,4)*100,s1PT2(:,4)-s1PT2(:,2),'m');
hold on
plot(e1PT3(:,4)*100,s1PT3(:,4)-s1PT3(:,2),'b');
hold on
plot(e1PT4(:,4)*100,s1PT4(:,4)-s1PT4(:,2),'k');
hold on
plot(e1PT5(:,4)*100,s1PT5(:,4)-s1PT5(:,2),'y');
hold on
plot(e1PT6(:,4)*100,s1PT6(:,4)-s1PT6(:,2),'c');
legend('Lab°','Set #1','Set #2','Set #3','Set #4','Set #5','Set #6')
hold off
title ('Axial Strain \epsilon (%) VS. Deviatoric Stress q (kPa)');
xlabel('Axial Strain \epsilon (%)');
ylabel('q (kPa)');
set(gcf,'paperposition',fs);
grid on

figure(3); close 3; figure(3);
plot(pq1(:,1),pq1(:,2),'r');
hold on
plot(-(s1PT1(:,2)+s1PT1(:,3)+s1PT1(:,4))/3,s1PT1(:,4)-s1PT1(:,2),'g');
hold on
plot(-(s1PT2(:,2)+s1PT2(:,3)+s1PT2(:,4))/3,s1PT2(:,4)-s1PT2(:,2),'m');
hold on
plot(-(s1PT3(:,2)+s1PT3(:,3)+s1PT3(:,4))/3,s1PT3(:,4)-s1PT3(:,2),'b');
hold on
plot(-(s1PT4(:,2)+s1PT4(:,3)+s1PT4(:,4))/3,s1PT4(:,4)-s1PT4(:,2),'k');
hold on
plot(-(s1PT5(:,2)+s1PT5(:,3)+s1PT5(:,4))/3,s1PT5(:,4)-s1PT5(:,2),'y');
hold on
plot(-(s1PT6(:,2)+s1PT6(:,3)+s1PT6(:,4))/3,s1PT6(:,4)-s1PT6(:,2),'c');
legend('Lab°','Set #1','Set #2','Set #3','Set #4','Set #5','Set #6')
hold off
title ('Mean effective Stress p' (kPa) VS. Deviatoric Stress q (kPa)');
xlabel('confinement p' (kPa)');
ylabel('q (kPa)');
set(gcf,'paperposition',fs);
grid on

figure(4); close 4; figure(4);
plot(tq1(:,1),tq1(:,2),'r');
hold on
plot((s1PT1(:,1))-20001,s1PT1(:,4)-s1PT1(:,2),'g');
hold on
plot((s1PT2(:,1))-20001,s1PT2(:,4)-s1PT2(:,2),'m');

```

La información presentada en este documento es de exclusiva responsabilidad de los autores y no compromete a la EIA.

```

hold on
plot((s1PT3(:,1))-20001,s1PT3(:,4)-s1PT3(:,2),'b');
hold on
plot((s1PT4(:,1))-20001,s1PT4(:,4)-s1PT4(:,2),'k');
hold on
plot((s1PT5(:,1))-20001,s1PT5(:,4)-s1PT5(:,2),'y');
hold on
plot((s1PT6(:,1))-20001,s1PT6(:,4)-s1PT6(:,2),'c');
legend('Lab°','Set #1','Set #2','Set #3','Set #4','Set #5','Set #6')
hold off
title('Time(s) VS. Deviatoric Stress q (kPa)');
xlabel('Time(s)');
ylabel('q (kPa)');
set(gcf,'paperposition',fs);
grid on

figure(5); close 5; figure(5);
plot(trul(:,1),trul(:,2),'r');
hold on
plot(p1PT1(:,1)-20001,p1PT1(:,2)/100,'g');
hold on
plot(p1PT2(:,1)-20001,p1PT2(:,2)/100,'m');
hold on
plot(p1PT3(:,1)-20001,p1PT3(:,2)/100,'b');
hold on
plot(p1PT4(:,1)-20001,p1PT4(:,2)/100,'k');
hold on
plot(p1PT5(:,1)-20001,p1PT5(:,2)/100,'y');
hold on
plot(p1PT6(:,1)-20001,p1PT6(:,2)/100,'c');
legend('Lab°','Set #1','Set #2','Set #3','Set #4','Set #5','Set #6')
hold off
title('Time(s) VS. Excess pore water pressure ratio ru');
xlabel('Time(s)');
ylabel('r_u');
set(gcf,'paperposition',fs);
grid on
end

if num_test==222
figure(1); close 1; figure(1);
plot(e1PT1(:,4)*100,p1PT1(:,2),'g');%%%%%%%%%%%%%%
hold on
plot(e1PT2(:,4)*100,p1PT2(:,2),'m');
hold on
plot(e1PT3(:,4)*100,p1PT3(:,2),'b');
hold on
plot(e1PT4(:,4)*100,p1PT4(:,2),'k');
hold on
plot(e1PT5(:,4)*100,p1PT5(:,2),'y');
hold on
plot(e1PT6(:,4)*100,p1PT6(:,2),'r');
legend('d1=0.25','d1=0.5','d1=0.75','d1=1.0','d1=1.5','d1=2.0')
hold off
title('Axial Strain \epsilon (%) VS. Excess pore water pressure u(kPa)');
xlabel('Axial Strain \epsilon (%)');
ylabel('u (kPa)');
set(gcf,'paperposition',fs);
grid on

figure(2); close 2; figure(2);

plot(e1PT1(:,4)*100,s1PT1(:,4)-s1PT1(:,2),'g');

```

La información presentada en este documento es de exclusiva responsabilidad de los autores y no compromete a la EIA.



```

hold on
plot(e1PT2(:,4)*100,s1PT2(:,4)-s1PT2(:,2), 'm');
hold on
plot(e1PT3(:,4)*100,s1PT3(:,4)-s1PT3(:,2), 'b');
hold on
plot(e1PT4(:,4)*100,s1PT4(:,4)-s1PT4(:,2), 'k');
hold on
plot(e1PT5(:,4)*100,s1PT5(:,4)-s1PT5(:,2), 'y');
hold on
plot(e1PT6(:,4)*100,s1PT6(:,4)-s1PT6(:,2), 'r');
legend('d1=0.25', 'd1=0.5', 'd1=0.75', 'd1=1.0', 'd1=1.5', 'd1=2.0')
hold off
title ('Axial Strain \epsilon (%) VS. Deviatoric Stress q (kPa)');
xlabel('Axial Strain \epsilon (%)');
ylabel('q (kPa)');
set(gcf, 'paperposition', fs);
grid on

figure(3); close 3; figure(3);

plot(-(s1PT1(:,2)+s1PT1(:,3)+s1PT1(:,4))/3,s1PT1(:,4)-s1PT1(:,2), 'g');
hold on
plot(-(s1PT2(:,2)+s1PT2(:,3)+s1PT2(:,4))/3,s1PT2(:,4)-s1PT2(:,2), 'm');
hold on
plot(-(s1PT3(:,2)+s1PT3(:,3)+s1PT3(:,4))/3,s1PT3(:,4)-s1PT3(:,2), 'b');
hold on
plot(-(s1PT4(:,2)+s1PT4(:,3)+s1PT4(:,4))/3,s1PT4(:,4)-s1PT4(:,2), 'k');
hold on
plot(-(s1PT5(:,2)+s1PT5(:,3)+s1PT5(:,4))/3,s1PT5(:,4)-s1PT5(:,2), 'y');
hold on
plot(-(s1PT6(:,2)+s1PT6(:,3)+s1PT6(:,4))/3,s1PT6(:,4)-s1PT6(:,2), 'r');
legend('d1=0.25', 'd1=0.5', 'd1=0.75', 'd1=1.0', 'd1=1.5', 'd1=2.0')
hold off
title ('Mean effective Stress p' (kPa) VS. Deviatoric Stress q (kPa)');
xlabel('confinement p' (kPa)');
ylabel('q (kPa)');
set(gcf, 'paperposition', fs);
grid on
figure(4); close 4; figure(4);

plot((s1PT1(:,1))-20001,s1PT1(:,4)-s1PT1(:,2), 'g');
hold on
plot((s1PT2(:,1))-20001,s1PT2(:,4)-s1PT2(:,2), 'm');
hold on
plot((s1PT3(:,1))-20001,s1PT3(:,4)-s1PT3(:,2), 'b');
hold on
plot((s1PT4(:,1))-20001,s1PT4(:,4)-s1PT4(:,2), 'k');
hold on
plot((s1PT5(:,1))-20001,s1PT5(:,4)-s1PT5(:,2), 'y');
hold on
plot((s1PT6(:,1))-20001,s1PT6(:,4)-s1PT6(:,2), 'r');
legend('d1=0.25', 'd1=0.5', 'd1=0.75', 'd1=1.0', 'd1=1.5', 'd1=2.0')
hold off
title ('Time(s) VS. Deviatoric Stress q (kPa)');
xlabel('Time(s)');
ylabel('q (kPa)');
set(gcf, 'paperposition', fs);
grid on

figure(5); close 5; figure(5);

plot(p1PT1(:,1)-20001,p1PT1(:,2)/100, 'g');

```

La información presentada en este documento es de exclusiva responsabilidad de los autores y no compromete a la EIA.

```

    hold on
    plot(p1PT2(:,1)-20001,p1PT2(:,2)/100,'m');
    hold on
    plot(p1PT3(:,1)-20001,p1PT3(:,2)/100,'b');
    hold on
    plot(p1PT4(:,1)-20001,p1PT4(:,2)/100,'k');
    hold on
    plot(p1PT5(:,1)-20001,p1PT5(:,2)/100,'y');
    hold on
    plot(p1PT6(:,1)-20001,p1PT6(:,2)/100,'r');
    legend('d1=0.25','d1=0.5','d1=0.75','d1=1.0','d1=1.5','d1=2.0')
    hold off
    title ('Time(s) VS. Excess pore water pressure ratio ru');
    xlabel('Time(s)');
    ylabel('r_u');
    set(gcf,'paperposition',fs);
    grid on
end
if num_test==99
figure(7); close 7; figure(7);
plot(-e1(:,4)*100,p1(:,2),'-');
title ('Axial Strain \epsilon (%) VS. Excess pore water pressure u(kPa)');
xlabel('Axial Strain \epsilon (%)');
ylabel('u (kPa)');
grid on

figure(8); close 8; figure(8);
plot(-e1(:,4)*100,-s1(:,4)+s1(:,2),'r');
title ('Axial Strain \epsilon (%) VS. Deviatoric Stress q (kPa)');
xlabel('Axial Strain \epsilon (%)');
ylabel('q (kPa)');
set(gcf,'paperposition',fs);
grid on

figure(9); close 9; figure(9);
plot(-(s1(:,2)+s1(:,3)+s1(:,4))/3,-s1(:,4)+s1(:,2),'r');
title ('Mean effective Stress p' (kPa) VS. Deviatoric Stress q (kPa)');
xlabel('confinement p' (kPa)');
ylabel('q (kPa)');
set(gcf,'paperposition',fs);
grid on

figure(10); close 10; figure(10);
plot((s1(:,1))-20001,-s1(:,4)+s1(:,2),'r');
title ('Time(s) VS. Deviatoric Stress q (kPa)');
xlabel('Time(s)');
ylabel('q (kPa)');
set(gcf,'paperposition',fs);
grid on

figure(11); close 11; figure(11);
plot(p1(:,1)-20001,p1(:,2)/100,'r');
title ('Time(s) VS. Excess pore water pressure ratio ru');
xlabel('Time(s)');
ylabel('r_u');
set(gcf,'paperposition',fs);
grid on

% figure(12); close 12; figure(12);
% plot(tSS1(:,1),tSS1(:,2),'r');
% title ('Time(s) VS. Shear Strain \gamma (%)');

```

La información presentada en este documento es de exclusiva responsabilidad de los autores y no compromete a la EIA.

```

%       xlabel('Time(s)');
%       ylabel('Shear Strain \gamma (%)');
%       grid on
end
% %integration point 1 p-q
% po=(s1(:,2)+s1(:,3)+s1(:,4))/3;
% for i=1:size(s1,1)
%     qo(i)=(s1(i,2)-s1(i,3))^2 + (s1(i,3)-s1(i,4))^2 + (s1(i,2)-s1(i,4))^2 + 6.0* s1(i,5)^2;
%     qo(i)=sign(s1(i,5))*1/3.0*qo(i)^0.5;
% end
%
% figure(1); close 1; figure(1);
% %integration point 1 stress-strain
% subplot(2,1,1), plot(e1(:,4),s1(:,5),'r');
% title ('shear stress \tau_x_y VS. shear strain \epsilon_x_y at integration point 1');
% xlabel('Shear strain \epsilon_x_y');
% ylabel('Shear stress \tau_x_y (kPa)');
% subplot(2,1,2), plot(-po,qo,'r');
% title ('confinement p VS. deviatoric stress q at integration point 1');
% xlabel('confinement p (kPa)');
% ylabel('q (kPa)');
% set(gcf,'paperposition',fs);
% saveas(gcf,'SS_PQ_p1','jpg');
%
%
% %integration point 5 p-q
% po=(s5(:,2)+s5(:,3)+s5(:,4))/3;
% for i=1:size(s5,1)
%     qo(i)=(s5(i,2)-s5(i,3))^2 + (s5(i,3)-s5(i,4))^2 + (s5(i,2)-s5(i,4))^2 + 6.0* s5(i,5)^2;
%     qo(i)=sign(s5(i,5))*1/3.0*qo(i)^0.5;
% end
%
% figure(5); close 5; figure(5);
% %integration point 5 stress-strain
% subplot(2,1,1), plot(e5(:,4),s5(:,5),'r');
% title ('shear stress \tau_x_y VS. shear strain \epsilon_x_y at integration point 5');
% xlabel('Shear strain \epsilon_x_y');
% ylabel('Shear stress \tau_x_y (kPa)');
% subplot(2,1,2), plot(-po,qo,'r');
% title ('confinement p VS. deviatoric stress q at integration point 5');
% xlabel('confinement p (kPa)');
% ylabel('q (kPa)');
% set(gcf,'paperposition',fs);
% saveas(gcf,'SS_PQ_p5','jpg');
%
%
% %integration point 9 p-q
% po=(s9(:,2)+s9(:,3)+s9(:,4))/3;
% for i=1:size(s1,1)
%     qo(i)=(s9(i,2)-s9(i,3))^2 + (s9(i,3)-s9(i,4))^2 + (s9(i,2)-s9(i,4))^2 + 6.0* s9(i,5)^2;
%     qo(i)=sign(s9(i,5))*1/3.0*qo(i)^0.5;
% end
%
% figure(6); close 6; figure(6);
% %integration point 9 stress-strain
% subplot(2,1,1), plot(e9(:,4),s9(:,5),'r');
% title ('shear stress \tau_x_y VS. shear strain \epsilon_x_y at integration point 9');
% xlabel('Shear strain \epsilon_x_y');
% ylabel('Shear stress \tau_x_y (kPa)');
% subplot(2,1,2), plot(-po,qo,'r');
% title ('confinement p VS. deviatoric stress q at integration point 9');
% xlabel('confinement p (kPa)');
% ylabel('q (kPa)');
% set(gcf,'paperposition',fs);
% saveas(gcf,'SS_PQ_p9','jpg');
%
% figure(2); close 2; figure(2);

```

La información presentada en este documento es de exclusiva responsabilidad de los autores y no compromete a la EIA.

```

% %node 3 displacement relative to node 1
% plot(d1(:,1),d1(:,4));
% title ('Lateral displacement at element top');
% xlabel('Time (s)');
% ylabel('Displacement (m)');
% set(gcf,'paperposition',fs2);
% saveas(gcf,'Disp','jpg');
%
% s=accMul*sin(0:pi/50:20*pi);
% s=[s';zeros(3000,1)];
% s1=interp1(0:0.01:40,s,a1(:,1));
%
% figure(3); close 3; figure(3);
% %node acceleration
% a = plot(a1(:,1),s1+a1(:,6),'r');
% title ('Lateral acceleration at element top');
% xlabel('Time (s)');
% ylabel('Acceleration (m/s^2)');
% set(gcf,'paperposition',fs2);
% saveas(gcf,'Acc','jpg');
%
% figure(4); close 4; figure(4);
% a=plot(p1(:,1),p1(:,2));
% title ('Pore pressure at base');
% xlabel('Time (s)');
% ylabel('Pore pressure (kPa)');
% set(gcf,'paperposition',fs2);
% saveas(gcf,'EPWP','jpg');

```